AD_____

Award Number: W81XWH-12-1-0579

TITLE: The Role of PP2A Methylation in Susceptibility and Resistance to TBI and AD-Induced Neurodegeneration.

PRINCIPAL INVESTIGATOR: Ottavio Arancio

CONTRACTING ORGANIZATION: Columbia University, New York NY 10032

REPORT DATE: September-2013

TYPE OF REPORT: Annual

PREPARED FOR: U.S. Army Medical Research and Materiel Command
Fort Detrick, Maryland 21702-5012

REPORT DOCUMENTATION PAGE

Form Approved
OMB No. 0704-0188

1. REPORT DATE
September 2013

2. REPORT TYPE
Annual

3. DATES COVERED
30September2012–29September2013

4. TITLE AND SUBTITLE
The Role of PP2A Methylation in Susceptibility and Resistance to TBI and AD-Induced Neurodegeneration

5a. CONTRACT NUMBER

5b. GRANT NUMBER
W81XWH-12-1-0579

5c. PROGRAM ELEMENT NUMBER

6. AUTHOR(S)
Ottavio Arancio, Barclay Morrison, Russell Nicholls, Edward Vogel, Christopher Hue

E-Mail: oa1@columbia.edu

5d. PROJECT NUMBER

5e. TASK NUMBER

5f. WORK UNIT NUMBER

7. PERFORMING ORGANIZATION NAME(S) AND ADDRESS(ES)
Columbia University

New York, NY 10032

8. PERFORMING ORGANIZATION REPORT NUMBER

9. SPONSORING / MONITORING AGENCY NAME(S) AND ADDRESS(ES)
U.S. Army Medical Research and Materiel Command
Fort Detrick, Maryland 21702-5012

10. SPONSOR/MONITOR'S ACRONYM(S)

11. SPONSOR/MONITOR'S REPORT NUMBER(S)

12. DISTRIBUTION / AVAILABILITY STATEMENT
Approved for Public Release; Distribution Unlimited

13. SUPPLEMENTARY NOTES

14. ABSTRACT
The focus of the current study is to test the effect of genetic manipulations that target the tau phosphatase, PP2A, on behavioral impairments resulting from shockwave exposure in a mouse model, and to compare those results with the effects of the same genetic manipulations on the sensitivity to AD-like impairments caused by acute beta-amyloid (Aβ) exposure. Our goal is to identify the molecular mechanisms that contribute to TBI or AD-related impairment so that this information can then be used to identify at-risk individuals and develop effective therapeutic approaches. The principal motivation behind this approach is the observation that aggregates of hyperphosphorylated tau are a common feature of multiple neurodegenerative conditions including Alzheimer's disease and traumatic brain injury-associated degeneration. We previously found that the two novel lines of transgenic mice will use in this study, altered sensitivity to Aβ-induced electrophysiological and behavioral impairments, and our hypothesis is that they will exert similar effects on shockwave-induced impairments. This effort has required a substantial investment in developing equipment and testing protocols for exposing mice to a range of shockwave exposure conditions that mimic militarily relevant exposures and then assessing the biochemical and behavioral consequences of those exposures. There is currently a pressing need for mouse models and methodologies that reproduce the key features of blast exposure observed in humans, and the results of our experiments are a significant contribution to that effort.

15. SUBJECT TERMS
none provided

16. SECURITY CLASSIFICATION OF:	**17. LIMITATION OF ABSTRACT**	**18. NUMBER OF PAGES**	**19a. NAME OF RESPONSIBLE PERSON**
			USAMRMC

a. REPORT	b. ABSTRACT	c. THIS PAGE			19b. TELEPHONE NUMBER *(include area code)*
U	U	U	UU	84	

Table of Contents

Page

INTRODUCTION:

Neurodegeneration resulting from both traumatic brain injury (TBI) and Alzheimer's disease (AD) is characterized by aggregates of hyperphosphorylated tau (Ballatore et al., 2007; Dekosky et al., 2013). This observation together with the involvement of tau in other neurodegenerative disorders suggests that a common neurodegenerative mechanism involving tau hyperphosphorylation may contribute to impairments associated with both TBI and AD. Tau phosphorylation is controlled by a balance between the activity of numerous kinases and the protein phosphatase, PP2A (Martin et al., 2013), and PP2A activity is in turn controlled by C-terminal methylation of its catalytic subunit (Sents et al., 2013). To examine the effects of altered PP2A activity and tau phosphorylation on TBI and AD-related impairments, we generated two lines of transgenic mice, one that expresses the PP2A methylesterase, PME-1, and one that over expresses the PP2A methyltransferase, LCMT-1. We found that PME-1 over expression increased sensitivity to electrophysiological and behavioral impairments caused by acute oligomeric Aβ exposure, and that LCMT-1 over expression protected animals from these impairments. In this project, we are using these novel transgenic animals to examine the relationships between shockwave exposure, tau phosphorylation, and behavioral impairment. If tau phosphorylation is involved in injury-induced and AD-related impairments, then we expect that these transgenes will exert similar sensitizing or protective effects on shockwave-induced impairments. Due to the emerging nature of the methodology for modeling blast exposure in mice, this effort has required a substantial investment to identify suitable shockwave exposure conditions, confirm biomechanical parameters, and to assess the biochemical consequences. One of the previously unforeseen benefits of this investment may be the identification of PME-1 over expressing mice as a sensitized background in which to model injury-related tauopathies that occur in humans, and we are actively exploring this possibility.

BODY:

In June of 2013 the statement of work for this project was modified to address the need for a more comprehensive assessment of the link between the shockwave characteristics and exposure conditions, and injury related increases in tau phosphorylation. The current statement of work seeks to address 4 main questions, numbered below. Here we outline our progress in addressing each of these questions in turn:

1) What are the parameters and characteristics of shockwave exposure that are necessary to produce increased tau phosphorylation in mouse brain?

Background:

Increased tau phosphorylation has been described in invasive models of traumatic brain injury in mice including fluid percussion and controlled cortical impact (Marklund and Hillered, 2011; Xiong et al., 2013), however data on increased tau phosphorylation in mice exposed to shockwaves is limited or just emerging (Goldstein et al., 2012; Huber et al., 2013). One recent report described increased tau phosphorylation using two phospho-

tau specific antibodies in brain homogenates from wild type mice prepared 2 weeks after injury (Goldstein et al., 2012). That study also reported that shockwave-related cognitive deficits in these animals were the result of shockwave-induced head acceleration and not shockwave exposure per se. As outlined in the amended statement of work, we exposed wild type control mice to shockwaves of different intensities to identify thresholds for exposure-induced tau phosphorylation. We exposed these animals to these different shockwave intensities under conditions where the head was either fixed or free to accelerate in response to the shockwave. We then compared the levels of tau phosphorylation by quantitative western blot on brain homogenates prepared from these different groups 2 weeks after shockwave exposure.

Shocktube and animal holder construction:

The second shock tube for exposing animals to shock waves mimicking real-world blast exposures has been constructed, instrumented, and is fully operational. The device was designed to be identical to our existing shock tube located at the Morningside Heights campus of Columbia University, in the Neurotrauma and Repair Laboratory, directed by Barclay Morrison, Ph.D. The aluminum shock tube consists of an adjustable length driver section (25 mm used for current studies) pressurized with compressed gas, a 1240 mm-long driven section with a 76 mm-diameter, and a Mylar burst diaphragm of adjustable-thickness (Figure 1). The shock tube design allows for modification of the type of compressed gas used, the volume of the driver section, and the thickness of the burst diaphragm in order to generate a range of overpressure and duration profiles similar to those observed in free-field blasts. Commercially available pressure transducers (Endevco) are flush-mounted at the tube outlet to record incident pressure of the shock wave. The blast parameters of peak incident overpressure, duration, and impulse are determined in the open-tube configuration in the absence of interacting structures downstream, as this arrangement represents an independent and consistent measure of the blast injury input. These methods have been established in accordance with our previous publications so that all blast injury experiments are standardized across both shock tube locations at Columbia University. Provided below is a representative averaged pressure history of a shock wave generated in a typical configuration using compressed helium gas (Figure 2).

To safely expose the animals to the necessary blast conditions, an animal holder was constructed (Figure 3). This brass tube (165.1 mm length, 38.1 mm inner diameter) is half-filled with polyurethane and lined with sorbothane in order to prevent any damaging impacts with the metal tube. One end of the tube has the top half removed and replaced with a detachable PVC plastic semi-cylinder, lined with sorbothane, to allow for easy loading of the animal while still providing effective thoracic protection. Another Endevco pressure transducer is positioned inside the tube and confirms minimal pressure levels exist within the holder, even during high blast intensities. The head of the subject rests on an exposed, padded section of the holder, where a nose bar can be attached to allow for restraint of the head and delivery of a pure primary blast exposure. If the restraint is removed, a combined primary & tertiary (inertial-driven) exposure can be delivered. The animal is positioned perpendicularly to the shock tube exit. In order to prevent reflections of the shock wave off the shielding portion of the holder, the edge of

the animal holder aligned with the inside edge of the shock tube exit. The animal head is aligned with the vertical center from of the shock tube exit and offset by 25mm.

Shockwave exposure conditions:

To test the effect of shockwave intensity and the presence or absence of concomitant head acceleration, we used our newly constructed shock tube apparatus and animal holder to expose wild type mice to 3 different shockwave intensities under conditions where the head was either restrained or free to accelerate in response to the shockwave. To do this, animals were given a prophylactic dose of buprenorphine (0.1 mg/kg) and anesthetized for 2 minutes in 5% isoflurane. Animals were then quickly transferred to the animal holder and positioned such that the head was located at the tube exit and the body was shielded from the blast. In all cases the shockwave was delivered to the right side of the animal's head. For the unrestrained configuration, the head rested on a sorbothane-covered support that protruded under the animal's chin. For the restrained condition, the support was placed against the left side of the head and a metal band was placed across the animal's nose to hold it in place. After positioning the animal, 2% isoflurane was delivered through a nose cone and anesthesia monitored for an additional 3 minutes before triggering the shock tube. High-speed video of the animal was captured during shockwave exposure for subsequent determination of head acceleration, and pressure transducers located at the tube exit and inside the animal holder recorded pressure traces at those locations. Following shockwave exposure, animals were placed on their backs and righting time was recorded (time for all 4 paws to contact the ground). To alleviate pain associated with the procedure, animals were given 3 more buprenorphine injections at 8-hour intervals.

The range of shockwave intensities used was specific to each configuration based on preliminary experiments to test viability thresholds. In each configuration, the highest intensity was near to the threshold for survivability. For animals exposed in the restrained head configuration, we exposed cohorts of 6 wild type animals to either a sham injury or one of three different shockwave intensities: 206±3.0 kPa overpressure / 0.53±0.006ms duration / 38.2±0.65 kPa-ms impulse; 244±6.6 kPa / 0.63±0.008 ms / 52.7±1.60 kPa-ms; 272±5.5 kPa / 0.69±0.007 ms / 65.3±1.38 kPa-ms. An additional 6 sham exposed animals were subject to all procedures including anesthesia, and positioning in the animal holder, but the shock tube was not fired. For animals exposed in the unrestrained head configuration, we exposed cohorts of 6 wild type animals to either a sham injury or one of three different shockwave intensities: 136±1.7 kPa overpressure / 0.34±0.011ms duration / 16.6±0.26 kPa-ms impulse; 179±3.0 kPa / 0.46±0.012 ms / 28.1±0.42 kPa-ms; 206±3.0 kPa / 0.53±0.006 ms / 38.2±0.65 kPa-ms. The mean shock wave parameters and corresponding righting times are listed in the table below.

TABLE 1

Blast Condition	Pressure (kPa)	Duration (ms)	Impulse (kPa-ms)	Holder Pressure (kPa)	Righting Time (sec)	Peak Horizontal Acceleration (m/s^2)	Peak Vertical Acceleration (m/s^2)
Sham	0	0	0	0	43 ± 7.7	0	0

Unrestrained	**1**	136 ± 1.7	0.34 ± 0.011	16.6 ± 0.26	23.1 ± 0.22	43 ± 8.5	13641 ± 809.3	11626 ± 394.7
	2	179 ± 3.0	0.46 ± 0.012	28.1 ± 0.42	29.4 ± 1.38	92 ± 20.2	20834 ± 1346.2	14355 ± 1059.5
	3	206 ± 3.0	0.53 ± 0.006	38.2 ± 0.65	32.2 ± 3.04	565 ± 280.9	22511 ± 1754.5	14548 ± 881.2
	Blast Condition	**Pressure (kPa)**	**Duration (ms)**	**Impulse (kPa-ms)**	**Holder Pressure (kPa)**	**Righting Time (sec)**	**Peak Horizontal Acceleration (m/s^2)**	**Peak Vertical Acceleration (m/s^2)**
	Sham	0	0	0	0	60 ± 12.9	0	0
Restrained	**1**	206 ± 3.0	0.53 ± 0.006	38.2 ± 0.65	19.4 ± 1.95	175 ± 41.2	12680 ± 1608.9	11549 ± 1278.2
	2	244 ± 6.6	0.63 ± 0.008	52.7 ± 1.60	20.8 ± 1.08	294 ± 51.0	16187 ± 1269.6	12907 ± 733.8
	3	272 ± 5.5	0.69 ± 0.007	65.3 ± 1.38	23.7 ± 1.14	657 ± 312.3	17463 ± 1453.7	15312± 2042.2

The largest exposure levels (Level 3) for both the unrestrained and restrained configurations produced significantly increased ($p < 0.05$) righting times as compared to sham exposures in the respective configurations.

Measure of shockwave related increases in tau phosphorylation:

To assess the level of tau phosphorylation in our shockwave-exposed animals, we carried out quantitative western blots on brain homogenates prepared 2 weeks after exposure. Animals were sacrificed by cervical dislocation and the brains were rapidly removed to ice cold, oxygenated ACSF. Ipsilateral and contralateral (relative to shock tube) cortex and hippocampi were rapidly dissected and snap frozen in liquid nitrogen. Tissue was homogenized using a motorized pestle in ice cold modified RIPA buffer supplemented with Halt protease plus phosphatase inhibitors (Pierce) and 25 nM okadaic acid (Calbiochem). Homogenates were gently agitated in buffer at 4°C for 15 min and cleared by centrifugation at 14,000xg. Protein concentration in each sample was determined by BCA (Pierce). 30 micrograms of protein was loaded per lane from each sample on a 1mm Nupage 4-12% Bis-Tris gel (Invitrogen). Resolved proteins were transferred to PVDF membrane using an I-blot apparatus (Invitrogen). Separate blots were prepared for each of 7 different phospho-tau specific antibodies. Blots were probed simultaneously with a single phospho-tau specific antibody (raised in either mouse or rabbit) and an antibody raised in sheep that recognizes both phosphorylated and unphosphorylated tau. Bound primaries were detected and distinguished with species specific secondary antibodies conjugated to infrared excitable fluorophores and detected and quantified using an Odyssey imager and associated software (Li-cor Biosciences). Total tau levels in these samples were determined similarly by probing simultaneously with the sheep anti-tau antibody to measure total tau immunoreactivity and a primary antibody recognizing β-actin to control for differences between lanes due to loading or transfer efficiency. Phospho-tau or total tau immunoreactivity in each lane was normalized to the signal from the loading control in that lane (total tau for phospho-tau signals and β-actin for total tau signals). Means for each group were calculated and expressed as percent of the mean for the sham control group.

The primary antibodies used were as follow:

Rabbit anti-phospho S262 (Invitrogen)
Rabbit anti-phospho S396 (Invitrogen)
Rabbit anti-phospho S422(Invitrogen)
Mouse anti-phospho tau clone AT8 (recognizes tau phosphorylated at S199/S202/S205) (Thermo Fisher)
Mouse anti-phospho tau clone AT100 (recognizes tau phosphorylated at T212/S214) (Thermo Fisher)
Mouse anti-phospho tau clone AT180 (recognizes tau phosphorylated at T231) (Thermo Fisher)
Mouse anti-phospho tau clone AT270 (recognizes tau phosphorylated at T181) (Thermo Fisher)
Sheep anti-total tau (Thermo Fisher)
Rabbit anti-β-actin (Li-Cor Biosciences)

We found no evidence for shock wave induced increases in tau phosphorylation at any of the phospho-tau epitopes examined from ipsilateral cortex harvested at 2 weeks post-exposure in any of our groups independent of blast level or the presence or absence of concomitant head acceleration (Figure 4). These data are in contrast to the results reported in Goldstein et al (Goldstein et al., 2012) on which we patterned our experimental design. We are currently unable to explain the basis for this difference. We employed multiple shockwave intensities and sampled a significantly larger battery of tau phosphorylation sites. The immunodetection conditions and quantitation methods we used in our analysis are widely regarded as among the most reliable and quantitative, particularly when compared with autoradiography of chemiluminescent signals measured by densitometry of blots that are stripped and reprobed with antibodies to loading control proteins. As described below in SOW Aim 2, this methodology successfully identified changes in baseline tau phosphorylation in the PME-1 over expressing mice. Importantly, the head acceleration that Goldstein et al. concluded was the critical factor for producing the impairments they reported was comparable in our experiments.

While our shockwave exposure conditions did produce comparable head acceleration to what was reported in Goldstein et al., the shockwaves we exposed our animals to were shorter in duration from those described by Goldstein et al. as well as from Huber et al. (Huber et al., 2013). The durations of the shockwaves in those studies is greater than 5ms, which has significant implications in terms of equivalent human-exposure delivered to a mouse. For example, from the original thoracic / lung injury tolerance studies reported by Bowen, the necessary shockwave to cause a 50% chance of lung injury varied with the size of the animal being tested (Bowen et al., 1968; Damon et al., 1966; Richmond et al., 1968). In fact, Bowen found that the critical parameter that needed to be scaled with respect to body mass for inducing the same level of injury was duration, not peak pressure. Bowen found that duration scaled with the relative mass of the animal to the 0.4 power. Practically, this meant that to apply a blast wave to a mouse that would cause similar injury as a blast in a human, the duration would need to be reduced by ~20 fold, but the peak pressure would remain constant. Or conversely, a 5ms long blast applied to a mouse would be the equivalent of a 100ms blast applied to a

human, which is not a realistic duration. More recently, this idea of scaling has been applied to other physiological outcome measures such as apnea. In this case, Wood et al. (Wood et al. 2013) found that duration scaled with respect to relative mass to the 0.33 power, similar but slightly lower than Bowen's scaling relationship. Taken together, these studies suggest that to appropriately model blasts due to improvised explosive devices, the durations of the experimental shockwave should be less than 1ms when applied to a mouse. In our studies, both un-scaled and scaled shockwave parameters equate to a range of real world blast exposure conditions from a small mortar round (M49A4 60 mm Mortar, standoff distance 0.25-2 m) to a large bomb (M118 Bomb, standoff distance 10-32 m; Conventional Weapons Effects, CONWEP).

While the Goldstein paper argues that shockwave induced head acceleration is the critical factor in producing associated impairments, it is also possible that the effects they describe were dependent on *combined* effects of the type of shockwaves they exposed their animals to and the accompanying head acceleration. Given the size of the animals' heads and the duration of the shockwave, significant deformation of the skull and underlying brain could be occurring in the Goldstein set-up, whereas our system has been designed to avoid this type of loading. To formally test this possibility and the possibility that the unique characteristics of the shockwaves these authors used are the basis of the difference in the effects we observe in tau phosphorylation, we will expose another group of wild type animals to shockwaves that more closely replicate those used by Goldstein et al and Huber et al. and again assess the levels of tau phosphorylation using our methodology.

In rodent models, there is substantial data showing acute increases in tau phosphorylation resulting from more traditional invasive rodent TBI methods. However, the use of mice to model the molecular and behavioral effects of blast exposure is relatively new and there remains very little data on the relationship between shockwave exposure and persistent changes in the level of tau phosphorylation. If the history of the development of murine AD models that exhibit tauopathy is an example, then mice may also be less susceptible to TBI associated tauopathy when compared to humans. Modeling the phenomenon in mice may therefore require the use of more robust TBI protocols such as repetitive TBI approaches or the use of sensitized genetic backgrounds. We will pursue the latter approach as part of Aims 2 and 3 of the SOW by examining the effects of shockwave exposure in the PME-1 over expressing transgenic mice. The decreased tau phosphatase activity and elevated levels of basal tau phosphorylation in these animals may sensitize them to blast-induced tauopathy.

In developing a successful blast-induced TBI model, it will be important to attempt to maintain normal physiological conditions to the extent possible. Data from mutant mouse models that lack the endogenous *MAPT* gene, over express heterologous or mutant tau and/or develop tauopathy independent of shock wave exposure may not be easily related to blast exposure in normal human patients that the model is attempting to reproduce. In this respect, our PME-1 over expressing mice may be useful. We know that PME-1 over expression produces modest increases in tau phosphorylation at specific sites see SOW Aim 2 below), and that it sensitizes animals to beta-amyloid induced impairments without any behavioral or physiological deficits that we have detected thus far (see Appendix 3). If shockwave exposure produces acute or persistent tau hyperphosphorylation and/or aggregate accumulation in the PME-1 mice (see SOW Aims

2 and 3 below), then these animals may constitute an extremely useful background in which to experimentally dissect, understand and ultimately develop treatments and preventative measures for blast-induced TBI impairments.

2) <u>What are the consequences of LCMT-1 and PME-1 transgene expression on bTBI-associated behavioral impairment and tau phosphorylation at 2 weeks and 3 months post injury?</u>

As outlined in the SOW, we will expose LCMT-1 and PME-1 over expressing animals and controls to shockwaves and assess the cognitive and behavioral performance of these animals at 2 weeks and 3 months post-injury as well as the level and distribution of total and phosphorylated tau species at these time points. Based on the results we obtained from experiments described in Aim 1 of the SOW, we will expose these animals to the highest survivable blast level (65.3kPa-ms impulse) in a fixed head configuration. In performing these experiments on genetically modified mice and including a longer post-exposure time point, we will explore three possibilities that not addressed by the experiments on wild type control animals described in Aim 1:

A) *The possibility that tauopathy develops at longer post-exposure time points.*
In humans, injury related tauopathy typically develops over time. There are multiple examples of professional football players described in the literature who do not report the first symptoms chronic traumatic encephalopathy (CTE) until several years after the end of their athletic career (McKee et al., 2012). By examining the level of tau phosphorylation by western blot and tau distribution by immunohistochemistry in animals 3 months after shockwave exposure we may identify changes that are not detectable at 2 weeks post-exposure.

B) *The possibility that shockwave exposure produces tauopathy in PME-1 over expressing mice*.
As discussed above, mice may be relatively more resistant to injury-induced tauopathy when compared to humans. Producing a successful model of blast-induced neurodegeneration in mice might therefore require the use of modified injury protocols or sensitized genetic backgrounds. We found that PME-1 over expression in our animals resulted in small but significant increases in basal tau phosphorylation at specific residues. By exposing these animals to shockwaves and assessing tau phosphorylation and distribution after injury, we will determine whether shockwave exposure in *combination* with PME-1 over expression is sufficient to produce injury related tauopathy. If this proves to be the case, then the PME-1 over expressing mice may be a useful genetic background in which to model blast-induced neurodegeneration.

C) *The possibility that LCMT-1 and/or PME-1 transgene expression affect shockwave induced cognitive and behavioral impairments independent of the presence of persistent increases in tau phosphorylation or aggregation.*
Persistent and progressive tau hyperphosphorylation and aggregation are clearly central to a number of neurodegenerative conditions, including chronic traumatic encephalopathy (Blennow et al., 2012), and may well play a role in the response to blast exposure (Goldstein et al., 2012). However, blast exposure affects the brain in multiple ways via

multiple molecular pathways. It is possible therefore, that PME-1 and LCMT-1 over expression may affect the response to shockwave exposure via a mechanism that doesn't affect persistent changes in injury-induced tau hyperphosphorylation or aggregation. For example, transgene expression could affect tau phosphorylation or another pathway during the acute response to shockwave exposure and that could well produce long-term effects on behavioral and cognitive performance. We will determine whether this may be the case through behavioral examination of shockwave exposed PME-1 and LCMT-1 transgenic animals at 2 and 3 months post-exposure.

In preparation for these experiments, we have substantially expanded our colonies of these animals and now have sufficient numbers for behavioral analysis. We have optimized our protocols for successfully measuring the level of tau phosphorylation by western blot (see discussion of SOW Aim 1 and below). We have successfully performed anti-tau and phospho-tau immunohistochemistry on paraffin sections from shockwave-exposed mice (see discussion of SOW Aim 3), and we have piloted the behavioral battery we will use to examine behavioral and cognitive performance in these animals. With the identification, in SOW Aim 1, of a sublethal shockwave exposure protocol that is analogous to real world blast exposures in humans, we are now set to begin and complete this behavioral analysis in the second and final year of the award.

Effect of PME-1 over expression on basal P-tau levels

To measure basal levels of tau phosphorylation in PME-1 over expressing mice we prepared hippocampal homogenates from naïve animals and performed quantitative western blotting as described above in SOW Aim 1. This analysis revealed significant increases in tau phosphorylation at specific sites in the PME-1 over expressing mice (Figure 5). Given published data showing that the presence and phosphorylation state of tau affects behavioral and physiological impairments in mouse models of Alzheimer's (Lewis et al., 2001; Mairet-Coello et al., 2013; Perez et al., 2008; Perez et al., 2005; Rhein et al., 2009; Ribe et al., 2005; Roberson et al., 2007; Shipton et al., 2011), we propose that elevated levels of tau phosphorylation in the PME-1 over expressing mice may be responsible for the increased sensitivity to Aβ-induced electrophysiological and behavioral impairments we observe in these animals (see Appendix 3 for further discussion). In this regard, increased phosphorylation at tau residue Ser262 in the PME-1 over expressing mice is particularly interesting in light of recently published data implicating Ser262 phosphorylation in Aβ sensitivity (Mairet-Coello et al., 2013).

If Alzheimer's disease-associated neurodegeneration and blast-induced neurodegeneration both entail mechanisms that involve tau hyperphosphorylation, then increases in basal tau phosphorylation in the PME-1 over expressing mice may sensitize these animals to shockwave induced cognitive and behavioral impairments as well as Aβ-induced impairments. It may also be possible to identify synergistic effects of shock wave exposure and PME-1 over expression on the level of tau phosphorylation and/or aggregation. The observation that AT8 anti-phospho-tau immunoreactivity is increased both in response to traumatic brain injury (Tran et al., 2011) and under basal conditions in the PME-1 transgenic mice suggests that this may prove to be the case.

Validating a behavioral battery for TBI associated impairments

Traumatic brain injury (TBI) can result in cognitive and behavioral impairments that include impaired motor function, depression or aggression, and impaired learning and memory (Blennow et al., 2012). We will examine the effects of shockwave exposure in mice on these behavioral and cognitive impairments as well as the ability of our genetic manipulations to sensitize or protect animals from these impairments. To do this, we have designed a unique behavioral battery that incorporates measures of motor function (rotarod, openfield, visible platform water maze), depression (forced swim, tail suspension), anxiety (elevated plus, open field) and cognitive function (radial arm water maze, contextual fear conditioning). To validate our behavioral protocols and their use in the behavioral battery, we carried out a pilot study using control animals in the same genetic background that we plan to use for our transgenic animal experiments. The behavioral protocols were carried out according to the following schedule:

Days -4 to -1: Rotarod pretraining
Day 0: no testing (shockwave exposure day)
Battery Day 1: openfield (AM) and accelerating rotarod (PM) (for experiments on transgenic animals this day will be 2 weeks, or 3 months after shockwave exposure)
Battery Day 2: elevated plus maze (AM) and forced swim test (PM)
Battery Day 3 and 4: radial arm water maze task
Battery Day 5: tail suspension test (AM) and contextual fear conditioning task training (PM)
Battery Day 6 : contextual fear conditioning task testing
Battery Day 7 and 8: visible platform water maze task
Battery Day 9: sensory threshold assessment

Accelerating rotarod task:

We assessed motor performance of mice using a rotarod apparatus (Med Associates) essentially as described previously (Clausen et al., 2011; Wang et al., 2011; Yu et al., 2012). This apparatus consists of a 32 mm diameter rotating rod suspended 16.5 cm above a pressure sensitive tray. The rod passes through large plastic discs that create 57 mm lanes along the rod in which lateral movement of the mice are constrained. Training on this task was carried out on 4 successive days. The first day of training consisted of 4 x 5 minute trials. On the first trial, animals were placed on the apparatus and the rotation speed was set at 4 rpm, on the second and third trials, the rotation speed was slowly ramped up from 4 to 10 rpm over the course of the trial, and on the third trial the rotation speed was ramped from 4 to 40 rpm. On this first day of training, animals that fell were returned to the rod and the trial continued for the specified 5 min period. On this and all subsequent days, animals were returned to their home cages for 45 min between trials. The second through fourth days of training consisted of 3 x 5 min trials per day with the rotation speed ramped from 4 to 40 rpm over the course of the trial. When animals fell from the apparatus the trial was terminated and the animal returned to its home cage. Rotarod testing was carried out in the morning of the second day of the behavioral battery. Testing consisted of 4 trials conducted in the same manner as described for pre-training days 2 -4.

As shown in Figure 6, this pilot study produced a level of performance consistent with similar studies described in the literature that is suitable for detecting motor deficits in our shockwave-exposed animals. The fact that the performance of our animals did not improve across training trial and failed to reach a plateau as high as that reported in some studies is of some theoretical, if not practical, concern. We are therefore repeating this test on a second group of control animals using a different rotarod apparatus to ascertain if these results were a function of the particular apparatus used for the initial tests.

Open field testing:

To assess the effects of shockwave exposure and our genetic manipulations on activity level, response to novelty, and anxiety, we will assess the behavior of our animals in a novel open field environment essentially as described in (Tweedie et al., 2007). In our pilot experiment, we placed animals in a plexiglass chamber (43.2 cm long × 43.2 cm wide × 30.5 cm high) for a total of 30 min during which time their movements were tracked and analyzed using a video tracking system and behavioral analysis software (Ethovision, Noldus). This analysis revealed levels of activity (ambulatory distance) and thigmotaxis (center time) (Figure 7) that were consistent with published literature and suitable for assessing the effects of shockwave exposure and transgene expression in our planned experiments.

Elevated plus maze task:

To assess any possible anxiogenic or anxiolytic effects of shockwave exposure and our genetic manipulations, we will examine the behavior of our animals in an elevated plus maze essentially as described in (Schwarzbold et al., 2010; Siopi et al., 2012). The apparatus consists of a plus shaped track with arms 18 cm long and 6 cm wide, elevated 60 cm above the bench top by a single central pillar. Two non-adjacent arms are surrounded by walls on 3 sides, and the remaining two arms are exposed. Animals were placed into the center of the apparatus and the number and duration of open vs. closed arm entries are used as an index of anxiety. Animal location during single 5 min exposure to this behavioral apparatus was monitored and analyzed using a video tracking system and accompanying behavioral analysis software (Ethovision, Noldus). After each trial, animals were returned to their home cages and the apparatus was thoroughly cleaned and deodorized with MB-10 and distilled water. We found that control animals showed strong preference for the closed vs. open arms of the maze spending 19 and 52% of their time in these locations respectively. This level of performance is consistent with published literature and appropriate for detecting differences in anxiety levels in our genetically modified, shockwave-exposed animals.

Forced swim test:

To assess the effects of shockwave exposure and our genetic manipulations on depressive behavior, we assessed the behavior or our animals in forced swim test essentially as described in (Milman et al., 2008; Tweedie et al., 2007). In our pilot experiment, we placed control animals into a 4 liter plastic beaker filled half way with tap water (22-25C) for a total of 6 minutes. During this time, the animals' movements were recorded using a video camera, and the recordings were subsequently offline by a blinded observer for number, timing, and duration of periods of immobility. Following the forced

swim trial, animals were dried using paper towels and returned to clean home cages partially illuminated by a heat lamp for a period of 10 minutes to prevent hypothermia. As shown in Figure 8, our pilot study produced a level of performance consistent with published literature and suitable for detecting differences in depressive behavior in our genetically modified, shockwave-exposed animals.

Radial arm water-maze task:

To assess the effects of shockwave exposure and our genetic manipulations on cognitive performance, we will test our animals in a 2-day radial arm water-maze task as described previously (Goldstein et al., 2012). The test will be performed in a 120 cm diameter pool containing a 6-arm radial maze insert and opaque water maintained at 24°C. On each day of the task, animals are subjected to a total of 15 trials. During the first 11 odd-numbered trials of the first day, the location of the escape platform is indicated by a marker protruding above the surface of the water, while on all other trials, the submerged platform is not visible to the animals. In each trial, the number of errors (entries into arms that do not contain the platform) will be recorded. At the end of testing, the mice will be dried off and placed in a clean cage with extra paper towels to prevent hypothermia.

We used this task previously to demonstrate increased sensitivity and resistance to Aβ-induced cognitive impairments in our PME-1 and LCMT-1 transgenic mice respectively (see Appendix 3). In our pilot experiment, conducted on control animals in the same genetic background, we noted a more rapid acquisition of this task and a higher level of performance once acquired (Figure 9) than what we observed previously. We attributed this to the more extensive history of behavioral testing and handling that animals experience when subjected to our behavioral battery and our concern was that the more rapid acquisition may be less sensitive for detecting the protective or sensitizing effects of our transgenic manipulations. To compensate, we reduced the number of visible platform trails used in our protocol from 7 to 2, and conducted a second pilot experiment on another group of control animals, but found that this had a negligible effect on acquisition (Figure 9).

While it may be possible to further adjust the behavioral protocol to achieve a more gradual increase in spatial memory acquisition (for example by substituting an abbreviated version of a traditional hidden-platform Morris water maze for the radial water maze task we currently use), we believe that this is unnecessary. The existing 2-day radial arm water maze task was successful in detecting transgene dependent alterations in Aβ-induced cognitive impairment and is therefore an excellent candidate for detecting similar transgene-dependent alterations in shockwave-induced cognitive impairment. Its use for the shockwave experiments, also allows a more direct comparison with our data on the effects of these transgenes on sensitivity to Aβ-induced cognitive impairment.

Tail suspension test:

As a second test of the effects of shockwave exposure and our genetic manipulations on depressive behavior, we will assess the behavior or our animals in a tail suspension test essentially as described in (Schwarzbold et al., 2010). In our pilot experiment, animals' tails were gently taped approximately 2 cm from the end to a horizontal bar elevated 30 cm above the benchtop. The animals were then suspended in

this position for 6 minutes while their movements were recorded using a digital video camera. Videos were later scored offline by a blinded observer for number, timing, and duration of periods of immobility. Immediately after testing animals were removed from the apparatus returned to their home cages. As shown in Figure 10, our pilot study produced a level of performance consistent with published literature and suitable for detecting differences in depressive behavior in our genetically modified, shockwave-exposed animals.

Contextual and cued fear conditioning

As a second test of the effects of shockwave exposure and our genetic manipulations on cognitive performance, we will test animals on a contextual fear conditioning task as described previously (Francis et al., 2009; Puzzo et al., 2008). In this task, animals are placed into a conditioning chamber located inside a sound-attenuating box (72cm x 51cm x 48cm). A clear Plexiglas window (2cm thick, 12cm x 20cm) will allow the experimenter to record the animal's behavior with a video camera connected to a computer running Freeze Frame software (MED Associates Inc.). Background white noise (72dB), will be provided by a single computer fan will installed in one of the side of the sound-attenuating chamber. The conditioning chamber (33cm x 20cm x 22cm) is made of transparent Plexiglas on two sides and metal on the other two. One of the metal sides has a speaker and the other one a 24 V light. The chamber has a 36-bar insulated shock grid floor. The floor is removable to facilitate its cleaning with MB-10 and then with distilled after each experimental subject. Animals will be placed in the conditioning one animal at a time chamber once on each of two consecutive days. The first day of exposure mice will be placed in the conditioning chamber for 2 minutes before the onset of a discrete tone (CS) (a sound that will last 30s at 2800Hz and 85dB). In the last 2s of the CS, mice will be given a foot shock (US) of 0.50mA for 2s through the bars of the floor. After the tone and shock exposure, the mice will be left in the conditioning chamber for another 30s and then placed back in their home cages. 24 hours after their first exposure animals will be returned to the conditioning chamber for a total of 5 min without foot shock or tone presentation. During each of these exposures, freezing behavior will be scored using FreezeFrame software (Med Associates) and this parameter will be used as a measure of the strength of the context-shock association (ie. memory on the second exposure) and the general level of anxiety (baseline pre-shock exposure).

We found that this protocol produced low levels of baseline freezing in our control animals prior to shock exposure (7% freezing) that increased dramatically during reexposure to the shock context 24 hours later (50% freezing). This level of performance is consistent with our previous experiments and published literature, and is appropriate for detecting differences in contextual learning and memory performance in our genetically modified, shockwave-exposed animals when included as part of our behavioral battery.

Sensory threshold assessment:

As part of our pilot experiment, we also tested animals on the sensory threshold assessment task that we will to use to rule out any differences in shock perception that could interfere with our interpretation of the performance of animals in the contextual fear conditioning task. We conducted this assessment as described previously (Francis et

al., 2009; Puzzo et al., 2008). Animals were placed into an apparatus similar to that used for contextual fear conditioning. A sequence of single, 1sec foot shocks was then given at 30 sec intervals and 0.1 mA increments from 0 to 0.7 mA. Each animal's behavior was evaluated to identify shock intensities that produced the first visible response to the shock (flinch), the first extreme motor response (run/jump), and the first vocalized distress (Figure 11). This analysis produced results similar to data we obtained previously and to published results.

Visible platform water maze task:

To complete the pilot testing of our behavioral battery, we subjected our cohort of control animals to a visible platform water maze task as described previously (Francis et al., 2009; Puzzo et al., 2008). We will use this task in our behavioral battery both as another assessment of motor function and also to test for any performance deficits that might interfere with our analysis of the radial arm water maze task. We performed this task in the same 120 cm diameter pool used for the radial arm water maze task, except that the partitions were removed. Training for this task was carried out over 2 days with 3 morning and 3 afternoon trials on each day. Intertrial intervals were 15 to 20 min and rest periods between morning and afternoon sessions were at least 3 hrs. Each trial lasted for a maximum of 120 sec during which animals were required to swim to a visible escape platform located just above the water surface. Animals that did not reach the platform within the allotted time were guided to it and allowed to sit there for 15 sec before being returned to their home cage. The location of the platform was rotated among 4 different locations such that it was not be present in the same location on any two successive trials. Water temperature was maintained at approximately 24°C, and at the end of testing, the mice were dried off and placed in a clean cage with extra paper towels to prevent hypothermia. Measures of both time required to reach the hidden platform (latency) and swim speed (Figure 12) were conducted using a video-tracking system and behavioral analysis software (Ethovision, Noldus), and were consistent with the previous data from these animals and published literature.

3) Do LCMT-1 and PME-1 transgene expression alter the acute shockwave-induced changes in tau phosphorylation at 1 hr and 24 hrs post-injury?

Blast exposure-induced TBI has been found to elicit acute biochemical and physiological responses in the brains of exposed individuals. However, the relationship between acute biochemical changes and short or long-term cognitive and behavioral impairment remain poorly understood. To address this question and examine the effects of our transgenic manipulations on this relationship, we will measure the level of tau phosphorylation and aggregation in the brains as well as the level of tau present in the CSF of shockwave-exposed transgenic and control animals at acute post-exposure time points. To validate our protocol for carrying out these measures, we completed pilot experiments on wild type animals as detailed below:

Shockwave exposure conditions:

We exposed a group of 16 wild type animals to shockwaves with peak overpressures of approximately 267 ± 7 kPa (mean ± SEM), durations of 0.662 ± 0.009

ms, and impulses of 53 ± 0.9 kPa*ms. According to the Conventional Weapons Effects Program (CONWEP), this level of blast severity can be considered approximately equivalent to exposure to an explosion experienced 0.8 m away from 90 g of C4 explosive (unscaled duration),, which is within a range of realistic blast threats in a military setting. With exposure duration scaled to the mouse, according to scaling laws used for pulmonary blast injury, this level is comparable to exposure to an M117 bomb (222 kg TNT) at close range. These animals were placed in the specially designed animal holder described above that supported the head from below, and shielded the body to prevent confounding lung/bowel injury and to reproduce the presence of body armor. In these experiments, shockwaves were directed at the head from above. These conditions produced no lethality in any of the animals tested.

Phospho-tau levels in brain homogenates 1 and 24 hours after shockwave exposure

To determine the acute effect of shockwave exposure on the level of tau phosphorylation, we carried out western blots on hippocampal homogenates prepared 1 and 24 hours after exposure using the phospho-tau specific antibodies AT8 and AT270 as described above for SOW Aim 1. We also measured total tau levels in these homogenates using an antibody that detects phosphorylated and dephosphorylated tau in conjunction with an antibody to β-actin for normalization as described above in SOW Aim 1. These methods were effective in detecting both increased tau expression and increased tau phosphorylation in positive control samples obtained from tau transgenic mice (Figure 13). However, like our measures of tau phosphorylation conducted 2 weeks after exposure to a range of shockwave conditions, these acute measures did not reveal any injury-associated changes in tau levels or phosphorylation in the shock-wave exposed animals at the time points tested and under the exposure conditions used (Figure 13).

We will now conduct similar measures on PME-1 and LCMT-1 transgenic animals and controls exposed to the higher shockwave intensities described in SOW Aim 1. It is possible that this higher shockwave intensity may produce detectable changes in tau phosphorylation in control animals in these experiments. However, we will also test the possibility that PME-1 transgene expression may sensitize animals to acute increases in shockwave-induced tau phosphorylation as discussed above for the longer post-exposure phospho-tau measures we will perform as part of SOW Aim 2.

Tau distribution in brains of shockwave exposed mice

As an additional initial test of the effects of shockwave exposure on total and phospho-tau distribution, we carried out immunohistochemical staining using the phospho-tau specific AT8 antibody and an antibody that recognizes phosphorylated and dephosphorylated tau isoforms. These measures were carried out in paraffin sections of brains isolated from wild type animals 1 week after shockwave exposure. As shown in Figure 14, we saw no evidence for increased tau phosphorylation, expression or aggregation in our shockwave exposed wild type animals under the exposure conditions we used. However, in a control experiment, we did find that this methodology readily detected increased total and phospho-tau levels in brain sections prepared from mutant tau transgenic P301L mice (Figure 15). We now plan to use this protocol to examine total and phospho-tau distribution at acute (1 and 24 hours for SOW Aim 2) and chronic (2

weeks and 3 months for SOW Aim 2) post-exposure time points in PME-1 and LCMT-1 transgenic exposed to the higher intensity shockwaves described in SOW Aim1.

CSF tau measures in shockwave-exposed mice

Increases in tau levels have been reported in both the CSF and serum of patients and rodents following traumatic brain injury and its presence and level have been proposed as a potential biomarker for TBI. We plan to measure CSF levels of tau in shockwave exposed control and transgenic animals to examine any effects of transgene expression on this phenomenon and correlate it with the effects of transgene expression on chronic cognitive and behavioral impairments. As an initial step toward this goal, we collected cerebral-spinal fluid (CSF) from shockwave exposed animals and measured the level of total tau in CSF at 1 and 24 hours post-injury using a Mesoscale Discovery ELISA kit together with electrochemiluminescent detection on a Sector Imager. This preliminary analysis identified elevated levels of CSF tau in shockwave-exposed animals 1 hour after exposure (Figure 16), however, these values were near the detection limits of the apparatus (Figure 16). We are currently optimizing our sampling methodology to obtain larger volumes CSF from these animals, and plan to use this improved methodology to measure CSF tau levels in PME-1 and LCMT-1 transgenic mice 1 and 24 hours after shockwave exposure.

4) Do LCMT-1 and PME-1 transgene over expression affect tau hyperphosphorylation induced by acute beta-amyloid exposure?

Neurodegeneration resulting from traumatic brain injury and Alzheimer's disease are both characterized by the presence of aggregates of hyperphosphorylated tau, suggesting that similar molecular mechanisms involving tau phospohorylation may underlie degeneration and behavioral impairments in both of these conditions. As described in more detail in the attached manuscript and abstracts (see Appendix), we found that transgenic PME-1 over expression increased sensitivity to electrophysiological and behavioral impairments resulting from Aβ exposure, and that LCMT-1 over expression protected animals from these impairments. These transgenes regulate the methylation and consequently the activity of PP2A, which is the principal tau phosphatase, so one way they might affect Aβ sensitivity is by altering Aβ-induced increases in tau phosphorylation. This increase in tau phosphorylation might then contribute to the electrophysiological and behavioral impairments we observe. This relationship between tau and Aβ has been compared to a bullet and gun, where Aβ is the trigger for tau related neurodegeneration.

One of our objectives in testing the effects of PME-1 and LCMT-1 over expression on the response to shockwave exposure is to examine the involvement of tau phosphorylation in this process and determine whether transgene expression also affect shockwave-induced behavioral impairments. In the case of neurodegeneration resulting from brain injury, a similar "bullet and gun" relationship might exist between tau phosphorylation and injury, where injury is now the trigger. We will examine the relationship between injury, tau phosphorylation, behavioral impairment and transgene expression as described in SOW Aims 2 and 3. In SOW Aim 4, we will extend the comparison between injury and Alzheimer's disease associated neurodegeneration by

examining the effects of PME-1 and LCMT-1 over expression on Aβ-induced increases in tau phosphorylation.

As described above in SOW Aim 2 and Figure 5, we found that PME-1 over expression increases basal levels of tau phosphorylation at specific residues. We are now in the process of testing the effects of PME-1 expression on tau phosphorylation following exposure to oligomeric Aβ preparations. To do this we are preparing acute 400 μm hippocampal slices from PME-1 over expressing animals and control siblings. These slices are allowed to recover for 90 minutes in oxygenated artificial cerebral spinal fluid at 29°C. Oligomeric Aβ is then applied to a final concentration of 200 nM and slices incubated for an additional 2 hours. The slices are then snap frozen in liquid N2 and stored at -80°C until use. Homogenates are prepared and analyzed by quantitative phospho-tau immunoblotting as described above in SOW Aim 2. Our hypothesis is that this analysis may reveal a synergistic interaction between Aβ exposure and PME-1 transgene expression with respect to Aβ-induced increases in tau phosphorylation.

We will carry out similar experiments to measure the effect of LCMT-1 over expression on Aβ-induced increases in tau phosphorylation. Our analysis of basal levels of tau phosphorylation in these animals revealed no significant differences compared to controls in tau phosphorylation at any of the sites examined (Figure 17). This result is likely affected by the already low levels of tau phosphorylation that exist in mice under basal conditions. It is therefore possible that our analysis of Aβ-induced tau phosphorylation in these animals will reveal a protective effect of LCMT-1 over expression that is analogous to the protective effects of this transgene on Aβ-induced electrophysiological and behavioral impairments.

KEY RESEARCH ACCOMPLISHMENTS:

- Constructed a shock tube apparatus and animal holder capable of mimicking military-relevant blast exposure restricted to the head of mice.
- Preliminary demonstrated elevated tau levels in the CSF of blast exposed mice detected at 1 hour after injury.
- Found that sublethal exposure of wild type mice to shockwaves that recapitulate real world blast exposure (i.e. durations scaled for mouse mass using Bowen's relationships), do not produce increases in tau phosphorylation at multiple residues at two weeks post-exposure.
- Found that PME-1 over expression increases basal levels of tau phosphorylation at specific residues implicated in beta-amyloid sensitivity and/or the response to traumatic brain injury.
- Validated all protocols necessary for the planned immunohistochemical, biochemical and behavioral analysis of shockwave-exposed mice.

REPORTABLE OUTCOMES:

- We presented an abstract describing the effects of PME-1 and LCMT-1 transgene expression on Aβ-induced impairments at the 2012 Society for Neuroscience Meeting (see appendix 1).

- We presented an abstract describing the effects of PME-1 and LCMT-1 transgene expression on Aβ-induced impairments at the 2013 Alzheimer's Disease/Parkinson's Disease Meeting (see appendix 2).
- We prepared a manuscript describing the effects of PME-1 and LCMT-1 transgene expression on Aβ-induced impairments that is currently being revised for journal submission (see appendix 3).
- We contributed descriptions of our animal models, shock tube, and animal holder to the MRPRA Products database.
- We presented our experimental design and preliminary data at the May 9, 2013 MRPRA Progress Review at Ft. Detrick MD.

CONCLUSION:

The study of the long-term consequences of traumatic brain injury (TBI) is still an emerging field and the long-term consequences of TBI due to blast exposure is an even more recent problem due to both the nature of recent military conflicts and the fact that improvements in body armor are allowing individuals to survive blast exposures that were previously lethal. While there is a considerable and growing body of evidence that repetitive TBI produces a neurodegenerative tauopathy (Blennow et al., 2012). The data on neurodegeneration and tauopathy following a single blast exposure is much more limited. Reliable, reproducible and realistic animal models of blast exposure and other forms of TBI are urgently needed if we are to understand and ultimately treat or prevent these conditions. We have confronted the difficulties in establishing an animal model of human blast-induced TBI head-on by examining the biochemical response of wild type mice to a range of shockwave intensities and different exposure conditions. The experience we gained from this effort has contributed to the collective effort of the TBI research community to developing effective methodologies with which to study this phenomenon. This experience together with our investment in validating methods for biochemical and behavioral analysis of shockwave exposed mice has also positioned us to test our original hypotheses regarding the role of PP2A and tau phosphorylation in the behavioral and cognitive impairments that can result from blast-induced TBI. A previously unforeseen outcome of this analysis and our use of PME-1 over expressing mice may be the identification of a genetically sensitized background for studying the relationships between shockwave exposure, tau phosphorylation and behavioral impairment.

REFERENCES:

Ballatore, C., Lee, V.M., and Trojanowski, J.Q. (2007). Tau-mediated neurodegeneration in Alzheimer's disease and related disorders. Nat Rev Neurosci *8*, 663-672.

Blennow, K., Hardy, J., and Zetterberg, H. (2012). The neuropathology and neurobiology of traumatic brain injury. Neuron *76*, 886-899.

Bowen, I.G., Fletcher, E.R., Richmond, D.R., Hirsch, F.G., and White, C.S. (1968). Biophysical mechanisms and scaling procedures applicable in assessing

responses of the thorax energized by air-blast overpressures or by nonpenetrating missiles. Annals of the New York Academy of Sciences *152*, 122-146.

Clausen, F., Hanell, A., Israelsson, C., Hedin, J., Ebendal, T., Mir, A.K., Gram, H., and Marklund, N. (2011). Neutralization of interleukin-1beta reduces cerebral edema and tissue loss and improves late cognitive outcome following traumatic brain injury in mice. Eur J Neurosci *34*, 110-123.

Damon, E.G., Richmond, D.R., and White, C.S. (1966). Effects of ambient pressure on the tolerance of mice to air blast. Aerospace medicine *37*, 341-347.

Dekosky, S.T., Blennow, K., Ikonomovic, M.D., and Gandy, S. (2013). Acute and chronic traumatic encephalopathies: pathogenesis and biomarkers. Nature reviews Neurology *9*, 192-200.

Francis, Y.I., Fa, M., Ashraf, H., Zhang, H., Staniszewski, A., Latchman, D.S., and Arancio, O. (2009). Dysregulation of histone acetylation in the APP/PS1 mouse model of Alzheimer's disease. J Alzheimers Dis *18*, 131-139.

Goldstein, L.E., Fisher, A.M., Tagge, C.A., Zhang, X.L., Velisek, L., Sullivan, J.A., Upreti, C., Kracht, J.M., Ericsson, M., Wojnarowicz, M.W.*, et al.* (2012). Chronic traumatic encephalopathy in blast-exposed military veterans and a blast neurotrauma mouse model. Science translational medicine *4*, 134ra160.

Huber, B.R., Meabon, J.S., Martin, T.J., Mourad, P.D., Bennett, R., Kraemer, B.C., Cernak, I., Petrie, E.C., Emery, M.J., Swenson, E.R.*, et al.* (2013). Blast exposure causes early and persistent aberrant phospho- and cleaved-tau expression in a murine model of mild blast-induced traumatic brain injury. J Alzheimers Dis *37*, 309-323.

Lewis, J., Dickson, D.W., Lin, W.L., Chisholm, L., Corral, A., Jones, G., Yen, S.H., Sahara, N., Skipper, L., Yager, D.*, et al.* (2001). Enhanced neurofibrillary degeneration in transgenic mice expressing mutant tau and APP. Science *293*, 1487-1491.

Mairet-Coello, G., Courchet, J., Pieraut, S., Courchet, V., Maximov, A., and Polleux, F. (2013). The CAMKK2-AMPK kinase pathway mediates the synaptotoxic effects of Abeta oligomers through Tau phosphorylation. Neuron *78*, 94-108.

Marklund, N., and Hillered, L. (2011). Animal modelling of traumatic brain injury in preclinical drug development: where do we go from here? British journal of pharmacology *164*, 1207-1229.

Martin, L., Latypova, X., Wilson, C.M., Magnaudeix, A., Perrin, M.L., and Terro, F. (2013). Tau protein phosphatases in Alzheimer's disease: the leading role of PP2A. Ageing research reviews *12*, 39-49.

McKee, A.C., Stein, T.D., Nowinski, C.J., Stern, R.A., Daneshvar, D.H., Alvarez, V.E., Lee, H.S., Hall, G., Wojtowicz, S.M., Baugh, C.M.*, et al.* (2012). The spectrum of disease in chronic traumatic encephalopathy. Brain.

Milman, A., Zohar, O., Maayan, R., Weizman, R., and Pick, C.G. (2008). DHEAS repeated treatment improves cognitive and behavioral deficits after mild traumatic brain injury. Eur Neuropsychopharmacol *18*, 181-187.

Perez, M., Moran, M.A., Ferrer, I., Avila, J., and Gomez-Ramos, P. (2008). Phosphorylated tau in neuritic plaques of APP(sw)/Tau (vlw) transgenic mice and Alzheimer disease. Acta Neuropathol *116*, 409-418.

Perez, M., Ribe, E., Rubio, A., Lim, F., Moran, M.A., Ramos, P.G., Ferrer, I., Isla, M.T., and Avila, J. (2005). Characterization of a double (amyloid precursor protein-tau) transgenic: tau phosphorylation and aggregation. Neuroscience *130*, 339-347.

Puzzo, D., Privitera, L., Leznik, E., Fa, M., Staniszewski, A., Palmeri, A., and Arancio, O. (2008). Picomolar amyloid-beta positively modulates synaptic plasticity and memory in hippocampus. J Neurosci *28*, 14537-14545.

Rhein, V., Song, X., Wiesner, A., Ittner, L.M., Baysang, G., Meier, F., Ozmen, L., Bluethmann, H., Drose, S., Brandt, U.*, et al.* (2009). Amyloid-beta and tau synergistically impair the oxidative phosphorylation system in triple transgenic Alzheimer's disease mice. Proc Natl Acad Sci U S A *106*, 20057-20062.

Ribe, E.M., Perez, M., Puig, B., Gich, I., Lim, F., Cuadrado, M., Sesma, T., Catena, S., Sanchez, B., Nieto, M.*, et al.* (2005). Accelerated amyloid deposition, neurofibrillary degeneration and neuronal loss in double mutant APP/tau transgenic mice. Neurobiol Dis *20*, 814-822.

Richmond, D.R., Damon, E.G., Fletcher, E.R., Bowen, I.G., and White, C.S. (1968). The relationship between selected blast-wave parameters and the response of mammals exposed to air blast. Annals of the New York Academy of Sciences *152*, 103-121.

Roberson, E.D., Scearce-Levie, K., Palop, J.J., Yan, F., Cheng, I.H., Wu, T., Gerstein, H., Yu, G.Q., and Mucke, L. (2007). Reducing endogenous tau ameliorates amyloid beta-induced deficits in an Alzheimer's disease mouse model. Science *316*, 750-754.

Schwarzbold, M.L., Rial, D., De Bem, T., Machado, D.G., Cunha, M.P., dos Santos, A.A., dos Santos, D.B., Figueiredo, C.P., Farina, M., Goldfeder, E.M.*, et al.* (2010). Effects of traumatic brain injury of different severities on emotional, cognitive, and oxidative stress-related parameters in mice. J Neurotrauma *27*, 1883-1893.

Sents, W., Ivanova, E., Lambrecht, C., Haesen, D., and Janssens, V. (2013). The biogenesis of active protein phosphatase 2A holoenzymes: a tightly regulated process creating phosphatase specificity. The FEBS journal *280*, 644-661.

Shipton, O.A., Leitz, J.R., Dworzak, J., Acton, C.E., Tunbridge, E.M., Denk, F., Dawson, H.N., Vitek, M.P., Wade-Martins, R., Paulsen, O.*, et al.* (2011). Tau protein is required for amyloid {beta}-induced impairment of hippocampal long-term potentiation. J Neurosci *31*, 1688-1692.

Siopi, E., Llufriu-Daben, G., Fanucchi, F., Plotkine, M., Marchand-Leroux, C., and Jafarian-Tehrani, M. (2012). Evaluation of late cognitive impairment and anxiety states following traumatic brain injury in mice: the effect of minocycline. Neurosci Lett *511*, 110-115.

Tran, H.T., LaFerla, F.M., Holtzman, D.M., and Brody, D.L. (2011). Controlled cortical impact traumatic brain injury in 3xTg-AD mice causes acute intra-axonal amyloid-beta accumulation and independently accelerates the development of tau abnormalities. J Neurosci *31*, 9513-9525.

Tweedie, D., Milman, A., Holloway, H.W., Li, Y., Harvey, B.K., Shen, H., Pistell, P.J., Lahiri, D.K., Hoffer, B.J., Wang, Y.*, et al.* (2007). Apoptotic and behavioral sequelae of mild brain trauma in mice. J Neurosci Res *85*, 805-815.

Wang, Y., Wei, Y., Oguntayo, S., Wilkins, W., Arun, P., Valiyaveettil, M., Song, J., Long, J.B., and Nambiar, M.P. (2011). Tightly coupled repetitive blast-induced traumatic brain injury: development and characterization in mice. J Neurotrauma *28*, 2171-2183.

Wood, G.W., Panzer, M.B., Yu, A.W., Rafaels, K.A., Matthews, K.A., Bass, C.R. "Scaling in blast neurotrauma", 2013 Proceedings of the IRCOBI Conference, Gotenberg, Sweden.

Xiong, Y., Mahmood, A., and Chopp, M. (2013). Animal models of traumatic brain injury. Nat Rev Neurosci *14*, 128-142.

Yu, F., Wang, Z., Tchantchou, F., Chiu, C.T., Zhang, Y., and Chuang, D.M. (2012). Lithium ameliorates neurodegeneration, suppresses neuroinflammation, and improves behavioral performance in a mouse model of traumatic brain injury. J Neurotrauma *29*, 362-374.

SUPPORTING DATA:

Figure 1: Schematic of *in vivo* bTBI model consisting of shock tube and custom-designed mouse holder (left) and photo of assembled second shock tube (right).

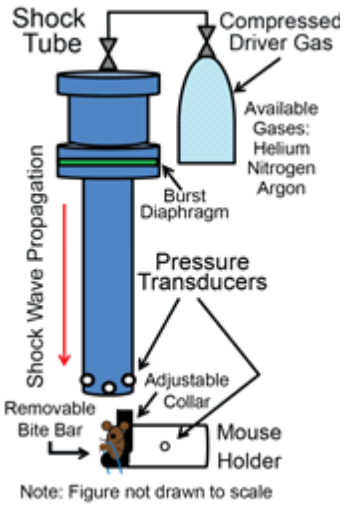

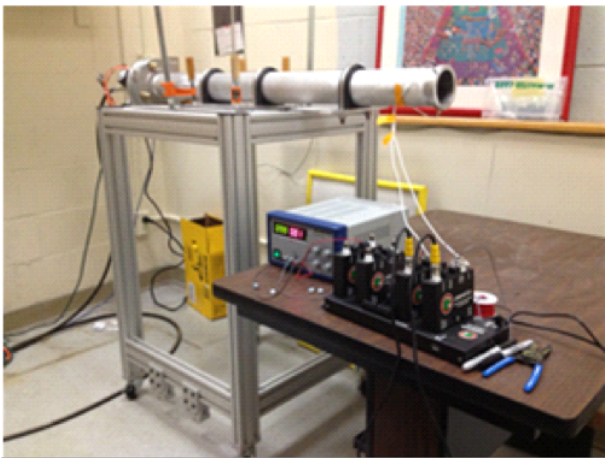

Figure 2: Shock wave recorded in the open-tube configuration with biomechanical injury parameters including a peak overpressure of 230 kPa, duration of 0.56 ms, and impulse of 45 kPa*ms.

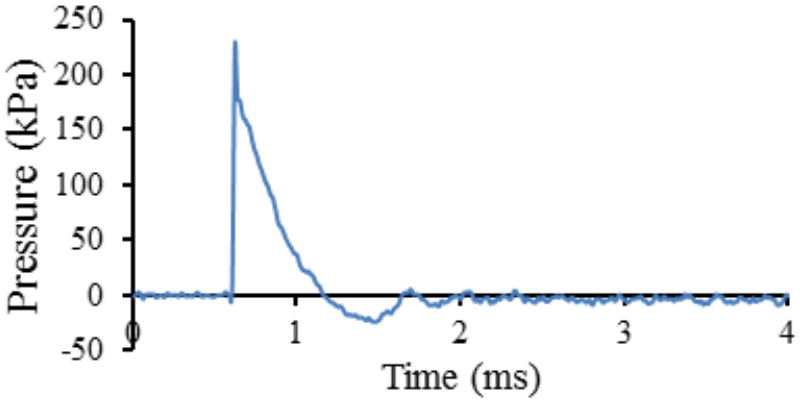

Figure 3: Image of mouse placed in our specially constructed animal holder. The head protrudes from the tube and is supported by a padded chin rest, which can be rotated to the side and used in conjunction with a nose piece to immoblize the head during blast exposure. The body of the animal is shielded by the tube and the head is positioned directly at the exit of the shock tube on the left.

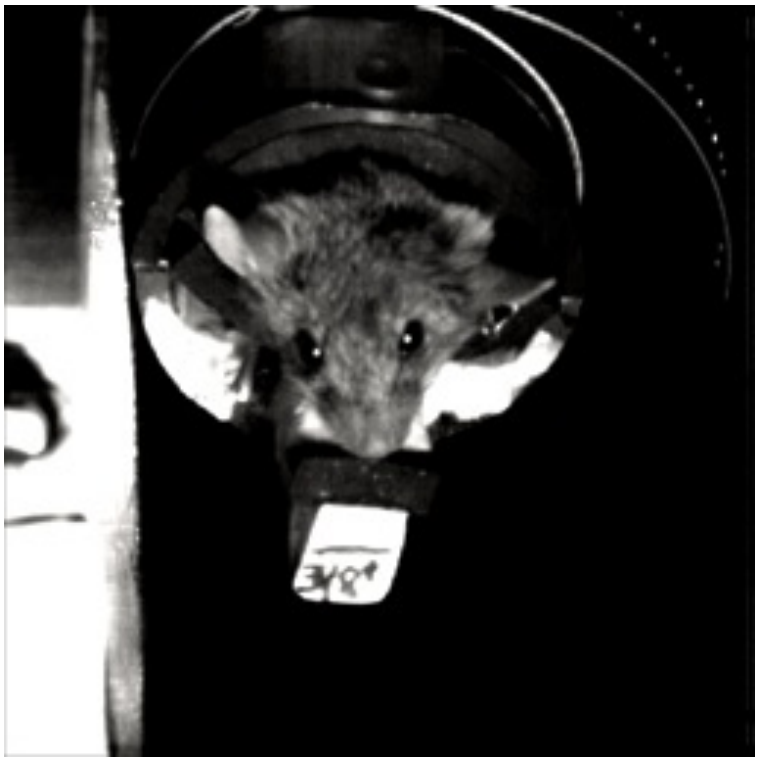

Figure 4A. Quantitative western blot analysis of phospho-tau levels in ipsilateral cortex of wild type mice exposed to shockwave in the unrestrained head configuration. Upper panels show representative images of western blots used to determine levels phosphorylated and total tau. Lanes are samples from unique individuals and antibodies are indicated at left with corresponding images of loading control beneath each. Signals in each lane were normalized to the loading control and mean values +/- SEM for each group and are expressed as percent of control in the graph at the bottom.

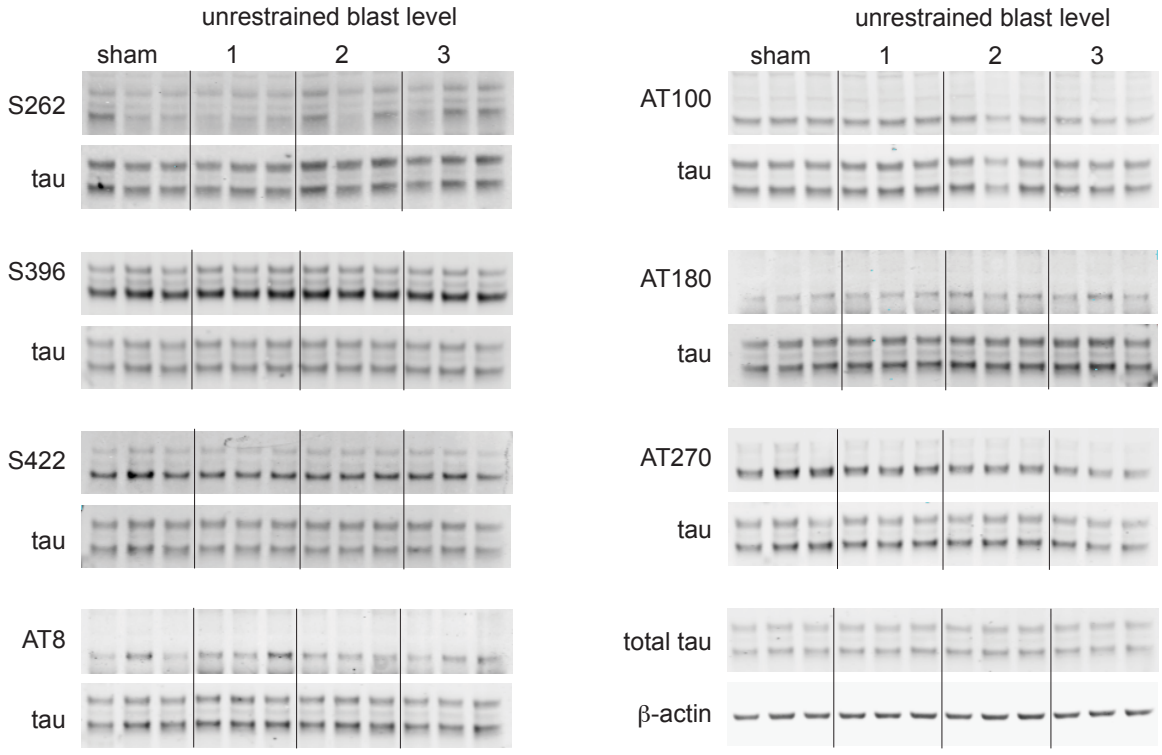
unrestrained blast level
sham
1
2
3
S262
tau
S396
tau
S422
tau
AT8
tau
unrestrained blast level
sham
1
2
3
AT100
tau
AT180
tau
AT270
tau
total tau
β-actin

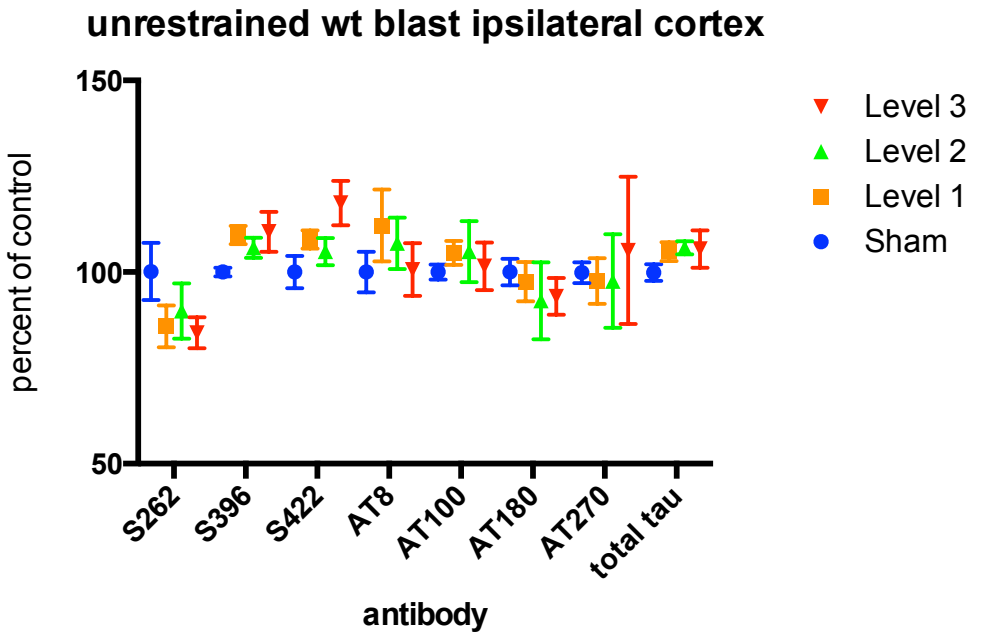
unrestrained wt blast ipsilateral cortex
percent of control
150
100
50
S262
S396
S422
AT8
AT100
AT180
AT270
total tau
antibody
Level 3
Level 2
Level 1
Sham

Figure 4B. Quantitative western blot analysis of phospho-tau levels in ipsilateral cortex of wild type mice exposed to shockwave in the restrained head configuration.

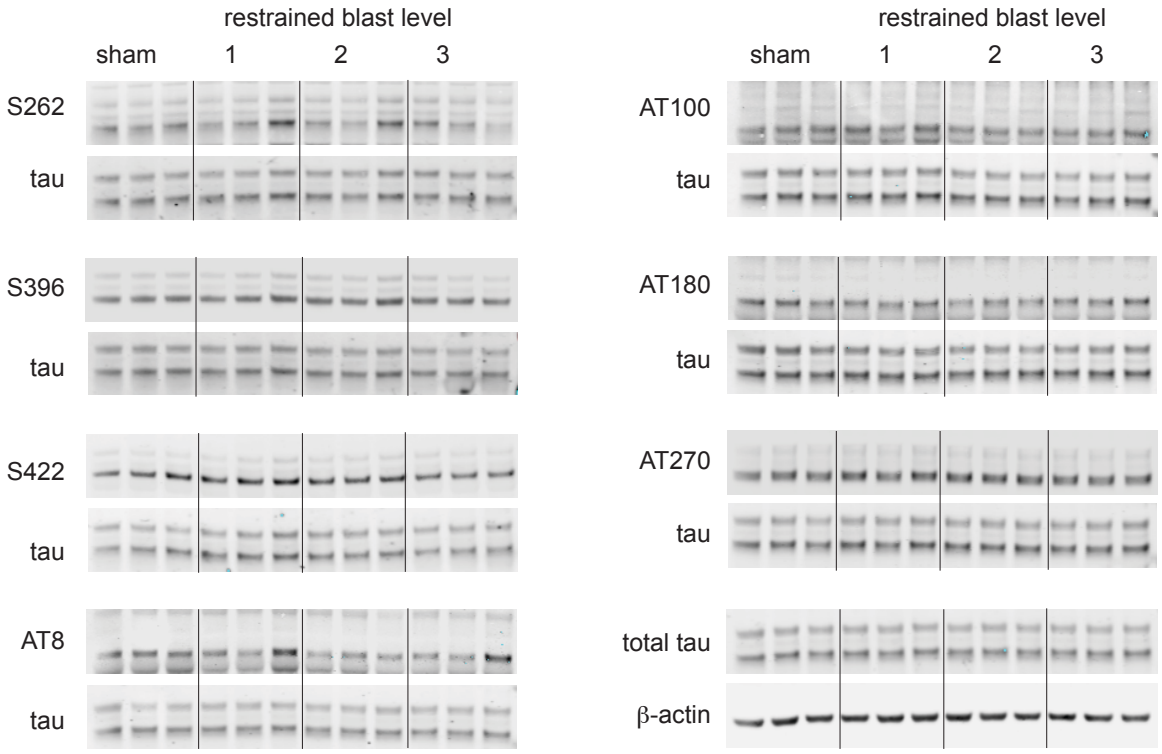

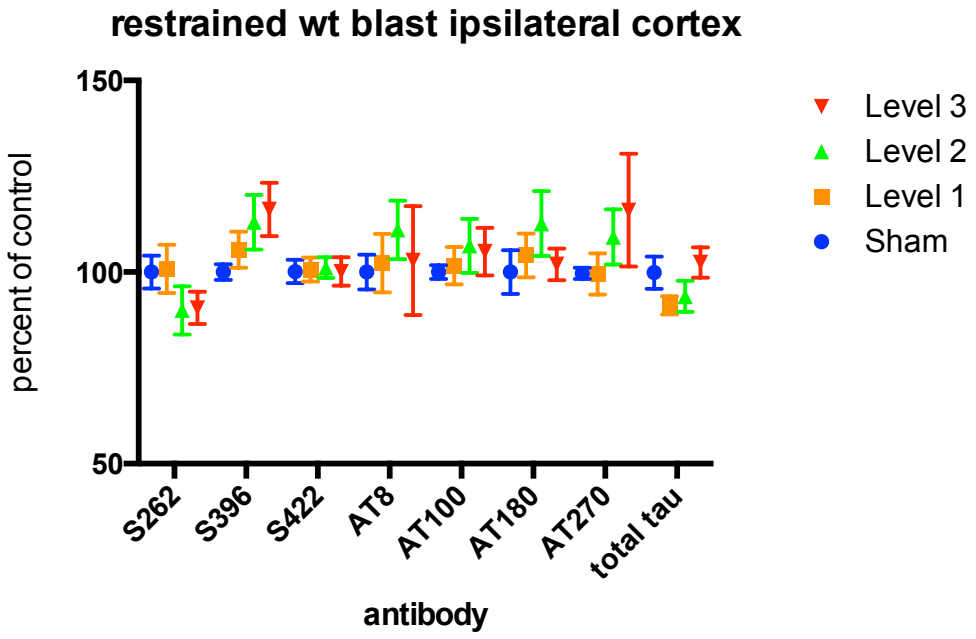

Figure 5. Quantitative western blot analysis of phospho-tau levels in hippocampal homogenates from naive PME-1 over expressing mice. Blots loaded with independent samples from PME-1 over expressing animals (tetO-PME/CaMKtTA) or control animals (tetO-PME and CaMKtTA) were probed simultaneously with the phospho-tau specific antibodies indicated and an antibody to total tau as a loading control. In the case of total measures, an anti-β-actin antibody was used as a loading control. Signals in each lane were normalized to the loading control and mean values +/- SEM for each group are expressed as percent of control in the graph at the bottom. Asterix indicates statistically significant difference between PME-1 over expressing animals and controls (T-test, $p<0.05$).

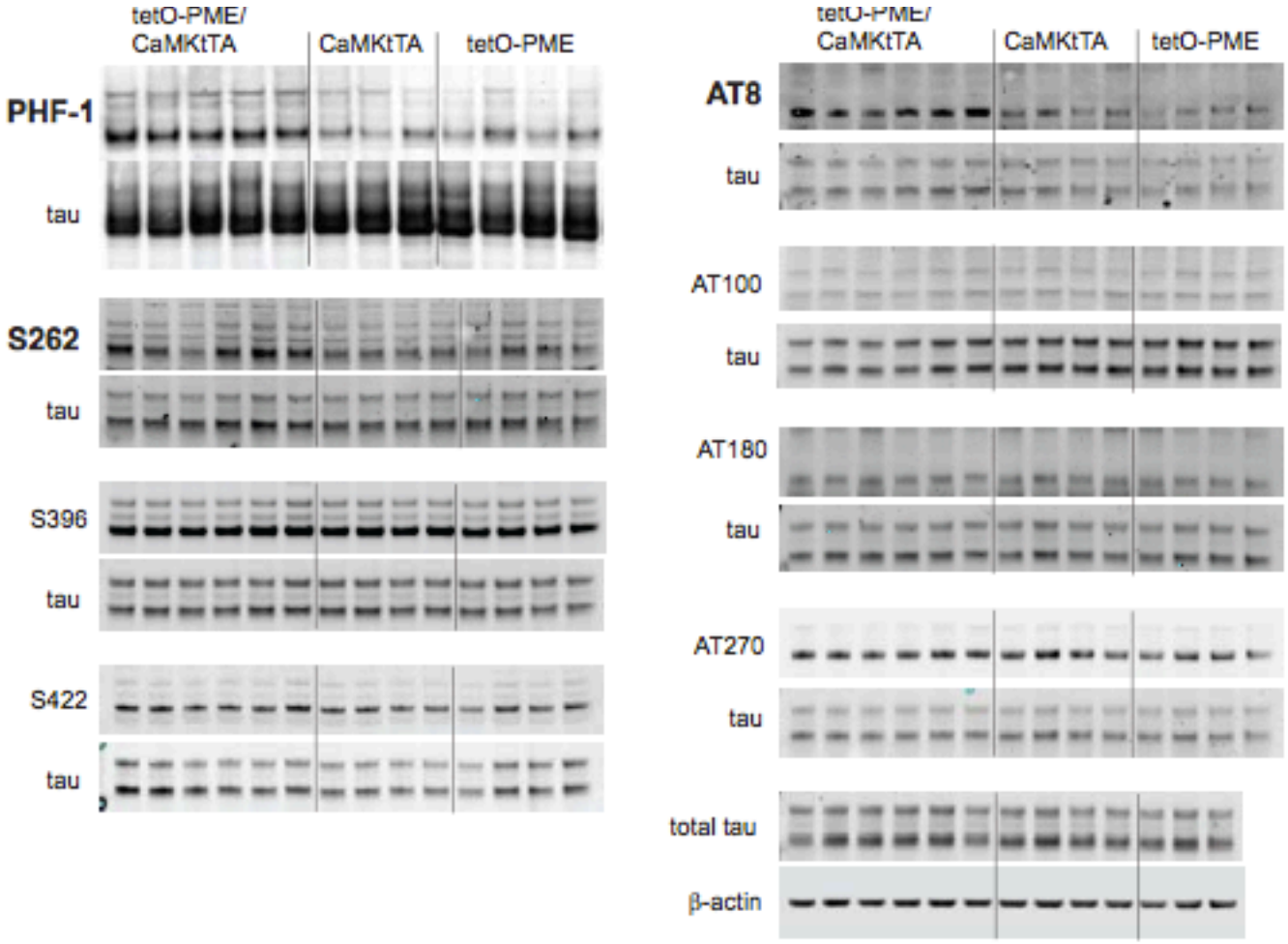
tetO-PME/
CaMKtTA
CaMKtTA
tetO-PME
PHF-1
tau
S262
tau
S396
tau
S422
tau
AT8
tau
AT100
tau
AT180
tau
AT270
tau
total tau
β-actin

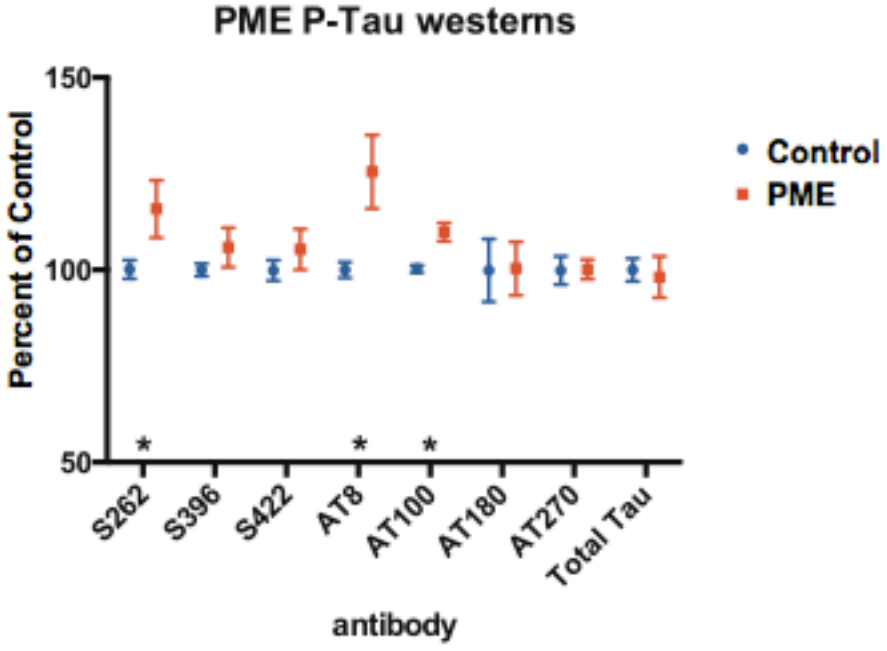
PME P-Tau westerns
Percent of Control
150
100
50
Control
PME
S262
S396
S422
AT8
AT100
AT180
AT270
Total Tau
antibody

Figure 6. Graph of the performance (latency to fall) of a cohort of 16 control animals was tested on a rotarod apparatus. Animals were subjected to 3 training trials on each of 3 successive days and then to 3 additional trials on a fourth day 1 week after the third training day.

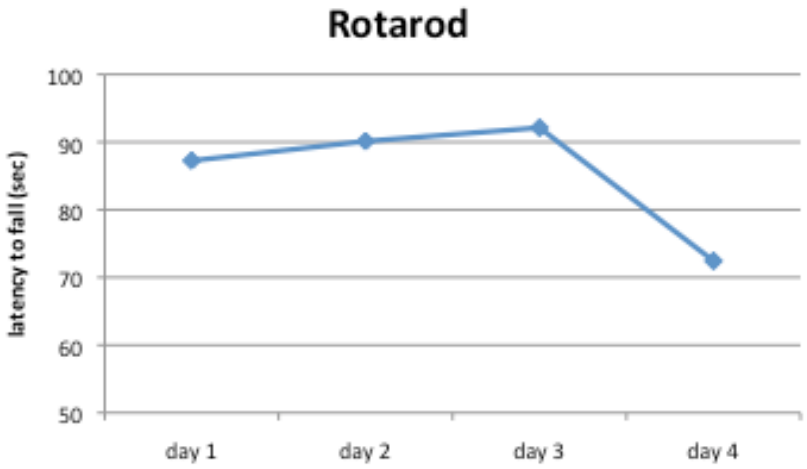

Figure 7. Behavioral analysis of a cohort of 16 control animals during exposure to a novel open field environment. Behavior assessed by calculating the percent of time spent in the center (>10 cm from the wall) (left), and total distance moved (right) during each 5 minute block of a single 30 minute exposure.

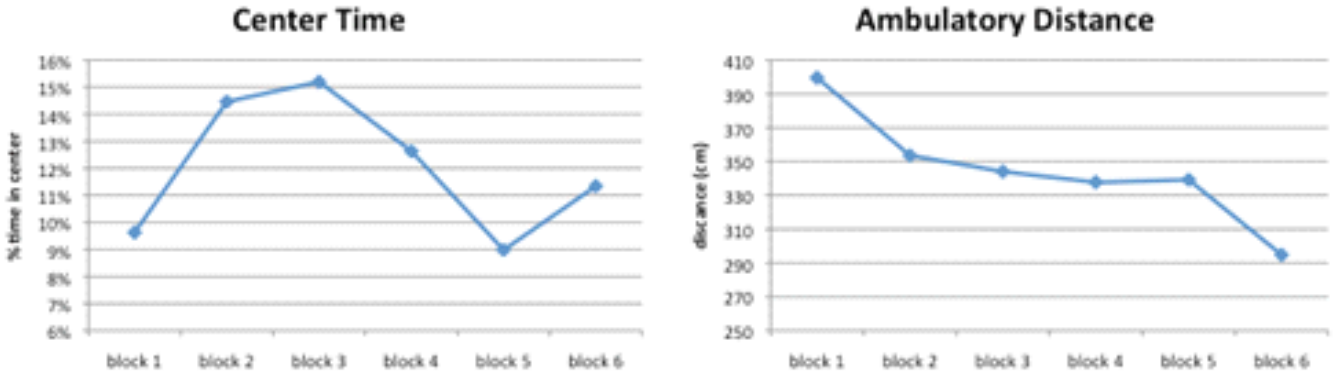

Figure 8. Behavioral analysis of a cohort of 16 control animals during a forced swim task. Graph shows average time spent immobile during each one-minute block of a single 5-minute exposure.

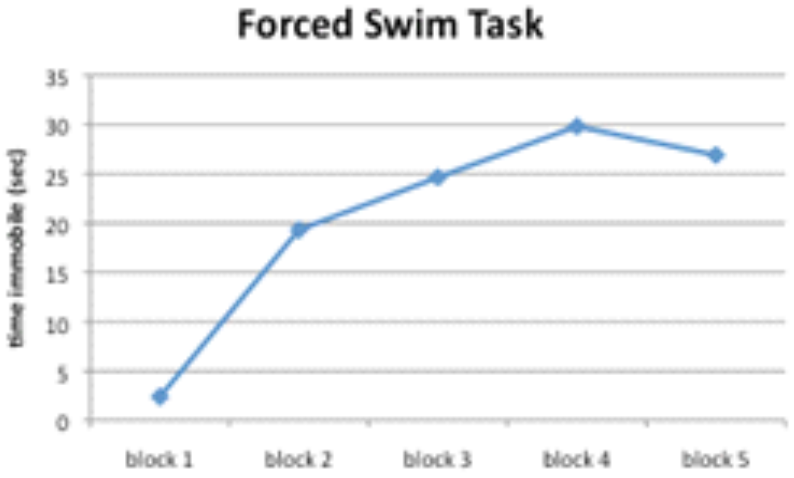

Figure 9. Behavioral performance in a radial arm water maze task. A group of 16 control animals were trained on a radial arm water maze task and the number of incorrect arm entries were scored (left). Another group of 6 animals was tested on a version of the task where training during day 1 included only 2, rather than the typical 7 visible platform training trials.

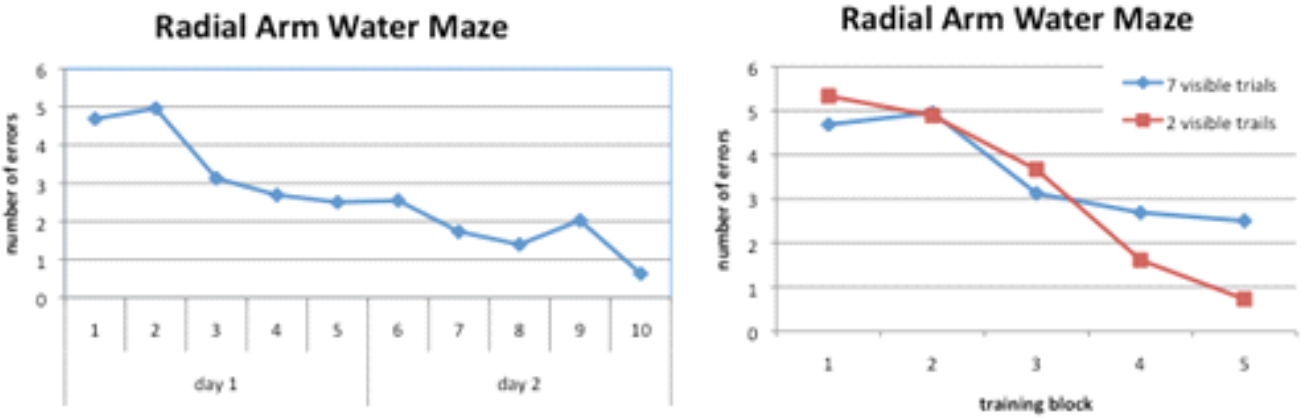

Figure 10. Behavioral analysis of a cohort of 16 control animals during a tail suspension task. Graph shows average time spent immobile during each one-minute block of a single 5-minute exposure.

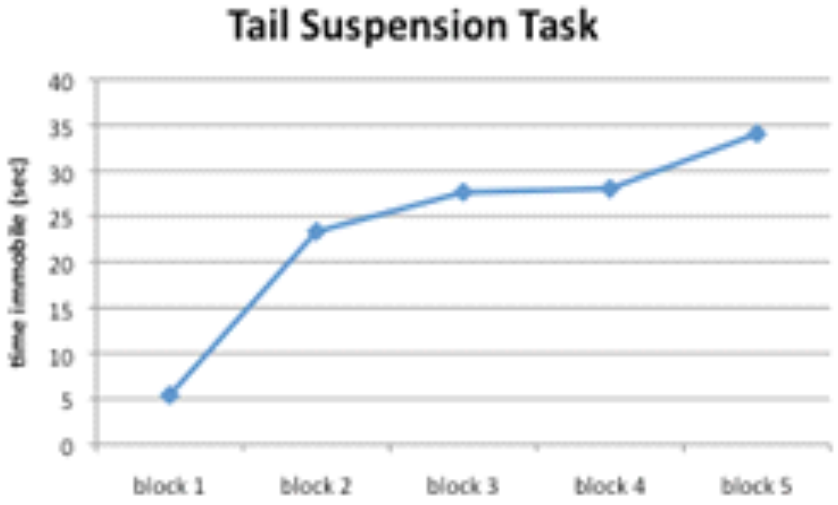

Figure 12. Sensory threshold assessment in a cohort of 16 control mice. Animals were also placed in a fear conditioning apparatus. The response of each animal (first visible response, first gross motor response, and first vocalization) to increasing foot shock intensities was recorded.

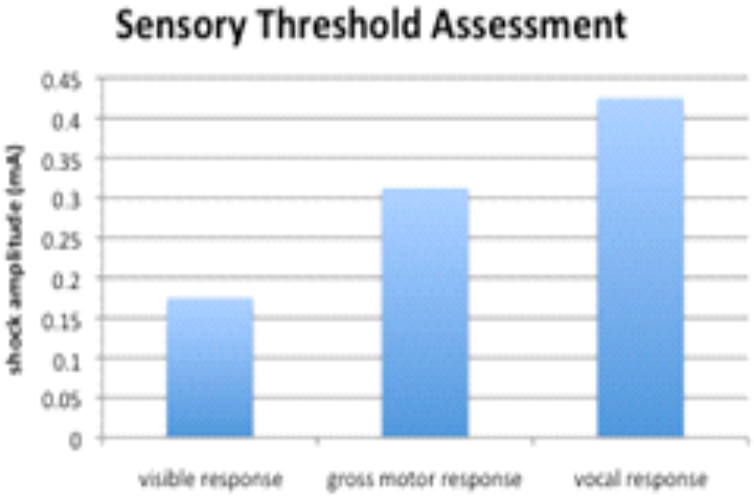

Figure 13. Graph of the performance of 16 control animals was assessed in a visible platform water maze task. Animals were placed in a water maze apparatus containing a visibly marked escape platform. Shown is the average latency to reach the platform for each of 4 x 2 trial training blocks conducted over the course of two days.

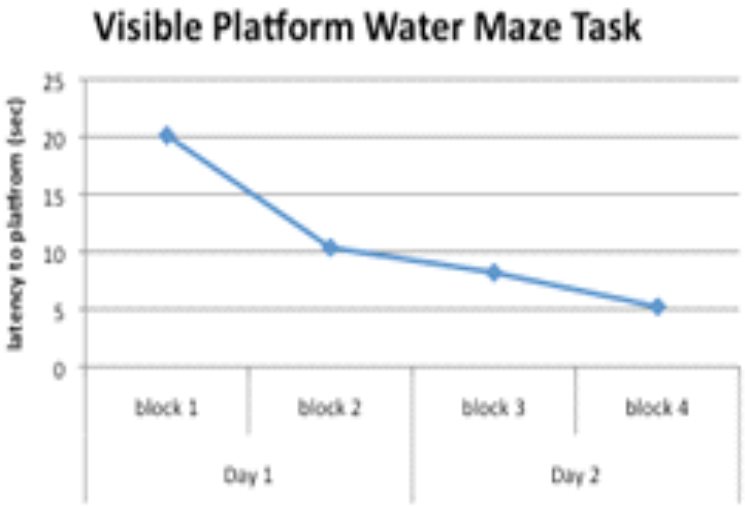

Figure 14. Western blots on hippocampal and cortical homogenates from shockwave and sham exposed animals simultaneously double labeled with the antibodies indicated (AT8/total tau, AT270/total tau, beta-actin/total tau). Order of lanes is as follows: 1,2 homogenates harvested at 1 hr from shockwave exposed animals, 3,4 homogenates harvested at 1 hr from sham exposed animals, 5,6 homogenates harvested at 24 hr from shockwave exposed animals, 7,8 homogenates harvested at 24 hr from sham exposed animals. Graphs of average band intensity for each treatment normalized to either total tau or beta-actin as a loading control are shown at right together with positive control blots comparing signals obtained from homogenates of hippocampi from wild type and tau P310L transgenic mice.

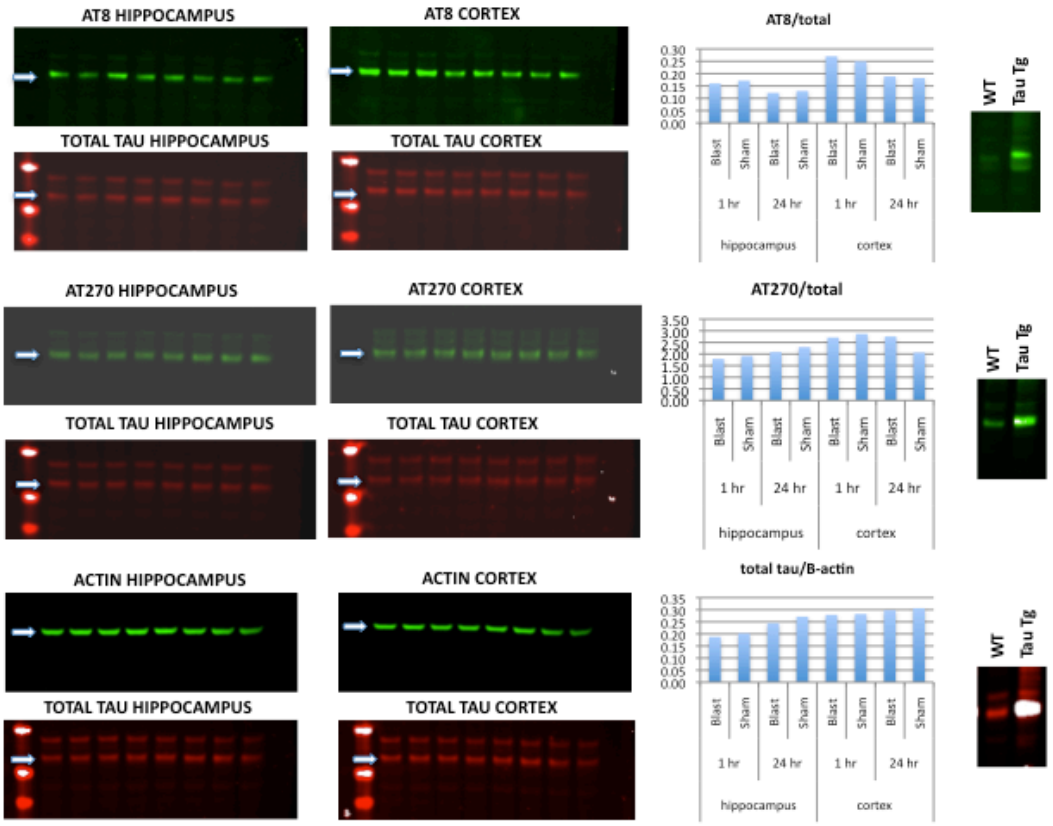

Figure 15. Representative images of perfused paraffin embedded brain sections from shockwave exposed and non-exposed mice stained with either phospho-specific tau antibody AT8 (upper) or an antibody recognizing all forms of tau (lower).

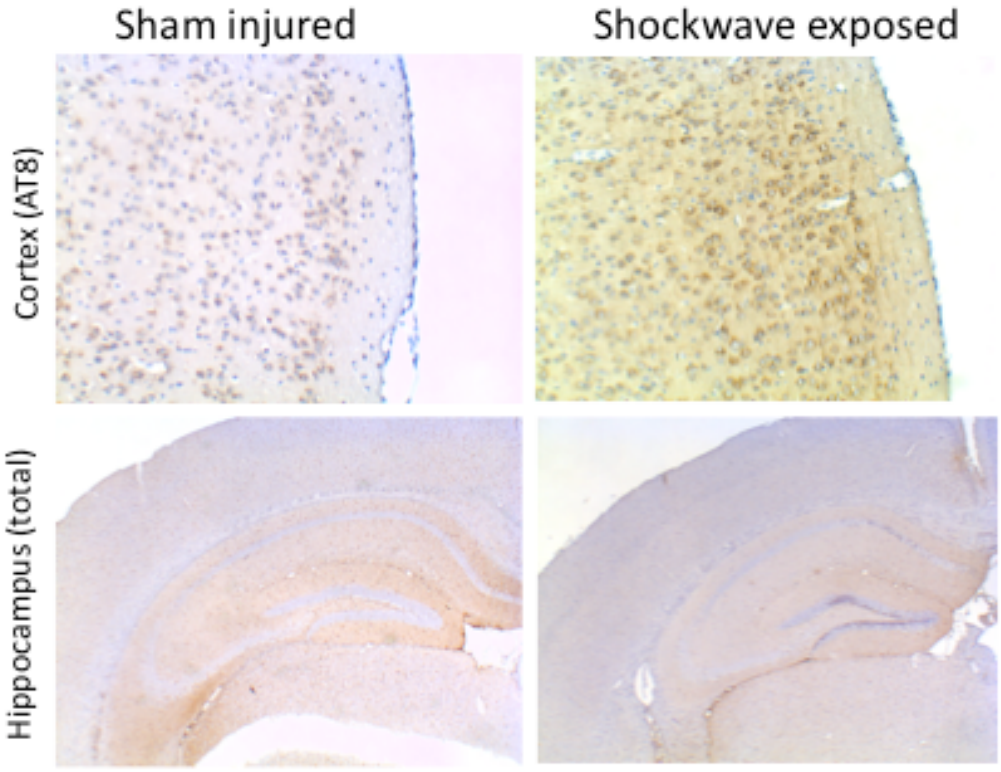

Figure 16. Representative images of perfused paraffin embedded brain sections from a tau P301L transgenic animal and wild type control stained with either phospho-specific tau antibody AT8 (upper) or an antibody recognizing all forms of tau (lower). Upper panels show staining in cortex whie lower panels show staining in hippocampus and adjacent structures.

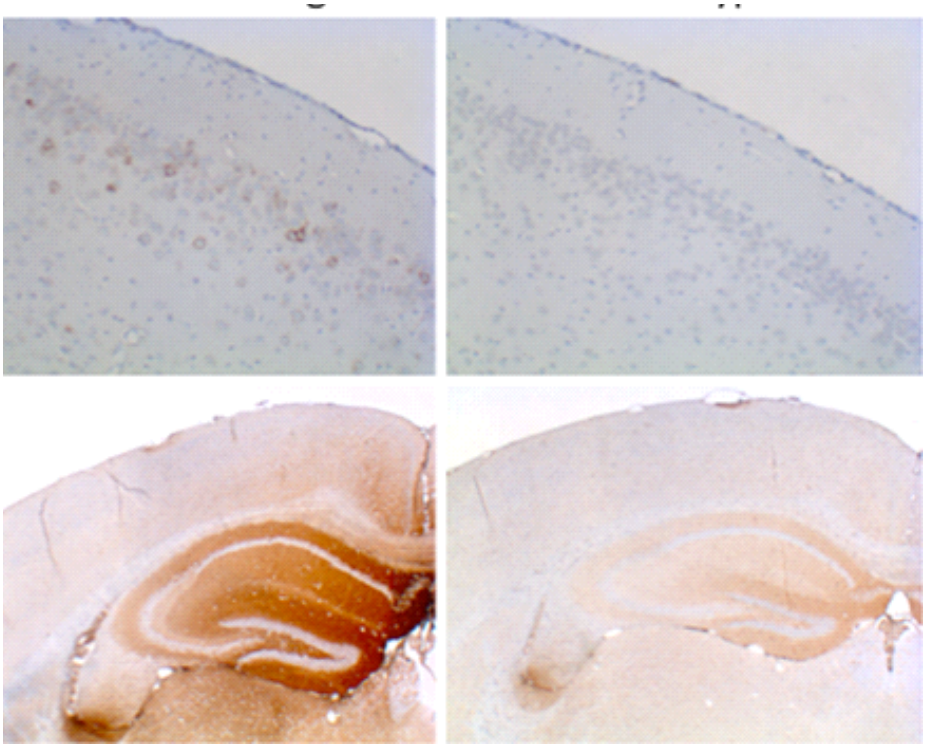

Figure 17. Results of ELISA measurements of total tau in CSF taken from shockwave and sham exposed mice at 1 and 24 hours after injury. Graph at left shows signal intensities obtained at each indicated concentration of a known standard. Graph at right shows signals obtained from CSF samples from each of two animals (A and B) for each treatment/timepoint examined.

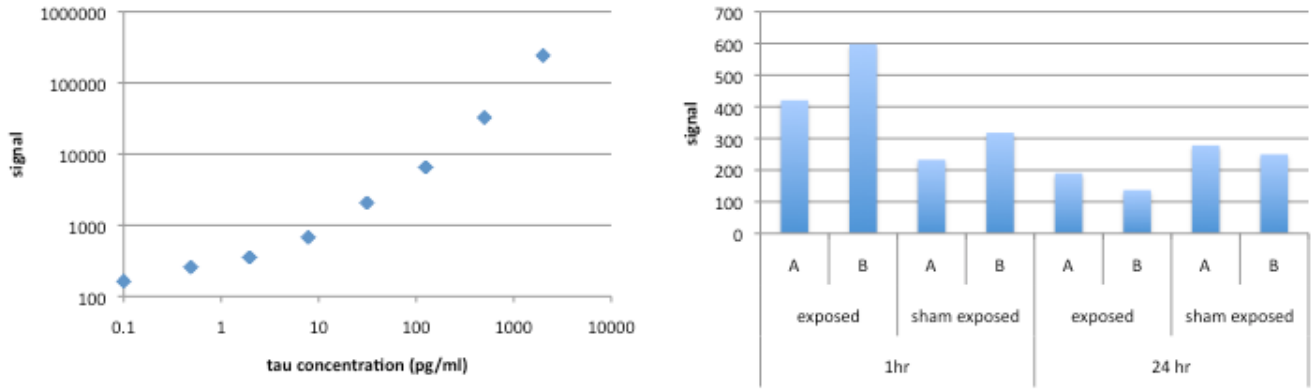

Figure 18. Quantitative western blot analysis of phospho-tau levels in hippocampal homogenates from naive LCMT-1 over expressing mice. Blots loaded with independent samples from individual LCMT-1 over expressing animals (tetO-LCMT/CaMKtTA) or controls (tetO-LCMT and CaMKtTA) were probed simultaneously with the phospho-tau specific antibodie indicated and an antibody recognizing total tau as a loading control. In the case of total measures, an anti-β-actin antibody was used as a loading control. Signals in each lane were normalized to the loading control and mean values +/- SEM for each group are expressed as percent of control in the graph at the bottom.

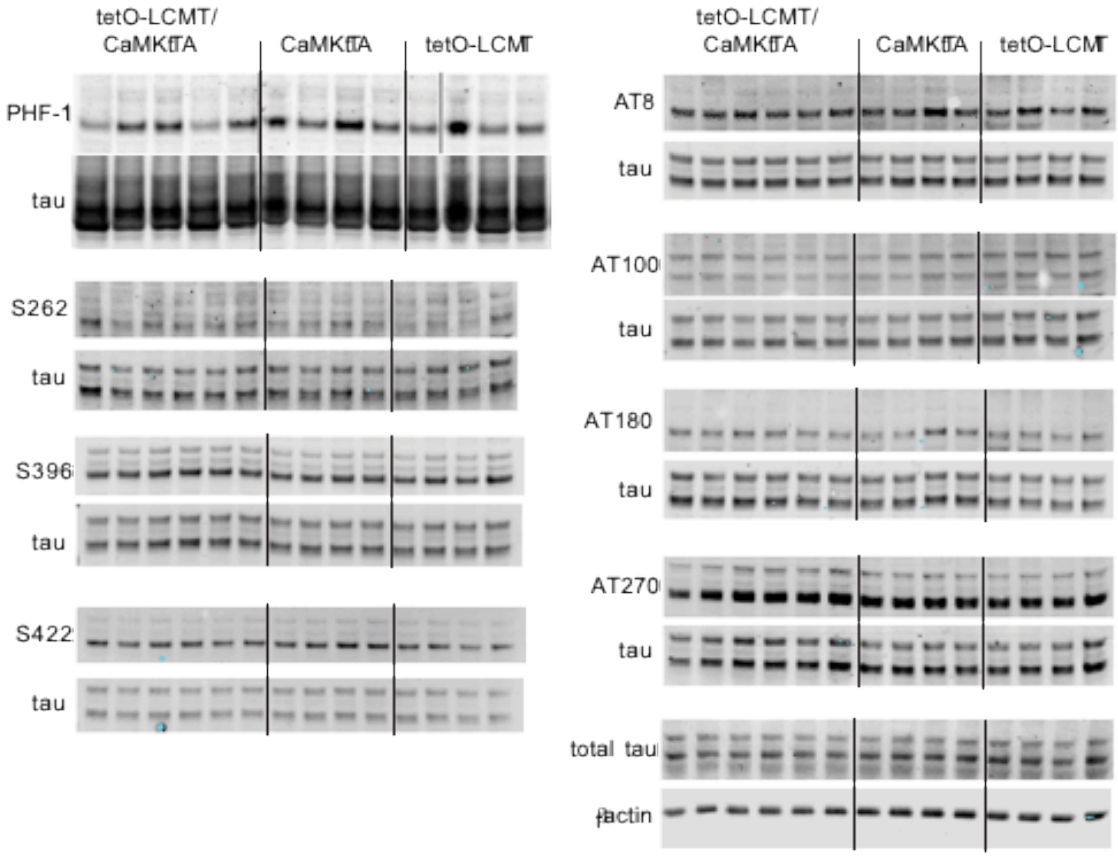
tetO-LCMT/
CaMKIIA
CaMKIIA
tetO-LCMT
PHF-1
tau
S262
tau
S396
tau
S422
tau
tetO-LCMT/
CaMKIIA
CaMKIIA
tetO-LCMT
AT8
tau
AT100
tau
AT180
tau
AT270
tau
total tau
β-actin

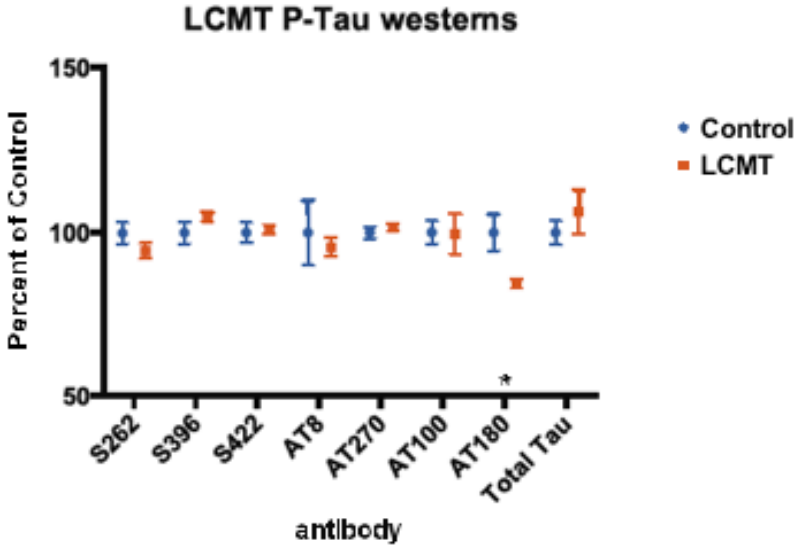
LCMT P-Tau westerns
Percent of Control
150
100
50
Control
LCMT
S262
S396
S422
AT8
AT270
AT100
AT180
Total Tau
antibody

APPENDICES:

Appendix 1:

Title: The role of PP2A methylation in beta-amyloid sensitivity and resistance.

Authors:
Russell E. Nicholls, Jean-Marie Sontag, Hong Zhang, Agnieszka Staniszewski, Caitlin M. Woodruff, Michael Yim, Erland Arning, Brandi Wasek, Carla Y. Kim, Deqi Yin, Teodoro Bottiglieri, Estelle Sontag, Eric R. Kandel, and Ottavio Arancio

Abstract:
Elevated levels of homocysteine and impaired methyl-donor metabolism have been linked to increased Alzheimer's disease (AD) risk in humans and increased AD-related pathology in cell and animal models. The substrate specificity of the serine/threonine phosphatase, PP2A, is regulated by site-specific methylation, and misregulated PP2A activity has been suggested to mediate the effects of impaired methyl-donor metabolism on AD development. To test this link, we generated transgenic mice that over express the PP2A methylesterase, PME-1 or the PP2A methyl transferase, LCMT-1, and examined the effects of these manipulations on the physiological and behavioral impairments caused by acute exposure to oligomeric beta-amyloid (Aβ). Over expression of PME-1 reduced PP2A methylation and sensitized animals to physiological and behavioral impairments caused by acute application of Aβ oligomer. PME-1 over expression increased both the LTP impairment caused by sub threshold doses of Aβ as well as Aβ-induced cognitive impairments in a radial arm water maze and a contextual fear conditioning task. Conversely, LCMT-1 over expression increased PP2A methylation and reduced Aβ-induced physiological and behavioral impairments. These data support a role for reduced PP2A methylation in increasing AD risk and suggest potential therapeutic actions for increased PP2A methylation in the treatment or prevention of AD.

Affiliations:
Russell E. Nicholls: Department of Pathology, Columbia University, Taub Institute for Research on Alzheimer's Disease and Aging Brain, New York, NY 10032, USA.
Jean-Marie Sontag: School of Biomedical Sciences and Pharmacy, University of Newcastle, Callaghan, NSW 2308, Australia.
Hong Zhang: Department of Pathology, Columbia University, Taub Institute for Research on Alzheimer's Disease and Aging Brain, New York, NY 10032, USA.
Agnieszka Staniszewski: Department of Pathology, Columbia University, Taub Institute for Research on Alzheimer's Disease and Aging Brain, New York, NY 10032, USA.
Caitlin M. Woodruff: Department of Neuroscience, College of Physicians and Surgeons, Columbia University, 1051 Riverside Drive, New York, NY 10032, USA.
Michael Yim: Department of Neuroscience, College of Physicians and Surgeons, Columbia University, 1051 Riverside Drive, New York, NY 10032, USA.

Erland Arning: Baylor University Medical Center, Institute of Metabolic Disease, Dallas, TX 75226, USA.
Brandi Wasek: Baylor University Medical Center, Institute of Metabolic Disease, Dallas, TX 75226, USA.
Carla Kim: Department of Neuroscience, College of Physicians and Surgeons, Columbia University, 1051 Riverside Drive, New York, NY 10032, USA.
Deqi Yin: Department of Neuroscience, College of Physicians and Surgeons, Columbia University, 1051 Riverside Drive, New York, NY 10032, USA.
Teodoro Bottiglieri: Baylor University Medical Center, Institute of Metabolic Disease, Dallas, TX 75226, USA.
Estelle Sontag: School of Biomedical Sciences and Pharmacy, University of Newcastle, Callaghan, NSW 2308, Australia.
Eric R. Kandel: Department of Neuroscience, College of Physicians and Surgeons, Columbia University Howard Hughes Medical Institute, and Kavli Institute for Brain Science, 1051 Riverside Drive, New York, NY 10032, USA.
Ottavio Arancio: Department of Pathology, Columbia University, Taub Institute for Research on Alzheimer's Disease and Aging Brain, New York, NY 10032, USA.

Appendix 2:

Theme: A Alzheimer's Disease (AD) & Prodromal AD
Topic: 2 Cell, Molecular & Systems Biology
Subtopic: 2.y other

Title: The role of PP2A methylation in beta-amyloid sensitivity and resistance.

Author(s): **R.E. Nicholls**[1], J.-M. Sontag[2], H. Zhang[1], A. Staniszewski[1], C.M. Woodruff[3], M. Yim[3], E. Arning[4], B. Wasek[4], C. Kim[3], D. Yin[3], T. Bottiglieri[4], E. Sontag[2], E.R. Kandel[3,5,6], O. Arancio[1]

Institute(s): [1]Taub Institute for Research on Alzheimer's Disease and the Aging Brain and Department of Pathology and Cell Biology, Columbia University, New York, NY, USA, [2]School of Biomedical Sciences and Pharmacy, University of Newcastle, Callaghan, NSW, Australia, [3]Department of Neuroscience, College of Physicians and Surgeons, Columbia University, New York, NY, [4]Institute of Metabolic Disease, Baylor Research Institute, Dallas, TX, [5]Howard Hughes Medical Institute, [6]Kavli Institute for Brain Science, Columbia University, New York, NY, USA

Text: **Objectives:** Elevated levels of homocysteine and impaired methyl-donor metabolism have been linked to increased Alzheimer´s disease (AD) risk in humans and increased AD-related pathology in cell and animal models. We sought to examine the role of PP2A methylation in mediating these effects.

Methods: To do this, we generated transgenic mice that over express the PP2A methylesterase, PME-1 or the PP2A methyl transferase, LCMT-1, and examined the effects of these manipulations on the physiological and behavioral impairments caused by acute exposure to oligomeric beta-amyloid (Aβ).

Results: Over expression of PME-1 reduced PP2A methylation and sensitized animals to physiological and behavioral impairments caused by acute application of Aβ oligomer. PME-1 over expression increased both the LTP impairment caused by sub-threshold doses of Aβ as well as Aβ-induced cognitive impairments in a radial arm water maze and a contextual fear conditioning task. Conversely, LCMT-1 over expression reduced Aβ-induced physiological and behavioral impairments.

Conclusions: These data support a role for reduced PP2A methylation in increasing AD risk and suggest potential therapeutic actions for increased PP2A methylation in the treatment or prevention of AD.

Author Keywords: phosphatase, PP2A, methylation, A-beta sensitivity, PME-1, LCMT-1

Appendix 3:

Title: PP2A methylation controls sensitivity and resistance to beta-amyloid induced behavioral and physiological impairments.

Authors: R.E. Nicholls[1], J.-M. Sontag[2], H. Zhang[1], A. Staniszewski[1], C.M. Woodruff[3], M. Yim[3], E. Arning[4], B. Wasek[4], C. Kim[3], D. Yin[3], T. Bottiglieri[4], E. Sontag[2], E.R. Kandel[3,5,6], O. Arancio[1]

Affiliations: [1]Taub Institute for Research on Alzheimer's Disease and the Aging Brain and Department of Pathology and Cell Biology, Columbia University, New York, NY, USA, [2]School of Biomedical Sciences and Pharmacy, University of Newcastle, Callaghan, NSW, Australia, [3]Department of Neuroscience, College of Physicians and Surgeons, Columbia University, New York, NY, [4]Institute of Metabolic Disease, Baylor Research Institute, Dallas, TX, [5]Howard Hughes Medical Institute, [6]Kavli Institute for Brain Science, Columbia University, New York, NY, USA

Summary;
Elevated levels of homocysteine and impaired methyl-donor metabolism have been linked to increased Alzheimer's disease (AD) risk in humans and increased AD-related pathology in cell and animal models. The serine/threonine phosphatase, PP2A, is regulated by site-specific methylation, and misregulated PP2A activity has been proposed to mediate the effects of impaired methyl-donor metabolism on AD. To further examine the link between PP2A activity and AD, we generated transgenic mice that over express the PP2A methylesterase, PME-1 or the PP2A methyl transferase, LCMT-1, and found that PME-1 over expression enhanced, and LCMT-1 over expression reduced the physiological and behavioral impairments caused by acute oligomeric Aβ exposure. These transgenes were without effect on Aβ production or the response to physiological concentrations of Aβ, suggesting that they selectively affect the response of neurons to pathological Aβ levels. These data support a role for reduced PP2A methylation in increasing AD risk in hyperhomocysteinemic individuals and suggest potential therapeutic effects for increased PP2A methylation in AD treatment or prevention.

Running title (70 characters):
PP2A methylation and beta amyloid sensitivity

Highlights (up to 4 bullet points, 85 characters each):

- PP2A methylesterase over expression enhances Aβ–induced LTP and memory deficits.
- PP2A methyltransferase over expression reduces Aβ–induced LTP and memory deficits.
- PP2A methylesterase/transferase over expression alter Aβ sensitivity not production.

Introduction:

Alzheimer's disease (AD) is an incurable neurodegenerative disorder characterized by progressive dementia and the accumulation of extracellular aggregates of Aβ peptide in the brain. With the exception of rare dominantly inherited familial forms of AD (Tanzi, 2012), the disease is thought to result from a complex interaction of multiple genetic and environmental factors (reviewed in: (Chouliaras et al., 2010). Identifying the various factors that contribute to the development of AD and understanding the interactions among them is therefore critical to understanding and ultimately preventing or treating the disease.

Hyperhomocysteinemia is one of the risk factors thought to contribute to the development of AD. Elevated homocysteine levels in the blood or CSF of human subjects has been linked to an increased risk for AD (reviewed in : Zhuo et al., 2011 (Zhuo et al., 2011)), and this link between elevated levels of homocysteine and AD-like pathology or cognitive impairment has been reproduced in cell and animal models (Bernardo et al., 2007; Fuso et al., 2012b; Hasegawa et al., 2005; Kruman et al., 2002; Pacheco-Quinto et al., 2006; Rhodehouse et al., 2013; Sontag et al., 2007; Wei et al., 2011; Zhang et al., 2009; Zhuo et al., 2010; Zhuo and Pratico, 2010a, b). Several potential mechanisms have been proposed to explain the link between hyperhomocysteinemia and AD including oxidative stress, cerebrovascular damage, altered DNA methylation, Aβ elevation and tau protein phosphorylation (Fleming et al., 2012; Fuso et al., 2012a; Marlatt et al., 2008; Sontag et al., 2007; Sontag et al., 2008; Troen et al., 2008; Wei et al., 2011; Zhang et al., 2009; Zhuo et al., 2010). Homocysteine is a metabolite in the biochemical pathway that produces S-adenosly methionine, which acts as the donor for methylation reactions in the cell, so one of the consequences of hyperhomocysteinemia is impaired methylation (Schalinske and Smazal, 2012). Impaired methylation affects multiple processes in the brain including gene expression and the production of neurotransmitters, but one of the substrates for methylation that is thought to have particular relevance for hyperhomocysteinemia's influence on AD is protein phosphatase 2A (PP2A).

Several independent lines of evidence also suggest a role for PP2A in AD (reviewed in: (Braithwaite et al., 2012; Martin et al., 2013; Rudrabhatla and Pant, 2011)). Among these are a reduced level of PP2A activity in the post-mortem brains of AD patients (Gong et al., 1995; Gong et al., 1993; Sontag et al., 2004; Vogelsberg-Ragaglia et al., 2001) and the presence of AD-like pathology and cognitive deficits in PP2A-impaired animal models (Kins et al., 2001; Louis et al., 2011; Schild et al., 2006; Sun et al., 2003; Wang et al., 2010; Yin et al., 2010). PP2A is also the principal tau phosphatase, and tau hyperphosphorylation is also thought to play a critical role in AD (Martin et al., 2013). Manipulations that impair homocysteine metabolism both reduce PP2A methylation and increase tau phosphorylation suggesting that one of the ways that PP2A might link homocysteine metabolism to AD is via its action as a tau phosphatase (Nicolia et al., 2010; Sontag et al., 2007; Sontag et al., 2008; Yoon et al., 2007; Zhang et al., 2008).

Methylation regulates PP2A activity by controlling its subunit composition. The typical PP2A holoenzyme is a heterotrimer composed of a catalytic subunit, a structural subunit and a regulatory subunit that determines its substrate specificity (Janssens and Goris, 2001; Sents et al., 2013; Shi, 2009). Methylation of the C-terminal leucine residue of the catalytic subunit (Leu309) promotes the formation of isoforms containing the Bα regulatory subunit (Bryant et al., 1999; Janssens et al., 2008; Longin et al., 2007; Sontag

et al., 2007; Tolstykh et al., 2000; Yu et al., 2001), and Bα containing PP2A isoforms exhibit high tau phosphatase activity (Sontag et al., 1996; Sontag et al., 1999). PP2A methylation is catalyzed by a dedicated methylesterase and a dedicated methyltransferase (PME-1 and LCMT-1 in mouse respectively) via a mechanism that has been evolutionarily conserved from yeast to mammals (reviewed in: (Sents et al., 2013)). Over expression of PME-1 in cultured neuroblastoma cells causes a reduction in the level of methylated PP2A and a corresponding increase in phosphorylated tau and APP (Sontag et al., 2007). Conversely, LCMT-1 over expression in these cells causes increased PP2A methylation and reduced tau and APP phosphorylation (Sontag et al., 2007).

To examine the potential interaction between altered PP2A methylation and the propensity for AD-related impairments, we generated transgenic mice that over express either the PP2A methylesterase, PME-1, or the PP2A methyltransferase, LCMT-1, and compared their response to exogenous Aβ exposure. We found that reducing PP2A methylation through PME-1 over expression sensitized animals to the physiological and behavioral impairments caused by exposure to nanomolar concentrations of Aβ. We also found that LCMT-1 over expression exerted the opposite effect, protecting animals from the physiological and behavioral impairments caused by nanomolar Aβ exposure. Transgene expression did not affect baseline behavior or physiological responses, or physiological response to picomolar concentrations of Aβ, suggesting that PME-1 and LCMT-1 over expression in these animals selectively affect the response to pathological Aβ concentrations. Moreover, transgene expression was not accompanied by changes in Aβ levels suggesting that they act by altering the sensitivity of cells and animals to Aβ, not Aβ production. These results support a role for PP2A methylation as a contributing factor in the development of AD in hyperhomocysteinemic individuals, as well as the potential of PP2A methylation-targeting therapeutic approaches for the AD prevention or treatment.

Results:

PME-1 and LCMT-1 over expression *in vivo* in transgenic mice.

To test the effect of altered PP2A methylation on the sensitivity to beta amyloid (Aβ) exposure, we generated two lines of mice: one carrying a transgene encoding FLAG epitope-tagged murine PP2A methylesterase (PME-1) and a second encoding FLAG epitope-tagged murine PP2A methyltransferase (LCMT-1). To drive the expression of these transgenes in principal cells of the forebrain, we placed them under the control of a synthetic tetO promoter and combined them independently with a third transgene expressing a synthetic transactivator (tTA) under the control of a regulatory region from the calcium calmodulin kinase IIα (CaMKIIα) gene (Mayford et al., 1996). In this system, PME or LCMT transgene expression is activated when tTA binds to the tetO promoter in cells where tTA expression is driven by the CaMKIIα promoter (Fig. 1A). Oligonucleotide RNA in situ hybridization to saggital sections of brains from animals that carried both the tetO-PME and CaMK-tTA transgenes revealed PME-1 transgene RNA expression in principal cells throughout the forebrain including the striatum, olfactory bulb, cortex, and hippocampus (Fig. 1B and C). Immunohistochemistry on brain sections from these animals using an antibody specific to the FLAG epitope tag

showed that epitope-tagged transgenic protein was present throughout cell bodies and dendrites of pyramidal cells of the hippocampal CA1 region (Fig 1D). Oligonucleotide RNA *in situ* hybridization and anti-FLAG tag immunohistochemistry revealed a similar distribution of LCMT-1 transgene RNA and protein expression in brains of animals that carried both the tetO-LCMT and CaMK-tTA transgenes (Fig 1K-M). Oligonucleotide RNA in situ hybridization and immunohistochemistry on sections from sibling controls that carried only one of the three transgenes (tetO-PME, tetO-LCMT, or CaMK-tTA alone) did not reveal transgenic PME-1 or LCMT-1 RNA or protein expression in brains from these animals (Fig 1E-J, N-P).

Quantitative western blot analysis of hippocampal extracts from tetO-PME/CaMKtTA and tetO-LCMT/CaMKtTA double transgenic animals revealed a 379 +/- 44% increase in PME-1 expression and a 152 +/- 13% increase in LCMT-1 protein expression respectively (transgenic + endogenous) compared to single transgenic control animals (Fig. 1Q and R; $p<0.001$). Transgene expression in these lines did not affect PP2A catalytic subunit expression, PP2A Bα regulatory subunit expression (Fig S1), or methyl-donor metabolite levels, including S-adenosyl methionine and S-adenosyl homocysteine (Supplemental table 1). Endogenous LCMT-1 expression was not affected by PME-1 transgene expression and endogenous PME-1 expression was not affected by LCMT-1 transgene expression (Fig S1). Methylated PP2A levels in hippocampal homogenates from the tetO-PME/CaMKtTA double transgenic animals were 45.2 ± 6.6 % of control levels (Fig. 1S; $t = 7.11$, $p<0.001$). However, a similar analysis on hippocampal homogenates from tetO-LCMT/CaMKtTA double transgenic animals failed to reveal a corresponding increase in PP2A methylation in these animals (Fig. 1T; 105.9 ± 7.3% of controls; $t = 0.65$; $p > 0.05$). Our observation that methylated PP2A/C represented 85.5 ± 2.5% ($n = 10$) of total C levels in hippocampal homogenates from control animals under basal conditions suggests that our inability to detect a further increase in PP2A/C methylation in the LCMT-1 over expressing animals may be a consequence of near saturating levels of methylation under basal conditions.

PME-1 over expression increases behavioral and physiological impairments caused by exposure to subthreshold doses of oligomeric Aβ.

Both the PME-1 and LCMT-1 over expressing mice were overtly indistinguishable from their single transgenic control siblings. They were fertile and obtained in normal Mendelian ratios from crosses of double transgenic males to wild type females (data not shown). Analysis of these animals' behavior in a novel open field revealed no genotypic effects on distance traveled, ambulatory episodes, time spent in the center of the arena, time spent rearing, resting time, or time spent engaged in small stereotypic movements (Fig. S2 & S3). For all experiments, single transgenic animals that carried the CaMKIIα-tTA, tetO-PME, or tetO-LCMT transgenes were used as controls. In our experiments, we observed no differences among these control groups, suggesting that the phenotypes observed in the CaMKIIα-tTA/tetO-PME or CaMKIIα-tTA/tetO-LCMT double transgenic animals were dependent on PME-1 or LCMT-1 transgene expression and were not an artifact of transgene insertion.

To test the effect of PME-1 over expression on the behavioral impairments that result from acute Aβ exposure we tested these animals and their single transgenic control siblings in a contextual fear-conditioning task with or without administration of

oligomeric Aβ. This task is used to assess the ability of the animals to make an association between a novel conditioned stimulus, (the testing environment) and an aversive unconditioned stimulus (a foot shock) and has been found previously to be both dependent on hippocampus function and sensitive to Aβ administration (Fiorito et al., 2013; Maren et al., 2013). PME-1 over expressing and control animals were bilaterally implanted with cannulae targeting the dorsal hippocampus and infused with either an oligomeric synthetic human $A\beta_{1-42}$ preparation or vehicle 20 minutes before exposure to the conditioning chamber. A single 2 sec, 0.8 mA foot shock was given during the third minute of the 3 min conditioning trial. Twenty four hours later, the animals were returned to the conditioning chamber and the amount of time spent freezing during a 5 min exposure without foot shock was determined and used as a measure of cognitive performance on this task. Vehicle-treated PME-1 over expressing animals exhibited a level of freezing at 24 hours that was similar to vehicle-treated single transgenic control siblings (Fig 3A; 36.6% +/- 4.4% for vehicle-treated PME-1 over expressing vs. 34.3% +/- 5.1% for vehicle-treated controls; Bonferroni post hoc test $P>0.05$) and control animals infused with a sub-threshold dose of oligomeric Aβ also exhibited levels of freezing similar to the vehicle treated controls (Fig 3A; 34.2% +/- 5.5% for Aβ-treated controls; Bonferroni post hoc tests $P>0.5$). However, PME-1 over expressing animals that received the same sub-threshold dose of Aβ (1 μl bilateral injections of 75nM oligomeric Aβ preparation) exhibited significantly less freezing than the other three groups (Fig 3A; 17.7% +/- 3.4% for Aβ-treated PME-1 over expressing animals), suggesting that PME-1 over expressing animals are more sensitive to Aβ-induced cognitive impairment in this task (Fig 3A; 2-WAY ANOVA showed a significant effect of training over all: $F(1,48) = 138.45$, $P <0.0001$; and also a significant training x group interaction: $F(3,48) = 3.43$, $P = 0.0241$. Bonferroni post-hoc comparisons of freezing at 24 hours for treated PME expressing animals vs. all other groups were $P<0.01$). The initial exposure to the conditioning chamber produced low levels of freezing that did not differ among groups ($P> 0.05$ for all Bonferroni post-hoc comparisons of baseline freezing), suggesting that neither PME-1 over expression, Aβ treatment, nor the combination affected baseline levels of freezing in these animals. Subsequent behavioral tests conducted on these animals revealed similar responses to foot shock (Fig. S4), suggesting that the differences in contextual fear conditioning observed among these groups did not result from differences in perception of the unconditioned stimulus, and analysis of the activity of these animals in an open field environment revealed no effect of genotype or Aβ administration on ambulatory activity (Fig. S4).

As an independent test of the effect of PME-1 over expression on Aβ-induced cognitive impairments, we tested these animals on a 2-day radial arm water maze task that was found previously to be sensitive to hippocampal Aβ administration (Watterson et al., 2013). In this task animals must navigate from pseudorandomly selected arms of a 6-arm radial water maze to an escape platform located in a fixed position in one of the arms (Alamed et al., 2006). Each day of the task consists of 15 trials. During the first 11 odd-numbered trials of the first day, the location of the escape platform is indicated by a marker protruding above the surface of the water, while on all other trials, the submerged platform is not visible to the animals. PME-1 over expressing and control animals were infused bilaterally 20 min before the start of training and once again at the midpoint of

training with 1 μl of either 75 nM oligomeric Aβ or vehicle via cannulae implanted into the dorsal hippocampus. The number of entries each animal made into non-platform-containing arms (errors) was used to monitor its acquisition and cognitive performance in this task. As we saw in the contextual fear-conditioning task, PME-1 over expression did not affect the performance of vehicle infused animals (Fig 3B; 2-way RM-ANOVA with block and genotype as factors for control vehicle vs. PME-1 vehicle on day 2: $F(1,24) = 0.01$, $P = 0.9427$ for genotype) and the sub-threshold dose of Aβ we used did not affect performance in control animals (Fig 3B; 2-way RM-ANOVA with block and treatment as factors for control vehicle vs. control Aβ on day 2: $F(1,24) = 0.68$, $P = 0.4188$ for treatment), but sub-threshold Aβ administration did significantly impair performance in the PME-1 over expressing animals (Fig 3B; 2-way RM-ANOVA with block and treatment as factors for PME vehicle vs. PME + Aβ on day 2: $F(1,24) = 20.81$, $P = 0.0001$ for treatment). Subsequent tests of these animals on a visible platform version of the Morris water maze revealed no differences in escape latency or swim speed among these groups, suggesting that the combination of PME-1 over expression and sub-threshold Aβ exposure does not measurably impact motor performance, perception, or motivation in a non-spatial water maze task (Fig. S4).

Activity-dependent changes in the efficacy of synaptic transmission within the hippocampus are thought to be required for particular forms of memory, and interference with these changes, caused by elevated levels of Aβ, is thought to contribute to AD-associated memory impairments (Ondrejcak et al., 2010). Since we found that PME-1 over expression enhanced Aβ-induced, hippocampus-dependent memory impairments, we sought to determine whether PME-1 over expression might also impact the effects of Aβ on the cellular processes thought to underlie these memories. To do this we prepared acute hippocampal slices from PME-1 over expressing animals and controls and examined field EPSP responses at Schaffer collateral synapses following afferent stimulation using a theta burst stimulus protocol. This protocol produced robust, long-lasting potentiation of synaptic responses (LTP) that was comparable in both PME-1 over expressing animals and controls (Fig 3D; RM-ANOVA for genotype: $F(1,23) = 0.16$, $P = 0.6895$), suggesting that PME-1 over expression alone did not affect synaptic potentiation under these conditions. We also failed to observe any difference in the stimulus intensity/ response relationship at Schaffer collateral synapses, further suggesting that PME-1 over expression did not affect basal synaptic transmission in these animals (Fig. S5).

Previous studies have shown that theta-burst-induced potentiation at Schaffer collateral synapses is sensitive to exogenous Aβ application (Haass and Selkoe, 2007; Puzzo et al., 2008), so in a manner analogous to our behavioral experiments, we repeated this experiment while bath applying a sub-threshold dose of 50 nM Aβ for 20 min before stimulation. Under these conditions, 50 nM Aβ produced no significant effect on synaptic potentiation in slices from control animals (Fig 3D and E; RM-ANOVA for treatment: $F(1,23) = 0.00$, $P = 0.9734$). However, 50 nM Aβ did produce a significant impairment of synaptic potentiation in slices from PME-1 over expressing animals compared to controls (Fig 3E; RM-ANOVA for genotype: $F(1,22) = 5.23$, $P = 0.0322$). This increase in the sensitivity of PME-1 over expressing slices to Aβ-induced LTP impairment could also be seen in a shift in the relationship between Aβ concentration

and the corresponding LTP impairment (Fig 3C; RM-ANOVA for genotype: $F(1,132) = 5.42$, $P = 0.0214$). This enhancement of Aβ-induced LTP impairment parallels the behavioral data we describe above, suggesting that PME-1 mediated enhancement of Aβ's effects on synaptic plasticity may lead to the enhanced Aβ-induced behavioral impairments we observe.

LCMT-1 over expression reduces physiological and behavioral impairments caused by exposure to oligomeric Aβ.

Given that over expression of the PP2A methylesterase, PME-1, sensitizes transgenic mice to Aβ-induced physiological and behavioral impairments, we sought to determine whether over expression of the PP2A methyltransferase, LCMT-1, might have the opposite effect on Aβ's actions. To do this we subjected our tetO-LCMT/CaMKtTA double transgenic animals to the same contextual fear conditioning and radial arm water maze tasks described above, however, in these experiments, we infused animals with Aβ at a concentration that produced behavioral impairments in control animals (bilateral infusions of 1 μl of 200 nM oligomeric Aβ) to test for possible protective effects of LCMT-1 over expression.

In the contextual fear-conditioning task, LCMT-1 over expression did protect against Aβ-induced impairment. Vehicle treated control animals exhibited a robust freezing response when tested 24 hrs after training that was significantly reduced in Aβ-infused control animals (Fig 4A; 37.3% +/- 6.3% for vehicle-treated vs 15.0% +/- 2.6% for Aβ-treated controls; Bonferroni post hoc test $P>0.05$), and completely restored in Aβ-infused tetO-LCMT/CaMKtTA double transgenic animals (Fig 4A; 32.0% +/- 3.5% freezing for Aβ-treated tetO-LCMT/CaMKtTA double transgenics; Bonferroni post hoc test vs. vehicle-treated controls: $P>0.05$). Moreover, this effect was specific to the Aβ-induced impairment, and not the result of enhanced fear conditioning in the tetO-LCMT/CaMKtTA double transgenic animals, since vehicle-treated tetO-LCMT/CaMKtTA double transgenic animals showed levels of freezing comparable vehicle treated controls (Fig 4A; 31.7% +/- 5.2% freezing for vehicle-treated tetO-LCMT/CaMKtTA double transgenics; Bonferroni post hoc test vs. vehicle-treated controls: $P>0.05$). As was the case for our analysis of the PME-1 over expressing animals, we observed significant effects of training overall ($F(1,43) = 134.51$, $P<0.0001$) and a significant training x group interaction ($F(3,43) = 5.50$, $P = 0.0027$. Bonferroni post-hoc comparisons of freezing at 24 hours for Aβ treated control animals vs. all other groups were $P<0.01$). No differences among these groups were evident during initial exposure to the training context, however, suggesting that neither LCMT-1 over expression, Aβ treatment at this dose, nor the combination affected baseline levels of freezing. Subsequent behavioral tests conducted on these animals revealed similar responses to foot shock (Fig. S4), suggesting that the differences in contextual fear conditioning observed among these groups during testing did not result from differences in perception of the unconditioned stimulus. We also observed no effect of genotype or treatment on open field activity in these animals (Fig. S4) suggesting that the differences observed in contextual fear conditioning were not the result of changes in the general level of activity of these groups.

LCMT-1 over expression also protected against Aβ-induced behavioral impairment in

the radial arm water maze task. Aβ significantly impaired performance in control animals (Fig 4B; 2-way RM-ANOVA with block and treatment as factors for control vehicle vs. control + Aβ on day 2: $F(1,21) = 27.74$, $P < 0.0001$ for treatment), but not LCMT-1 over expressing animals (Fig 4B; 2-way RM-ANOVA with block and group as factors for control vehicle vs. LCMT-1 + Aβ on day 2: $F(1,21) = 0.07$, $P = 0.7991$ for group). As was the case for the contextual fear conditioning task, this effect could not be explained by increased performance resulting from LCMT-1 over expression alone since no difference was observed between the vehicle treated control and vehicle treated tetO-LCMT/CaMKtTA double transgenic groups (2-way RM-ANOVA with block and genotype as factors for day 2: $F(1,21) = 0.05$, $P = 0.8207$ for genotype). Subsequent tests of these animals on a visible platform version of the Morris water maze also failed to reveal differences in escape latency or swim speed among these groups, suggesting that the combination of LCMT-1 over expression and Aβ exposure did not measurably impact motor performance, perception, or motivation in a non-spatial water maze task (Fig. S4).

Given the protective action of LCMT-1 over expression with respect to Aβ-induced behavioral impairment, we wondered whether LCMT-1 over expression might also protect against Aβ-induced impairments at the electrophysiological level. To test this hypothesis, we carried out field recordings on acute hippocampal slices from tetO-LCMT/CaMKtTA double transgenic and control animals as described above. As was the case for PME-1 over expression, we found that LCMT-1 over expression affected neither the stimulus/response relationship, (Fig. S5), nor theta-burst-induced LTP at Schaffer collateral synapses (Fig 4C; RM-ANOVA for genotype on vehicle-treated tetO-LCMT/CaMKtTA double transgenic vs. vehicle-treated controls: $F(1,22) = 0.05$, $P = 0.8285$). We did find that bath application of 100 nM Aβ significantly impaired this LTP in slices from single transgenic controls (Fig 4C and D; RM-ANOVA for treatment on vehicle vs. Aβ treated controls: $F(1,22) = 10.73$, $P = 0.0035$), and that this Aβ-induced LTP impairment was significantly reduced in slices from LCMT-1 over expressing animals (Fig 4D; RM-ANOVA for genotype on Aβ treated LCMT vs. control slices: $F(1,20) = 5.13$, $P = 0.0348$). As was the case for the PME-1 over expressing mice, this correlation between LCMT's behavioral and electrophysiological effects suggests that LCMT-1 over expression may protect against Aβ-induced behavioral impairments by reducing Aβ-induced physiological impairments.

PME and LCMT transgene expression do not alter Aβ levels or response to picomolar Aβ concentrations

PP2A has been found to dephosphorylate the amyloid precursor protein (APP) at threonine 668, and phosphorylation at this site is thought to control Aβ production by regulating APP processing by BACE ((Ando et al., 2001; Lee et al., 2003; Matsushima et al., 2012; Pierrot et al., 2006), but see (Feyt et al., 2007; Sano et al., 2006)). PME-1 and LCMT-1 over expression in neuroblastoma cell lines has also been found to alter both APP Thr668 phosphorylation and Aβ production (Sontag et al., 2007). If Aβ production is altered in the PME-1 and LCMT-1 over expressing mice, then this might provide a mechanism for the changes in the Aβ sensitivity we observe in these animals. Consistent with the effects of these transgenes in neuroblastoma cell lines, we found that phospho-

APP levels were 150 ± 5 % of control levels in the PME-1 over expressing animals (Fig 4A; P = 8.68 or p< 0.001) and 56 ± 5% of control ((Fig 4B; t = 7.87 or p< 0.001) in the LCMT-1 over expressing animals. However, measures of $A\beta_{1-40}$ and $A\beta_{1-42}$ peptides in hippocampal homogenates using a commercially available sandwich ELISA failed to reveal any significant differences in basal levels for either $A\beta_{1-40}$ or $A\beta_{1-42}$ in the PME-1 or LCMT-1 over expressing animals and their corresponding controls (Fig. 4C, D; unpaired t test results: $A\beta_{1-40}$: PME vs. control t= 1.179, p= 0,2546; LCMT vs. control: t= 1.016, p= 0.3224; $A\beta_{1-42}$: PME vs. control t= 1.732, p= 0.1014; LCMT vs. control: t= 1.2221, p= 0.2369), suggesting that the altered behavioral and electrophysiological responses to exogenous Aβ in the PME-1 and LCMT-1 over expressing mice are not due to altered basal levels of Aβ.

As described above, Aβ application at nanomolar concentrations impairs LTP, however, at but at picomolar concentrations Aβ has been found to enhance LTP (Puzzo et al., 2008). While the impairments observed at high Aβ concentrations are thought to reflect the pathological actions of Aβ that occur in AD patients, the effects of Aβ at picomolar concentrations are thought to reflect a normal physiological role for Aβ in regulating synaptic activity and transmission (Puzzo and Arancio, 2013). To examine the possibility that PME-1 and LCMT-1 over expression also affect the sensitivity to picomolar concentrations of Aβ, we evoked LTP at Schaffer collateral synapses by theta-burst stimulation in the presence or absence of 200 pM oligomeric Aβ. In these experiments, picomolar Aβ application caused a significant enhancement of LTP over corresponding vehicle treated slices in both PME-1 and LCMT-1 over expressing animals (Fig. 4E, F; RM-ANOVA for treatment: PME Aβ vs. vehicle: $F(1,15) = 5.893$, $P = 0.0283$; LCMT Aβ vs. vehicle: $F(1,25) = 8.125$, $P = 0.0086$) that was similar among all genotypic groups (Fig. 4E, F; RM-ANOVA for genotype: PME Aβ vs. Control Aβ $F(1,20) = 0.6677$, $P = 0.4235$; LCMT Aβ vs. Control Aβ $F(1,26) = 0.4638$, $P = 0.5019$). These results are consistent with the observation that baseline LTP, behavior, and Aβ production are all normal in the PME-1 and LCMT-1 over expressing mice, and suggests that the over expression of these transgenes selectively affects the response of these animals to pathological levels of Aβ without affecting Aβ's normal physiological actions.

The microtubule associated binding protein, tau, also plays a central role in AD, and aggregates of hyperphosphorylated tau constitute another histological hallmark of the disease, neurofibrillary tangles. The presence and phosphorylation state of tau has been found to alter AD pathology in AD mouse models and the response to exogenously applied Aβ (Lewis et al., 2001; Mairet-Coello et al., 2013; Perez et al., 2008; Perez et al., 2005; Rhein et al., 2009; Ribe et al., 2005; Roberson et al., 2007; Shipton et al., 2011). Given the ability of tau to modulate Aβ responses, and PP2A's role as the principal tau phosphatase, we sought to determine whether the changes in Aβ sensitivity we observed in the PME-1 and LCMT-1 over expressing mice correlate with changes in tau phosphorylation. To do this, we performed quantitative western blot analysis on hippocampal homogenates from PME-1 and LCMT-1 over expressing mice and their corresponding controls using three phosphospecific antibodies: PHF-1, which detects tau phosphorylated at Ser396/Ser 404; AT8, which detects tau phosphorylated at Ser202/Thr205; and a third antibody that detects tau phosphorylated at Ser262. The increased Aβ sensitivity exhibited by the PME-1 over expressing mice correlated with

increased immunoreactivity for each of these three phosphospecific antibodies when compared to controls (Fig 4G; PHF-1: 210 ± 7%, p< 0.001; AT8: 139 ± 15%, P=0.02; S262: 116 ± 7.5%, P=0.04), which was not accompanied by a change in the level of tau itself (Fig 4G; 98 ± 5.4%, P= 0.74). However, we did not observe a corresponding decrease in phospho-tau immunoreactivity in LCMT-1 over expressing animals and controls, perhaps due to the relatively low levels of phosphorylation that exist at these sites under basal conditions (Matsuo et al., 1994) (Fig 4H; PHF-1: 79.5 ± 12.4% of control; p >0.05; AT8: 95 ± 2.9%, p=0.71; S262: 95 ± 2.4%, p=0.23; total tau: 106 ± 6.7%, p=0.40).

Discussion:

We find that over expression of the PP2A methylesterase, PME-1, sensitizes animals to the pathological effects of acute Aβ exposure and that over expression of the PP2A methyltransferase, LCMT-1 protects animals from ~~the~~ these effects. These data add to the growing body of evidence suggesting that altered PP2A activity can contribute to the development of AD and that increasing PP2A activity may have therapeutic benefits for the prevention or treatment of the disease (Braithwaite et al., 2012; Martin et al., 2013; Rudrabhatla and Pant, 2011).

To examine the effect of altered PP2A methylation on the pathological effects of Aβ exposure, we generated a novel line of transgenic mice that over express the PP2A methylesterase, PME-1. In our behavioral and biochemical analysis of these animals, we found that they exhibit a reduced proportion of methylated PP2A catalytic subunit in vivo, as well as increased cognitive and electrophysiological impairments when exposed to nanomolar concentrations of exogenously applied oligomeric Aβ. The data we obtained from our analysis are consistent with impaired PP2A methylation contributing to the increased AD risk observed in hyperhomocysteinemic individuals, and suggest that reduced PP2A methylation may do so by altering the susceptibility of these individuals to the pathological effects of elevated Aβ concentrations. These results, however, do not exclude the possible contribution of additional downstream effects of elevated homocysteine in increasing AD risk (Fleming et al., 2012; Fuso et al., 2012a; Marlatt et al., 2008; Sontag et al., 2007; Sontag et al., 2008; Troen et al., 2008; Wei et al., 2011; Zhang et al., 2009; Zhuo et al., 2010). They also do not exclude the possibility that PME-1 over expression may affect PP2A activity and Aβ sensitivity via a mechanism that is independent of PME-1's methylesterase activity (Longin et al., 2008).

In contrast to PME-1 over expressing mice, we found that a novel line of transgenic mice that over express the PP2A methyltransferase, LCMT-1, exhibit reduced sensitivity to Aβ-induced behavioral and electrophysiological impairments. These data suggest that strategies designed to pharmacologically increase LCMT-1 activity may be an effective strategy for preventing or treating AD. The opposing effects of PME-1 and LCMT-1 over expression on Aβ sensitivity are consistent with the opposing actions of these enzymes on PP2A methylation. However, one caveat to the interpretation that LCMT-1 over expression reduces Aβ sensitivity in these animals by promoting PP2A methylation is the fact that we were unable to detect corresponding increases in PP2A methylation in LCMT-1 over expressing mice. Our inability to detect a difference PP2A methylation may be influenced by the high proportion of basal methylated PP2A levels that exist under basal conditions, as previously observed in cultured cells (Xu et al.,

2001), and/or the inherent limits in the sensitivity of quantitative western blotting. However, it is also possible that LCMT-1 may influence PP2A regulation via a mechanism that does not depend on its methyltransferase activity. The association of LCMT-1 with PP2A alone may influence PP2A's subcellular distribution (Sontag et al., 2013), stability, or interaction with other proteins in a manner analogous to that proposed for several other PP2A regulatory proteins (Sents et al., 2013).

How might PME-1 and LCMT-1 over expression affect Aβ sensitivity?

One way to increase the sensitivity of animals to exogenously applied Aβ would be to alter basal levels of endogenous Aβ. In animals with elevated endogenous Aβ levels, the threshold for Aβ-induced impairment would be reached at lower exogenous Aβ concentrations. PME-1 and LCMT-1 over expression does alter Aβ production in neuroblastoma cells (Sontag et al., 2007) where these changes correlate with changes in the level of Thr668 phosphorylated APP, which is thought to affect Aβ production ((Ando et al., 2001; Lee et al., 2003; Matsushima et al., 2012; Pierrot et al., 2006), but see (Feyt et al., 2007; Sano et al., 2006)). We also observe transgene-dependent changes in the amount of Thr668-phosphorylated APP in the PME-1 and LCMT-1 over expressing mice. However, several of our observations suggest that altered Aβ production is not the basis for the increased Aβ sensitivity or resistance we observe. First, direct measurement of $A\beta_{40}$ and $A\beta_{42}$ levels in brain homogenates by ELISA revealed no difference in Aβ levels between PME-1 or LCMT-1 over expressing mice and their corresponding controls. Second, a change in Aβ level sufficient to shift the threshold for sensitivity to impairments caused by exposure to nanomolar concentrations of exogenous Aβ, would likely occlude the response to picomolar concentrations of Aβ, and we observe normal LTP enhancement in response to 200 picomolar Aβ in both the PME-1 or LCMT-1 over expressing mice. Third, normal levels of Aβ production are also consistent with the normal theta-burst LTP and normal behavioral performance we observe in the PME-1 and LCMT-1 over expressing animals in the absence of exogenous Aβ.

Another way in which PME-1 and LCMT-1 may affect Aβ sensitivity is through PP2A mediated tau dephosphorylation. PP2A is the principal tau phosphatase (Martin et al., 2013), and several studies have found that tau affects the response of cells and animals to elevated levels of Aβ. Transgenic expression of mutant, tau has been found to enhance AD related phenotypes in AD mouse models (Lewis et al., 2001; Perez et al., 2008; Perez et al., 2005; Rhein et al., 2009; Ribe et al., 2005). Conversely, the absence of tau was found to prevent AD related phenotypes in APP mutant mice (Roberson et al., 2007) as well as Aβ-induced LTP impairment (Shipton et al., 2011). Consistent with this mode of action, we observed increased tau phosphorylation in our PME-1 over expressing mice using three different phospho-tau specific antibodies. The observation that tau phosphorylation at Ser262 is increased in these animals is particularly noteworthy since a recent report has implicated phosphorylation at this site increased Aβ sensitivity (Mairet-Coello et al., 2013). The fact that the reduced Aβ sensitivity we observe in the LCMT-1 over expressing mice does not correlate with an analogous decrease in tau phosphorylation at these sites suggests that LCMT-1 over expression may act by preventing Aβ-induced tau hyperphosphorylation rather than by reducing the already low levels of tau phosphorylation that exist under basal conditions. While the extensive literature linking tau and its phosphorylation to Aβ sensitivity strongly suggest that PME-

1 and LCMT-1 mediated changes in tau phosphorylation are the most likely mechanism for the altered Aβ sensitivity we observe in these animals, we cannot rule out the possibility that altered phosphorylation of other PP2A substrates (for example: ERK (Chong et al., 2006)) may contribute to this altered sensitivity. While PME-1 and LCMT-1 are known only to regulate PP2A methylation, we also cannot rule out the potential involvement of PME-1 or LCMT-1 interactions with other unknown substrates.

PME and LCMT as potential drug targets for the prevention or treatment of AD.

The data we obtained from our PME-1 and LCMT-1 over expressing mice lend support to a growing interest in developing therapeutic approaches for AD that act by targeting PP2A methylation (Braithwaite et al., 2012; Martin et al., 2013; Voronkov et al., 2011), and suggest that this approach may afford some distinct advantages over current alternative strategies. First, Unlike AD therapeutic strategies that seek to reduce Aβ production (Schenk et al., 2012), we found that PME-1 and LCMT-1 over expression instead target the *response* to Aβ. Second, our data suggest that, PME-1 and LCMT-1 over expression selectively affect response to *pathological* Aβ concentrations while preserving responses to normal physiological concentrations. Thus, given that Aβ is thought to have an important role in regulating normal neuronal activity (Puzzo and Arancio, 2013), a PP2A methylation-based therapeutic strategy for AD may offer the prospect of preventing the pathological effects of Aβ without affecting normal physiological functions – a contention supported by the normal baseline behavioral and electrophysiological responses in the PME-1 and LCMT-1 over expressing animals, as well as their normal electrophysiological responses to picomolar Aβ concentrations. However, a successful strategy based on this approach will likely require precise modulation of PME-1 or LCMT-1 activity. PP2A plays a number of critical functions in numerous cell types throughout the body (Janssens and Goris, 2001; Shi, 2009), and mice homozygous for a knock-out mutation of the murine PME-1 or LCMT-1 genes exhibit early postnatal or embryonic lethality respectively (Lee and Pallas, 2007; Ortega-Gutierrez et al., 2008). Additionally, we observed that greater than 10 fold LCMT-1 over expression in second line of transgenic mice resulted in behavioral impairments on its own (data not shown). Given the scale of the social and economic problems caused by AD, and the lack of any effective disease modifying treatments, the pursuit of such a strategy and the insights into the mechanisms underlying AD pathology it will provide is certainly warranted.

Acknowledgements:

We thank Peter Davies (Albert Einstein College of Medicine) for the gift of the PHF-1 antibody. This work was supported by a Department of Defense grant W81XWH-12-1-0579 (OA and REN), a generous gift from the Broitman family (ERK), and a grant from the National Health and Medical Research Council of Australia (ES and JMS).

Methods:

Transgenic animals: tetO promoter driven constructs expressing either Flag tagged murine PME-1 or Flag tagged murine LCMT-1 were generated using standard molecular cloning techniques and used to generate transgenic mice by pronuclear injection into C57BL6/J oocytes. Transgene containing animals were crossed to an existing CaMKIIα-tTA line (Mayford et al., 1996) also in a C57BL6/J background, and double transgenic

animals were outcrossed to wild type 129SVEV/TAC mice to generate the C57BL6/J x 129SVEV/TAC F1 animals used for experiments. We used adult animals between 3 and 6 months of age for all experiments. Only males were used for behavioral experiments and both males and females were used in equal proportions for all other experiments.

Oligonucleotide in situ hybridization and immunohistochemistry: RNA in situ hybridization was carried out on 20 μm saggital sections as described previously (Wisden and Morris, 2002) using a radiolabeled oligonucleotide probe specific to the 3'UTR of both the LCMT-1 and PME-1 transgenes. Immunohistochemistry was carried out on 30 μm free floating vibratome sections from paraformaldehyde perfused animals using a primary antibody against the Flag epitope tag and a fluorescently labeled secondary antibody. Images were obtained by confocal microscopy.

Western blots: For all blots except total tau, AT8 and S262, hippocampal homogenates were prepared from microwave fixed samples homogenized by sonication in hot 0.5% SDS solution. Western blotting was carried out as described previously (Bottiglieri et al., 2012; Sontag et al., 2007). To control for differences in loading or transfer efficiency, signals were normalized to the corresponding total PP2A/C, APP, tau or β-actin signal in each lane detected simultaneously or after stripping and reprobing. Western blots shown in figure 4, using total tau, AT8 and S262 antibodies were carried out similarly except that samples were homogenized in modified RIPA buffer supplemented with protease and phosphatase inhibitors and 25 nM okadaic acid. Quantitation of these blots was carried out using infrared dye labeled secondary antibodies and an Odyssey imager (Li-cor).

Aβ preparation and infusion: Oligomeric Aβ was prepared from synthetic Aβ 1-42 peptides (American Peptide) as described previously (Puzzo et al., 2008; Stine et al., 2003). For behavioral experiments, Aβ was infused into the dorsal hippocampus via bilaterally implanted cannulae (coordinates: 2.46 mm posterior to bregma, 1.50 mm lateral to midline suture, and to a depth of 1.50 mm from the skull surface). The quality of oligomeric Aβ preparations were routinely assessed by immunoblotting.

Contextual fear conditioning and radial arm water maze tasks were carried out as described previously (Fiorito et al., 2013). The contextual fear conditioning protocol consisted of a 3 minute exposure to a novel context during which a 2 sec. 0.8 mA foot shock was delivered 30 seconds before the end of the trial. 24 hours after this training session animals were re-exposed to the training environment and the amount of time spent freezing was measured using an automated system (Actimetrix). Radial arm water maze training was carried out over two days with 15 trials per day in a 6-arm radial arm water maze. A visible or hidden platform was located at a fixed position in one of the arms and the starting positions for the animals were pseudorandomly alternated among the non-platform-containing arms across trials. Visible platform trials were conducted on odd-numbered trials 1-11 on the first day and hidden platform trials were carried out on all others. Trials were videotaped and animal entries into non-platform containing arms were scored as errors by an observer blinded to treatment and genotype.

Electrophysiological recordings: Field EPSP recordings of synaptic responses at Schaffer collateral synapses were carried out in 400 μm acute hippocampal slices maintained in an interface chamber at 29°C as described previously (Puzzo et al., 2008). LTP was evoked at these synapses by afferent stimulation using a theta-burst protocol

consisting of 10-burst trains separated by 15 seconds. Each train consisted of 10 bursts delivered at 5 Hz and each burst consisted of 4 pulses at 100 Hz.

Aβ ELISA measures: Aβ 1-40 and 1-42 levels were determined by commercially available ELISA kits (Wako), and hippocampal homogenates were prepared as described previously (Teich et al., 2013).

Figure Legends:

Figure 1: PME-1 and LCMT-1 over expression in the forebrain of transgenic mice. **(A)** Diagram of the tetO/tTA system in which either FLAG tagged PME or LCMT transgene expression is driven by the tTA transactivator, the expression of which is driven by a second transgene under the control of a calcium/calmodulin kinase IIα promoter fragment. **(B,E,H,K,N)** Representative autoradiographic images of transgene-specific oligonucleotide RNA in situ hybirdization of whole brain saggital sections from animals of the indicated genotypes. **(C,F,I,L,O)** Higher magnification views of the hippocampal regions from the corresponding images in panels B,E,H,K, and N. **(D,G,J,M,P)** Representative immunofluorescent images of hippocampal CA1 region pyramidal cells in animals of the indicated genotypes generated using an antibody specific the FLAG epitope tag contained within the PME and LCMT transgenes. **(Q-T)** Western blots of hippocampal homogenates from tetO-PME/CaMKtTA or tetO-LCMT/CaMKtTA double transgenic animals and single transgenic siblings carried out using primary antibodies directed against the proteins indicated at left. Blots were probed simultaneously or stripped and reprobed with individual primary antibodies as indicated in the methods section. Lanes in each blot contain samples from unique animals.

Figure 2: PME-1 over expression increases behavioral and electrophysiological impairments caused by sub-threshold doses of Aβ. **(A)** Histogram of average percent of time spent freezing (+/- SEM) during an initial exposure to the training context (baseline) and during a second exposure 24 hours after single foot shock in that context (test at 24 hrs) for PME-1 over expressing and control animals infused with either a sub-threshold dose of Aβ or vehicle (N = 13 animals per group). **(B)** Graph of average number of errors committed (+/- SEM) during each 3 trial training block of a 2-day radial arm water maze task for PME over expressing and control animals infused with either a sub-threshold dose of Aβ or vehicle (N = 13 animals per group). **(C)** Dose response curve showing increased Aβ-induced LTP inhibition in PME expressing animals compared to controls. Plotted are average potentiated responses (+/-SEM) in hippocampal CA1 pyramidal cells measured 105 to 115 min. after theta-burst stimulation in acute slices following bath application of oligomeric Aβ at the indicated concentration for 20 min. prior to potentiating stimulation (N > 10 slices per group). **(D, E)** Complete time course of averaged responses for vehicle treated (D) and 50 nM Aβ-treated (E) slices shown in C. Oligomeric Aβ or vehicle (solid bar) was bath applied for 20 min prior to delivery of a potentiating theta-burst stimulus protocol at the indicated time (arrow).

Figure 3: LCMT-1 over expression reduces behavioral and electrophysiological impairments caused by oligomeric beta-amyloid without affecting Aβ levels or Aβ-mediated LTP enhancement. **(A)** Histogram of average percent of time spent freezing (+/- SEM) during an initial exposure to the training context (baseline) and during a second exposure 24 hours after single foot shock in that context (test at 24 hrs) for LCMT-1 over expressing and control animals infused bilaterally with either 1 μl of 200 nM Aβ or vehicle (N = 11 to 12 animals per group). **(B)** Graph of average number of errors committed (+/- SEM) during each 3 trial training block of a 2-day radial arm water maze task for LCMT-1 over expressing and control animals infused with either the same dose

of Aβ or vehicle (N = 11 to 12 animals per group). **(C)** LCMT-1 over expression alone does not affect theta-burst evoked LTP. Shown is the time course of the average evoked responses (+/- SEM) at hippocampal Schaffer collateral synapses in acute slices prepared from LCMT-1 over expressing animals and controls following vehicle treatment (solid bar) and theta-burst stimulation (arrow) (N= 9 LCMT/11 control slices). **(D)** LCMT-1 over expression reduces Aβ-induced LTP impairment. Shown is the time course of the average evoked responses (+/- SEM) at hippocampal Schaffer collateral synapses in acute slices prepared from LCMT-1 over expressing animals and controls following 20 min bath application of 100 nM Aβ (solid bar) and theta-burst stimulation (arrow) (N= 9 LCMT/13 control slices).

Figure 4: PME-1 and LCMT-1 over expression do not alter basal Aβ levels or responses to picomolar Aβ concentrations. **(A,B)** Western blots of hippocampal homogenates from tetO-PME/CaMKtTA (A), or tetO-LCMT/CaMKtTA (B) double transgenic and corresponding single transgenic siblings probed first using a primary antibody specific to APP phosphorylated at threonine-668 (upper panels) then stripped and reprobed with a primary antibody that detects both phosphorylated and unphosphorylated APP (lower panels). **(C,D)** PME-1 and LCMT-1 transgene over expression do not alter basal levels of $A\beta_{1-40}$ or $A\beta_{1-42}$. Shown are values and means (+/- SEM) obtained by ELISA for $A\beta_{1-40}$ (left) or $A\beta_{1-42}$ (right) conducted on hippocampal homogenates from PME-1 over expressing animals (N= 9) and controls (N= 10) (C) or LCMT-1 over expressing animals (N= 8) and controls (N= 13) (D) and normalized to the total amount of protein in each sample. **(E)** PME-1 transgene over expression does not affect enhanced LTP caused by application of 200 pM Aβ. Shown is the time course of the average evoked responses (+/- SEM) at hippocampal Schaffer collateral synapses in acute slices prepared from PME-1 over expressing animals (triangles) and controls (circles) following treatment (solid bar) with vehicle (filled symbols) or 200 pm oligomeric Aβ (open symbols) and theta-burst stimulation (arrow) (N= 8 PME + vehicle/ 9 PME + Aβ/ 11 control + vehicle/ 13 control + Aβ slices). **(F)** LCMT-1 transgene over expression does not affect enhanced LTP caused by application of 200 pM Aβ. Shown is the time course of the average evoked responses (+/- SEM) at hippocampal Schaffer collateral synapses in acute slices prepared from LCMT-1 over expressing animals (triangles) and controls (circles) following treatment (solid bar) with vehicle (filled symbols) or 200 pm oligomeric Aβ (open symbols) and theta-burst stimulation (arrow) (N= 12 LCMT + vehicle/ 15 LCMT + Aβ slices). Pooled control data is plotted in both E and F for comparison. **(G)** PME-1 over expression increases tau phosphorylation. Western blots of hippocampal homogenates from tetO-PME/CaMKtTA double transgenic and single transgenic siblings probed using an antibody to total tau, or the phospho-specific tau antibodies: PHF-1, S262, or AT8. Blots were either stripped and reprobed (PHF-1) or probed simultaneously (S262, AT8, total tau) with antibodies recognizing both phosphorylated and non-phosphorylated tau (PHF-1, S262, AT8) or β-actin (total tau) as a control for loading and transfer efficiency. **(H)** Western blots of hippocampal homogenates from tetO-LCMT/CaMKtTA double transgenic and single transgenic siblings probed as described in G did not reveal significant changes in total or phospho-tau levels.

Supplemental figures:

Supplemental Table 1: Table of methyl-donor metabolite levels in hippocampal homogenates prepared from PME-1 and LCMT-1 over expressing animals and controls.

Supplemental figure S1: PP2A catalytic subunit, Bα regulatory subunit, PME-1 and LCMT-1 expression in PME-1 and LCMT-1 over expressing transgenic mice. Hippocampal homogenates from tetO-PME/CaMKtTA (panel A) and tetO-LCMT/CaMKtTA (panel B) double transgenic and corresponding single transgenic siblings were prepared from microwave fixed tissue by sonication in hot SDS buffer. Western blotting was carried out using primary antibodies to the PP2A catalytic subunit (PP2A/C), the PP2A Bα regulatory subunit (PP2A/Bα), PME-1, LCMT-1 and β-actin. Immunoreactivity was measured by chemiluminescent detection, autoradiography and densitometry. For each antibody the signals were normalized to the corresponding β-actin immunoreactivity in that lane to control for differences in loading or transfer efficiency. This analysis revealed no statistically significant differences ($p > 0.05$) in PP2A catalytic or PP2A Bα regulatory subunit expression between PME-1 and LCMT-1 over expressing animals and their corresponding controls. Analysis of LCMT-1 immunoreactivity in PME-1 over expressing mice and analysis of PME-1 immunoreactivity in LCMT-1 over expressing mice revealed no significant difference in endogenous LCMT-1 or PME-1 expression compared to controls.

Supplemental figure S2: PME-1 over expressing animals show normal behavior in a novel open field environment. 24 PME-1 over-expressing double transgenic and 38 single transgenic control animals were placed individually into a novel open field and their movements tracked and recorded using an infrared beam system and associated computer software. In each graph, the average values (+/- SEM) for the indicated measure are plotted for each 5 min. interval of a 60 min exposure. No significant differences were detected in any of the measures conducted as assessed by 2-way repeated measures ANOVA and Bonferroni post-hoc tests. **(A)** Distance traveled: $F(1,60) = 0.63$, $P=0.4297$. **(B)** Ambulatory episodes: $F(1,60) = 0.82$, $P=0.3678$. **(C)** Center time: $F(1,60) = 0.67$, $P=0.4152$. **(D)** Rearing: $F(1,60) = 0.50$, $P=0.4801$. **(E)** Resting time: $F(1,60) = 0.06$, $P=0.8108$. **(F)** Stereotypic time: $F(1,60) = 3.26$, $P=0.0758$.

Supplemental figure S3: LCMT-1 over expressing animals show normal behavior in a novel open field environment. 16 LCMT-1 over-expressing double transgenic and 31 single transgenic control animals were placed individually into a novel open field and their movements tracked and recorded using an infrared beam system and associated computer software. In each graph, the average values (+/- SEM) for the indicated measure are plotted for each 5 min. interval of a 60 min exposure. No significant differences were detected in any of the measures conducted as assessed by 2-way repeated measures ANOVA and Bonferroni post-hoc tests. **(A)** Distance traveled: $F(1,45) = 1.52$, $P=0.2247$. **(B)** Ambulatory episodes: $F(1,45) = 1.94$, $P=0.1700$. **(C)** Center time: $F(1,45) = 0.92$, $P=0.3428$. **(D)** Rearing: $F(1,45) = 1.28$, $P=0.2640$. **(E)** Resting time: $F(1,45) = 0.01$, $P=0.9314$. **(F)** Stereotypic time: $F(1,45) = 0.40$, $P=0.5328$.

Supplemental figure S4: PME-1 and LCMT-1 over expressing animals show normal

sensory threshold for foot shock, normal open field ambulation, and normal visible platform water maze task performance. **(A)** Histogram of average shock intensities (+/- SEM) at which the first visible movement (eg. flinching) first gross motor movement (running or jumping) or first audible response occur for PME-1 over expressing double transgenic animals and single transgenic controls bilaterally infused into the dorsal hippocampus via cannulae with 1 μl of either 75 nM oligomeric Aβ preparation or vehicle, 20 min prior to testing. 2-way ANOVA revealed no effect of genotype or treatment and no genotype x treatment interaction for any of the response thresholds (ANOVA for genotype: $F(1,48) = 0.33$, $P = 0.5664$ for visible response, $F(1,48) = 0.13$, $P = 0.7224$ for motor response, $F(1,48) = 0.42$, $P = 0.5194$ for audible response); (ANOVA for treatment: $F(1,48) = 0.33$, $P = 0.5664$ for visible response, $F(1,48) = 0.13$, $P = 0.7224$ for motor response, $F(1,48) = 1.37$, $P = 0.2484$ for audible response); (ANOVA for interaction: $F(1,48) = 0.33$, $P = 0.5664$ for visible response, $F(1,48) = 1.15$, $P = 0.2891$ for motor response, $F(1,48) = 0.02$, $P = 0.8972$ for audible response). **(B)** Histogram of the same analysis described in (A) conducted on LCMT-1 over expressing double transgenic animals and single transgenic controls bilaterally infused into the dorsal hippocampus via cannulae with 1 μl of either 200 nM oligomeric Aβ preparation or vehicle, 20 min prior to testing. 2-way ANOVA these data also revealed no effect of genotype or treatment and no genotype x treatment interaction for any of the response thresholds (ANOVA for genotype: $F(1,43) = 0.28$, $P = 0.5987$ for visible response, $F(1,43) = 0.17$, $P = 0.6826$ for motor response, $F(1,43) = 0.06$, $P = 0.8118$ for audible response); (ANOVA for treatment: $F(1,43) = 0.28$, $P = 0.5987$ for visible response, $F(1,43) = 0.08$, $P = 0.7770$ for motor response, $F(1,43) = 0.25$, $P = 0.6175$ for audible response); (ANOVA for interaction: $F(1,43) = 3.25$, $P = 0.0785$ for visible response, $F(1,43) = 0.08$, $P = 0.7770$ for motor response, $F(1,43) = 0.08$, $P = 0.7752$ for audible response). **(B)** Histogram of average distance traveled (+/- SEM) for the indicated genotype x treatment groups during 10 min exposure to an open field environment on subsequent days. Animals were infused with1 μl of 75 nM oligomeric Aβ or vehicle per side via bilateral cannulae directed at the dorsal hippocampus 20 min before each exposure. 2-way ANOVA revealed no effect of genotype or treatment, and no genotype x treatment interaction on either testing day (ANOVA for genotype: $F(1,48) = 0.54$, $P = 0.4651$ for day 1 ; $F(1,48) = 0.04$, $P = 0.8500$ for day 2); (ANOVA for treatment: $F(1,48) = 0.005$, $P = 0.9450$ for day 1; $F(1,48) = 0.74$, $P = 0.3951$ for day 2); (ANOVA for interaction: $F(1,48) = 0.43$, $P = 0.5151$ for day 1; $F(1,48) = 0.29$, $P = 0.5945$ for day 2). **(C)** Histogram of the same analysis described in (B) conducted on LCMT-1 over expressing double transgenic animals and single transgenic controls. 2-way ANOVA on these data also revealed no effect of genotype or treatment, and no genotype x treatment interaction on either testing day (ANOVA for genotype: $F(1,43) = 2.18$, $P = 0.1473$ for day 1 ; $F(1,43) = 0.02$, $P = 0.9000$ for day 2); (ANOVA for treatment: $F(1,43) = 2.01$, $P = 0.1547$ for day 1; $F(1,43) = 0.09$, $P = 0.7667$ for day 2); (ANOVA for interaction: $F(1,43) = 0.01$, $P = 0.9122$ for day 1; $F(1,43) = 0.04$, $P = 0.8371$ for day 2).**(E)** Plot of the average escape latency (+/- SEM) for treated and untreated PME-1 over expressing and control animals during training on a visible platform Morris water maze task. Animals were trained on this task over the course of 2 days in 4 blocks of 3 trials each. 20 minutes before each block, animals were bilaterally infused into the dorsal hippocampus via cannulae with 1 μl of either 75 nM oligomeric Aβ preparation or vehicle. 2-way RM-ANOVA of these data with block and group as factors identified no

significant effect of group ($F(3, 48) = 0.15$, $P = 0.9260$). **(F)** Plot of the average escape latency (+/- SEM) for treated and untreated LCMT-1 over expressing and control animals during training on a visible platform Morris water maze task. Animals were trained on this task as described in C. 20 minutes before each block, animals were bilaterally infused into the dorsal hippocampus via cannulae with 1 μl of either 200 nM oligomeric Aβ preparation or vehicle. 2-way RM-ANOVA of these data with block and group as factors identified no significant effect of group ($F(3, 43) = 0.46$, $P = 0.7119$). **(G)** Plot of the average swim speed (+/- SEM) for treated and untreated PME-1 over expressing and control animals during training on the visible platform Morris water maze task described in C. 2-way RM-ANOVA with block and group as factors also identified no significant effect of group in these data ($F(3, 48) = 0.78$, $P = 0.5102$). **(H)** Plot of the average swim speed (+/- SEM) for treated and untreated LCMT-1 over expressing and control animals during training on the visible platform Morris water maze task described in D. 2-way RM-ANOVA with block and group as factors also identified no significant effect of group in these data ($F(3, 43) = 0.30$, $P = 0.8249$).

Supplemental figure S5: PME-1 and LCMT-1 over expressing animals show normal synaptic input/output relationships at hippocampal Schaffer collateral synapses. **(A)** Show are the averaged fEPSP slopes (+/- SEM) of responses elicited by afferent stimulation at the indicated voltages in acute hippocampal slices obtained from PME-1 over expressing (N= 13) and control animals (N= 12). **(B)** Plot analogous to that described in A obtained from LCMT-1 over expressing (N= 9) and control animals (N= 11).

Supplemental Methods:

PME and LCMT transgenic mice:

Construct generation: 1) A BamH1/Hind3 digested WRE-containing PCR product generated from template FUGW (Lois et al., 2002) with primers WRE-Bam-for and WRE-H3-rev was inserted into BamH1/Hind3 digested pCDNA3.1(-) (Invitrogen). 2) A Not1/BamH1 tetO promoter-containing fragment from mm400 was inserted into the Not1/BamH1 digested product of step 1. 3) A 3x Flag tagged PME fragment was generated by the PCR overlap method in two steps. A 3xFlag fragment was generated from p3XFLAG-myc-CMV24 plasmid template (Sigma) with primers Bam-Flag-for and Pme-Flag-rev and a Pme-containing fragment was generated from clone #BC014867 (Open Biosystems) with primers Flag-Pme-for and Bam-Pme-rev. The products of these two reactions were mixed and amplified with primers Bam-Flag-for and Bam-Pme-rev. 4) A 3x Flag tagged LCMT fragment was generated by PCR overlap similarly using CDNA clone #BC132507 (Open Biosystems) and primers: Bam-Flag-for, LCMT-Flag-rev, Flag-LCMT-for and Bam-LCMT-rev. 5) The BamHI digested product from step3 or 4 was inserted into the BamHI-digested, phosphatase-treated product from step 2. All constructs were verified by sequencing. Expression and activity were verified by transient transfection of N2A cells and western blotting using anti-flag or anti-demethyl PP2A antibodies (data not shown).

Generation of transgenic mice: teto-Flag-transgene-WPRE-BGH pA cassettes from step 5 were generated using primers: mm400-Not-for and BGH-Not-rev and inserted into vector PCR-BluntII (Invitrogen) as per manufacturer's instructions. The products were digested with Not1 to generate linear fragments for pronuclear injection of embryos in a pure C57BL6 background for generation of transgenic mice at the Columbia Cancer Center transgenic Core facility.

Progeny of founder animals were crossed with mice expressing the tTA transgene under the control of the CamKIIα promoter (Mayford et al., 1996). Double transgenic animals in a C57BL6/J background were outcrossed to wild type 129SVEV/Tac animals to generate double, and single transgenic animals in a C57BL6/J x 129SVEV/Tac F1 background for all biochemical, molecular, behavioral and physiological experiments. Genotypes were determined by PCR analysis on tail samples using the RedExtract and RedTaq reagents (Sigma) and transgene specific primer pairs. All animals were maintained and bred under standard conditions, and all experiments were carried out in a manner consistent with NIH guidelines and approved by the Columbia University Institutional Animal Care and Use Committee. Adult animals between 3 and 6 months of age were used for all experiments. Only males were used for behavioral experiments and both males and females were used in equal proportions for all other experiments. For all behavioral and electrophysiological experiments, the experimenter was blind to genotype.

Oligonucleotide in situ hybridization to PME and LCMT transgene RNA was carried out as described previously (Wisden and Morris, 2002). 20 μM fresh frozen cryostat sections were prepared, mounted on Superfrost plus microscope slides (Fisher Scientific) and hybridized using a radiolabelled transgene-specific oligonucleotide probe. Labeled sections were then exposed to autoradiographic film (Biomax MR, Kodak) and digital images generated using a flatbed scanner (Epson).

Immunohistochemistry against Flag epitope-tagged transgene protein was carried out on fixed floating brain sections from double transgenic and control animals. Animals were deeply anesthetized with ketamine/xylazine and transcardially perfused with 50 ml of ice-cold 4% paraformaldehyde in 0.1M Na2HPO4/NaH2PO4 pH 7.4 buffer. Brains were then removed and post-fixed at 4°C overnight. 30 μm coronal sections were made using a Vibratome slicer. Collected sections were rinsed in TBS (0.1M Tris pH7.4/0.9% (w/v) NaCl) plus 0.2% triton X-100 and blocked for 2 hrs in TBS + 1% BSA (Sigma). Sections were then incubated overnight at 4 C in anti-flag antibody (Sigma) diluted 1:1000 in TBS + 1% BSA (Sigma). Sections were then washed in TBS + 0.2% triton, incubated in secondary antibody (Alexa 568 donkey anti-mouse (Invitrogen)) diluted 1:1000 in block for 1 hr, and washed again before mounting in FluorSave aqueous mounting medium (Calbiochem). Z-stack confocal images were obtained using an Olympus confocal microscope.

Microwave tissue fixation: Mice were sacrificed by microwave fixation, a technique designed to inactivate enzyme activity and halt post mortem metabolism. Briefly mice (25 – 35 g) were placed in a cylindrical Perspex holder, which prevents any movement and keeps the head of the mouse in a fixed position. The holder and mouse were placed in the chamber of the microwave system, model TMW 4012 (Muramachi, Tokyo, Japan) and exposed to the microwave beam at an intensity of 6.5 kW for 0.8 seconds. The brain tissue was removed, dissected into various regions that were then stored at -80°C for analysis.

Western blots: Microwave fixed tissue was used for all western blot samples with the exception of S262, AT8, and total tau probed blots shown in figure 4G and H. Mouse hippocampal tissue was homogenized by sonication for 30 sec in 10 volumes (weight/volume) of 0.5% SDS solution followed by incubation for 10 min at 90°C. Aliquots were analyzed immediately or kept frozen at -80°C for future analyses. PP2A methylation, phosphorylated (Thr668) APP, and total and phosphorylated (PHF-1) tau expression levels were measured as described previously (Bottiglieri et al., 2012; Sontag et al., 2007). Protein samples were resolved on 4-12% Bis-Tris gels using the NU-PAGE system (Invitrogen) followed by quantitative Western blotting using fluorescent secondary antibodies and the OdysseyTM Infrared imaging system and Image Studio Lite version 3.1 Software (LI-COR Biosciences).

Western blots shown in figure 4G and H probed with the S262, AT8, and total tau primary antibodies were performed on samples obtained from animals sacrificed by cervical dislocation. Isolated brains were chilled in ice-cold oxygenated ACSF solution (see electrophysiology for composition). Dissected hippocampi were snap frozen in liquid N2 and homogenized on ice using a motorized pestle in mRIPA buffer supplemented with Halt protease + phosphatase inhibitor coctail (Pierce) and 25 nM okadaic acid (Calbiochem). Band intensity was determined using infrared dye-labeled secondary antibodies, an Odyssey imager (Li-cor) and associated software. For all blots, signal intensity was normalized to the corresponding non-methyspecific, non-phosphospecific, or β-actin loading control and expressed as percent of the average value for the pooled controls. All values are expressed as mean percent of

pooled controls ± SEM. Antibodies used in figures 4G and H were as follow: Rabbit anti-phospho tau S262 and goat anti-total tau antibodies from Invitrogen, and mouse anti-phospho tau antibody AT8 from Pierce. All other antibodies were as described previously (Bottiglieri et al., 2012; Sontag et al., 2007).

Aβ preparation: Oligomeric $A\beta_{42}$ was prepared from commercially available synthetic human $A\beta_{42}$ peptide (American Peptide Co, Sunnyvale, CA), as described previously (Puzzo et al., 2008; Stine et al., 2003). Briefly, lyophilized peptide was resuspended in cold 1,1,1,3,3,3-hexafluoro-2-propanol (HFIP, Sigma) to a concentration of 1 mM and aliquoted in polypropylene vials. The HFIP solution was allowed to evaporate in a fume hood for 24 hrs, and the dried preparation was stored in sealed vials at -20°C. Prior to use, anhydrous DMSO (Sigma) was added to obtain a pure monomeric Aβ/DMSO solution that was then sonicated for 10 min. Oligomeric $A\beta_{42}$ was obtained by incubating an aliquot of the monomeric Aβ/DMSO solution in sterile PBS at 4°C overnight. The quality of Aβ preparation was routinely assessed by immunoblots of non-denaturing gels followed by detection using the anti-human Aβ monoclonal antibody 6E10 (Signet Lab) that recognizes monomeric and oligomeric forms of $A\beta_{42}$ (data not shown).

Cannulation and Aβ infusion were conducted as described previously (Puzzo et al., 2008). Mice were anesthetized with 20 mg/kg Avertin and placed in a stereotaxic frame (Kopf). The skull was exposed and appropriately positioned holes were drilled in the skull using a dental drill (Fine Science Tools) and 0.9 mm burr. A bilateral 26-gauge guide cannula was then placed into the dorsal part of the hippocampus (coordinates: posterior = 2.46 mm, lateral = 1.50 mm to a depth of 1.30 mm) (Paxinos and Franklin, 2004) and fixed to the skull with acrylic dental cement (Paladur). Mice were administered 5 mg/kg carprofen at the end of surgery and again 24 hours later as analgesic, the skin was sutured, and the mice were allowed to recover for 1 week before behavioral testing. Infusions of $A\beta_{42}$ or vehicle at the indicated concentrations were performed over 1 min in a final volume of 1 μl through infusion cannulae that were connected to a 10 μl microsyringe (Hamilton) by polyethylene tubing. Infusion cannulae were retracted 1 minute after injection to allow for diffusion of the injected solution.

Contextual fear conditioning: Animals were placed in a conditioning chamber (Med Associates) for 2 min before onset of a 30 sec. tone presentation (2800 Hz at 85 dB). During the last 2 sec. of tone presentation a 0.8 mA foot shock was administered followed by 30 sec of exposure to the environment in the absence of tone or shock. On the next day animals were returned to the conditioning chamber for 5 min without shock or tone presentation. Freezing during each phase of training and testing was monitored continuously using a video tracking and analysis system (Freezeframe, Actimetrix Software).

A 2-day radial arm water maze task was carried out as described previously (Alamed et al., 2006; Fiorito et al., 2013). The behavioral apparatus consisted of a pool 1.2 meters in diameter filled with water made opaque with white paint. Dividers were placed into the pool to generate a contiguous space with 6

equidistantly spaced arms radiating from the center. A 10 cm escape platform was placed at the end of a designated goal arm which remained fixed for each mouse throughout the experiment. For trials 1, 3, 5, 7, 9, and 11 conducted on the first day, the platform was visible, marked with a 5 cm diameter bottle cap that protruded approximately 1 cm above the water's surface, but for all other trials the platform was hidden 1 cm below the water surface. Animals were subjected to 15 trials of up to 1 min each with an intertrial interval of 30 min. on each of two consecutive days. At the start of the trial the animal was placed at the end of a pseudo-randomly selected non-goal arm and allowed to swim to the escape platform. Entry into an arm with no platform, or failure to select an arm after 10 sec was scored as an error. Animals that entered an incorrect arm were guided back to the start arm. At the end of each trial, animals were allowed to rest on the platform for 20 sec. For analysis, the average number of errors was calculated for each mouse in each block of 3 trials.

Electrophysiological experiments were conducted as described previously (Puzzo et al., 2008). Transverse hippocampal slices (400 μm) were cut with a tissue chopper (EMS, PA) and maintained in an interface chamber at 29°C for 90 min before recording. The bath solution consisted of the following (in mM): 124.0 NaCl, 4.4 KCl, 1.0 Na_2HPO4, 25.0 $NaHCO_3$, 2.0 $CaCl_2$, 2.0 $MgSO_4$, and 10.0 glucose. The flow rate of the perfusion was 1 ml/min. The stimulating electrode, a bipolar tungsten electrode, was placed at the level of the Schaffer collateral fibers. A glass recording electrode, filled with bath solution, was placed at the level of CA1 stratum radiatum. Basal synaptic transmission was assayed by plotting the stimulus voltages against slopes of field EPSP. A 20 min baseline was recorded every minute at an intensity that evoked a response ~35% of the maximum evoked response. When stable baseline responses were obtained, slices were then perfused for 20 min with bath-applied oligomeric Aβ at the indicated concentration or vehicle before evoking LTP using a theta-burst protocol. The theta-burst protocol consisted of 10-burst trains separated by 15 seconds, and each train consisted of 10 bursts delivered at 5 Hz and each burst consisted of 4 pulses at 100 Hz.

Aβ ELISA: Levels of Aβ 1-40 and Aβ 1-42 were determined by sandwich ELISA (Human/Rat β Amyloid 40 Wako II and Human/Rat β Amyloid 42 Wako High Sensitivity respectively) as per manufacturers instructions. Hippocampal homogenates were prepared from PME and LCMT over expressing and control animals as described previously (Teich et al. 2013). Hippocampi were homogenized with motorized pestle in 400 μl of ice cold buffer composed of (in mM): 250 sucrose, 1 EDTA, 1 EGTA, 10 Tris pH 7.4, supplemented with protease and phosphatase inhibitors (Halt protease + phosphatase inhibitor mix , Pierce). An equal volume of 0.4% diethylamine/100 mM NaCl was added to each sample before rehomogenization and centrifugation at 21,000 x g at 4°C for 1 hr. Supernatants were neutralized by adding 1/10 volume of 0.5 M Tris pH 6.8 before 4 (Aβ 1-40) or 6 fold (Aβ 1-42) dilution in supplied diluent. Total protein concentration was determined for each sample by micro BCA assay (Pierce) as per manufacturers instructions.

Open field behavior was assessed in a novel open field environment consisting of Plexiglas activity chambers (model ENV- 520; Med Associates, St. Albans, Vermont)

(43.2 cm long × 43.2 cm wide × 30.5 cm high). Mice were placed in the open field and activity was automatically recorded for 60 min. Behavioral measures were calculated using the Activity Monitor program (Med Associates) and "center" was defined as an area beginning 10 cm from the walls. To test the combined effects of transgene expression and Aβ or vehicle administration, animals were placed in a 27.3 cm square open field environment (Med Associates) for 10 min on each of 2 consecutive days, and ambulatory activity was assessed using a digital video camera, PC and Ethovision XT software (Noldus).

Sensory threshold assessment: Animals were placed in a conditioning chamber (Med Associates) and subjected to 1 sec foot shocks of increasing intensity from 0.1 to 0.7 mA at 0.1 mA increments and 30 sec intervals. Behavior was recorded by video capture software (FreezeFrame, Actimetrics) and manually evaluated offline for the shock intensity that elicited the first visible response (flinch), the first extreme motor response (run/jump), and the first audible response (vocalization).

Visible platform water maze task: The experiment was carried out in a circular pool 120cm in diameter filled with water made opaque with white paint. A video tracking system (Ethovision XT) was used to record and analyze each animal's behavior. A 10cm circular platform concealed 1cm below the water surface was used as an escape platform, and marked with a 5 cm diameter bottle cap that protruded approximately 1 cm above the water's surface. Prior to each trial, the platform was rotated among 3 different locations equidistant from one another and 30 cm from the wall. Animals were trained on two blocks of three trials each on each of two successive days. Intertrial intervals were 20 sec and the daily interblock interval was 3 hours. The maximum trail time was trials 60 sec and animals that exceeded this time limit were guided to the platform before being returned to their home cage.

Oligonucleotide sequences:

in situ

WRE-D:ATCCGACTCGTCTGAGGGCGAAGGCGAAGACGCGGAAGAGG

Genotyping primers

tetO transgene pair:
tetO 1-17: 5'GCGGCCGCCAACTCTCG3'
tetO 419-395: 5'TCAAAACAGCGTGGATGGCGTCTC3'
tTA transgene pair:
tTA 209-232: 5'TAGAAGGGGAAAGCTGGCAAGATT3'
tTA 748-732: 5'CCGCGGGGAGAAAGGAC3'

Primers for cloning

WRE-Bam-for: TAAGGATCCTAATCAACCTCTGGATTA
WRE-H3-rev: TCTAAGCTTACTAGTGCGGGGAGG
Bam-Flag-for:TAGGGATCCGTCAGAATTAACCAT
PME-Flag-rev:CTTTTTTCAAGGGCCGACATCTTGTCATCGTCATCCTTGT
Flag-PME-for:ACAAGGATGACGATGACAAGATGTCGGCCCTTGAAAAAAG

Bam-PME-rev:GGAGGATCCAGCAGGTCACTAGCA
LCMT-Flag-rev:TCCCTCGAGCTGGAGGCCATCTTGTCATCGTCATCCTTGT
Flag-LCMT-for:ACAAGGATGACGATGACAAGATGGCCTCCAGCTCGAGGGA
Bam-LCMT-rev:GCAGGATCCTTCAGCAGATCAATA
mm400-Not-for:ACTCGAGCGGCCGCCAACTCTCGA
BGH-Not-rev:TAGAGCGGCCGCTGGTTCTTTCCG

References:

Alamed, J., Wilcock, D.M., Diamond, D.M., Gordon, M.N., and Morgan, D. (2006). Two-day radial-arm water maze learning and memory task; robust resolution of amyloid-related memory deficits in transgenic mice. Nature protocols *1*, 1671-1679.

Ando, K., Iijima, K.I., Elliott, J.I., Kirino, Y., and Suzuki, T. (2001). Phosphorylation-dependent regulation of the interaction of amyloid precursor protein with Fe65 affects the production of beta-amyloid. J Biol Chem *276*, 40353-40361.

Bernardo, A., McCord, M., Troen, A.M., Allison, J.D., and McDonald, M.P. (2007). Impaired spatial memory in APP-overexpressing mice on a homocysteinemia-inducing diet. Neurobiology of aging *28*, 1195-1205.

Bottiglieri, T., Arning, E., Wasek, B., Nunbhakdi-Craig, V., Sontag, J.M., and Sontag, E. (2012). Acute administration of L-DOPA induces changes in methylation metabolites, reduced protein phosphatase 2A methylation, and hyperphosphorylation of Tau protein in mouse brain. J Neurosci *32*, 9173-9181.

Braithwaite, S.P., Stock, J.B., Lombroso, P.J., and Nairn, A.C. (2012). Protein phosphatases and Alzheimer's disease. Progress in molecular biology and translational science *106*, 343-379.

Bryant, J.C., Westphal, R.S., and Wadzinski, B.E. (1999). Methylated C-terminal leucine residue of PP2A catalytic subunit is important for binding of regulatory Balpha subunit. The Biochemical journal *339 (Pt 2)*, 241-246.

Chong, Y.H., Shin, Y.J., Lee, E.O., Kayed, R., Glabe, C.G., and Tenner, A.J. (2006). ERK1/2 activation mediates Abeta oligomer-induced neurotoxicity via caspase-3 activation and tau cleavage in rat organotypic hippocampal slice cultures. J Biol Chem *281*, 20315-20325.

Chouliaras, L., Sierksma, A.S., Kenis, G., Prickaerts, J., Lemmens, M.A., Brasnjevic, I., van Donkelaar, E.L., Martinez-Martinez, P., Losen, M., De Baets, M.H.*, et al.* (2010). Gene-environment interaction research and transgenic mouse models of Alzheimer's disease. International journal of Alzheimer's disease *2010*.

Feyt, C., Pierrot, N., Tasiaux, B., Van Hees, J., Kienlen-Campard, P., Courtoy, P.J., and Octave, J.N. (2007). Phosphorylation of APP695 at Thr668 decreases gamma-cleavage and extracellular Abeta. Biochem Biophys Res Commun *357*, 1004-1010.

Fiorito, J., Saeed, F., Zhang, H., Staniszewski, A., Feng, Y., Francis, Y.I., Rao, S., Thakkar, D.M., Deng, S.X., Landry, D.W.*, et al.* (2013). Synthesis of quinoline derivatives: discovery of a potent and selective phosphodiesterase 5 inhibitor for the treatment of Alzheimer's disease. European journal of medicinal chemistry *60*, 285-294.

Fleming, J.L., Phiel, C.J., and Toland, A.E. (2012). The role for oxidative stress in aberrant DNA methylation in Alzheimer's disease. Curr Alzheimer Res *9*, 1077-1096.

Fuso, A., Cavallaro, R.A., Nicolia, V., and Scarpa, S. (2012a). PSEN1 promoter demethylation in hyperhomocysteinemic TgCRND8 mice is the culprit, not the consequence. Curr Alzheimer Res *9*, 527-535.

Fuso, A., Nicolia, V., Ricceri, L., Cavallaro, R.A., Isopi, E., Mangia, F., Fiorenza, M.T., and Scarpa, S. (2012b). S-adenosylmethionine reduces the progress of the Alzheimer-like features induced by B-vitamin deficiency in mice. Neurobiology of aging *33*, 1482 e1481-1416.

Gong, C.X., Shaikh, S., Wang, J.Z., Zaidi, T., Grundke-Iqbal, I., and Iqbal, K. (1995). Phosphatase activity toward abnormally phosphorylated tau: decrease in Alzheimer disease brain. Journal of neurochemistry *65*, 732-738.

Gong, C.X., Singh, T.J., Grundke-Iqbal, I., and Iqbal, K. (1993). Phosphoprotein phosphatase activities in Alzheimer disease brain. Journal of neurochemistry *61*, 921-927.

Haass, C., and Selkoe, D.J. (2007). Soluble protein oligomers in neurodegeneration: lessons from the Alzheimer's amyloid beta-peptide. Nature reviews Molecular cell biology *8*, 101-112.

Hasegawa, T., Ukai, W., Jo, D.G., Xu, X., Mattson, M.P., Nakagawa, M., Araki, W., Saito, T., and Yamada, T. (2005). Homocysteic acid induces intraneuronal accumulation of neurotoxic Abeta42: implications for the pathogenesis of Alzheimer's disease. J Neurosci Res *80*, 869-876.

Janssens, V., and Goris, J. (2001). Protein phosphatase 2A: a highly regulated family of serine/threonine phosphatases implicated in cell growth and signalling. The Biochemical journal *353*, 417-439.

Janssens, V., Longin, S., and Goris, J. (2008). PP2A holoenzyme assembly: in cauda venenum (the sting is in the tail). Trends in biochemical sciences *33*, 113-121.

Kins, S., Crameri, A., Evans, D.R., Hemmings, B.A., Nitsch, R.M., and Gotz, J. (2001). Reduced protein phosphatase 2A activity induces hyperphosphorylation and altered compartmentalization of tau in transgenic mice. J Biol Chem *276*, 38193-38200.

Kruman, II, Kumaravel, T.S., Lohani, A., Pedersen, W.A., Cutler, R.G., Kruman, Y., Haughey, N., Lee, J., Evans, M., and Mattson, M.P. (2002). Folic acid deficiency and homocysteine impair DNA repair in hippocampal neurons and sensitize them to amyloid toxicity in experimental models of Alzheimer's disease. J Neurosci *22*, 1752-1762.

Lee, J.A., and Pallas, D.C. (2007). Leucine carboxyl methyltransferase-1 is necessary for normal progression through mitosis in mammalian cells. J Biol Chem *282*, 30974-30984.

Lee, M.S., Kao, S.C., Lemere, C.A., Xia, W., Tseng, H.C., Zhou, Y., Neve, R., Ahlijanian, M.K., and Tsai, L.H. (2003). APP processing is regulated by cytoplasmic phosphorylation. The Journal of cell biology *163*, 83-95.

Lewis, J., Dickson, D.W., Lin, W.L., Chisholm, L., Corral, A., Jones, G., Yen, S.H., Sahara, N., Skipper, L., Yager, D*., et al.* (2001). Enhanced neurofibrillary degeneration in transgenic mice expressing mutant tau and APP. Science *293*, 1487-1491.

Lois, C., Hong, E.J., Pease, S., Brown, E.J., and Baltimore, D. (2002). Germline transmission and tissue-specific expression of transgenes delivered by lentiviral vectors. Science *295*, 868-872.

Longin, S., Zwaenepoel, K., Louis, J.V., Dilworth, S., Goris, J., and Janssens, V. (2007). Selection of protein phosphatase 2A regulatory subunits is mediated by the C terminus of the catalytic Subunit. J Biol Chem *282*, 26971-26980.

Longin, S., Zwaenepoel, K., Martens, E., Louis, J.V., Rondelez, E., Goris, J., and Janssens, V. (2008). Spatial control of protein phosphatase 2A (de)methylation. Experimental cell research *314*, 68-81.

Louis, J.V., Martens, E., Borghgraef, P., Lambrecht, C., Sents, W., Longin, S., Zwaenepoel, K., Pijnenborg, R., Landrieu, I., Lippens, G.*, et al.* (2011). Mice lacking phosphatase PP2A subunit PR61/B'delta (Ppp2r5d) develop spatially restricted tauopathy by deregulation of CDK5 and GSK3beta. Proc Natl Acad Sci U S A *108*, 6957-6962.

Mairet-Coello, G., Courchet, J., Pieraut, S., Courchet, V., Maximov, A., and Polleux, F. (2013). The CAMKK2-AMPK kinase pathway mediates the synaptotoxic effects of Abeta oligomers through Tau phosphorylation. Neuron *78*, 94-108.

Maren, S., Phan, K.L., and Liberzon, I. (2013). The contextual brain: implications for fear conditioning, extinction and psychopathology. Nat Rev Neurosci *14*, 417-428.

Marlatt, M.W., Lucassen, P.J., Perry, G., Smith, M.A., and Zhu, X. (2008). Alzheimer's disease: cerebrovascular dysfunction, oxidative stress, and advanced clinical therapies. J Alzheimers Dis *15*, 199-210.

Martin, L., Latypova, X., Wilson, C.M., Magnaudeix, A., Perrin, M.L., and Terro, F. (2013). Tau protein phosphatases in Alzheimer's disease: the leading role of PP2A. Ageing research reviews *12*, 39-49.

Matsuo, E.S., Shin, R.W., Billingsley, M.L., Van deVoorde, A., O'Connor, M., Trojanowski, J.Q., and Lee, V.M. (1994). Biopsy-derived adult human brain tau is phosphorylated at many of the same sites as Alzheimer's disease paired helical filament tau. Neuron *13*, 989-1002.

Matsushima, T., Saito, Y., Elliott, J.I., Iijima-Ando, K., Nishimura, M., Kimura, N., Hata, S., Yamamoto, T., Nakaya, T., and Suzuki, T. (2012). Membrane-microdomain localization of amyloid beta-precursor protein (APP) C-terminal fragments is regulated by phosphorylation of the cytoplasmic Thr668 residue. J Biol Chem *287*, 19715-19724.

Mayford, M., Bach, M.E., Huang, Y.Y., Wang, L., Hawkins, R.D., and Kandel, E.R. (1996). Control of memory formation through regulated expression of a CaMKII transgene. Science *274*, 1678-1683.

Nicolia, V., Fuso, A., Cavallaro, R.A., Di Luzio, A., and Scarpa, S. (2010). B vitamin deficiency promotes tau phosphorylation through regulation of GSK3beta and PP2A. J Alzheimers Dis *19*, 895-907.

Ondrejcak, T., Klyubin, I., Hu, N.W., Barry, A.E., Cullen, W.K., and Rowan, M.J. (2010). Alzheimer's disease amyloid beta-protein and synaptic function. Neuromolecular Med *12*, 13-26.

Ortega-Gutierrez, S., Leung, D., Ficarro, S., Peters, E.C., and Cravatt, B.F. (2008). Targeted disruption of the PME-1 gene causes loss of demethylated PP2A and perinatal lethality in mice. PLoS One *3*, e2486.

Pacheco-Quinto, J., Rodriguez de Turco, E.B., DeRosa, S., Howard, A., Cruz-Sanchez, F., Sambamurti, K., Refolo, L., Petanceska, S., and Pappolla, M.A. (2006). Hyperhomocysteinemic Alzheimer's mouse model of amyloidosis shows increased brain amyloid beta peptide levels. Neurobiol Dis *22*, 651-656.

Paxinos, G., and Franklin, K.B.J. (2004). The mouse brain in stereotaxic coordinates, Compact 2nd edn (Amsterdam ; Boston: Elsevier Academic Press).
Perez, M., Moran, M.A., Ferrer, I., Avila, J., and Gomez-Ramos, P. (2008). Phosphorylated tau in neuritic plaques of APP(sw)/Tau (vlw) transgenic mice and Alzheimer disease. Acta Neuropathol *116*, 409-418.
Perez, M., Ribe, E., Rubio, A., Lim, F., Moran, M.A., Ramos, P.G., Ferrer, I., Isla, M.T., and Avila, J. (2005). Characterization of a double (amyloid precursor protein-tau) transgenic: tau phosphorylation and aggregation. Neuroscience *130*, 339-347.
Pierrot, N., Santos, S.F., Feyt, C., Morel, M., Brion, J.P., and Octave, J.N. (2006). Calcium-mediated transient phosphorylation of tau and amyloid precursor protein followed by intraneuronal amyloid-beta accumulation. J Biol Chem *281*, 39907-39914.
Puzzo, D., and Arancio, O. (2013). Amyloid-beta peptide: Dr. Jekyll or Mr. Hyde? J Alzheimers Dis *33 Suppl 1*, S111-120.
Puzzo, D., Privitera, L., Leznik, E., Fa, M., Staniszewski, A., Palmeri, A., and Arancio, O. (2008). Picomolar amyloid-beta positively modulates synaptic plasticity and memory in hippocampus. J Neurosci *28*, 14537-14545.
Rhein, V., Song, X., Wiesner, A., Ittner, L.M., Baysang, G., Meier, F., Ozmen, L., Bluethmann, H., Drose, S., Brandt, U.*, et al.* (2009). Amyloid-beta and tau synergistically impair the oxidative phosphorylation system in triple transgenic Alzheimer's disease mice. Proc Natl Acad Sci U S A *106*, 20057-20062.
Rhodehouse, B.C., Erickson, M.A., Banks, W.A., and Bearden, S.E. (2013). Hyperhomocysteinemic mice show cognitive impairment without features of Alzheimer's disease phenotype. J Alzheimers Dis *35*, 59-66.
Ribe, E.M., Perez, M., Puig, B., Gich, I., Lim, F., Cuadrado, M., Sesma, T., Catena, S., Sanchez, B., Nieto, M.*, et al.* (2005). Accelerated amyloid deposition, neurofibrillary degeneration and neuronal loss in double mutant APP/tau transgenic mice. Neurobiol Dis *20*, 814-822.
Roberson, E.D., Scearce-Levie, K., Palop, J.J., Yan, F., Cheng, I.H., Wu, T., Gerstein, H., Yu, G.Q., and Mucke, L. (2007). Reducing endogenous tau ameliorates amyloid beta-induced deficits in an Alzheimer's disease mouse model. Science *316*, 750-754.
Rudrabhatla, P., and Pant, H.C. (2011). Role of protein phosphatase 2A in Alzheimer's disease. Curr Alzheimer Res *8*, 623-632.
Sano, Y., Nakaya, T., Pedrini, S., Takeda, S., Iijima-Ando, K., Iijima, K., Mathews, P.M., Itohara, S., Gandy, S., and Suzuki, T. (2006). Physiological mouse brain Abeta levels are not related to the phosphorylation state of threonine-668 of Alzheimer's APP. PLoS One *1*, e51.
Schalinske, K.L., and Smazal, A.L. (2012). Homocysteine imbalance: a pathological metabolic marker. Adv Nutr *3*, 755-762.
Schenk, D., Basi, G.S., and Pangalos, M.N. (2012). Treatment strategies targeting amyloid beta-protein. Cold Spring Harb Perspect Med *2*, a006387.

Schild, A., Ittner, L.M., and Gotz, J. (2006). Altered phosphorylation of cytoskeletal proteins in mutant protein phosphatase 2A transgenic mice. Biochem Biophys Res Commun *343*, 1171-1178.

Sents, W., Ivanova, E., Lambrecht, C., Haesen, D., and Janssens, V. (2013). The biogenesis of active protein phosphatase 2A holoenzymes: a tightly regulated process creating phosphatase specificity. The FEBS journal *280*, 644-661.

Shi, Y. (2009). Serine/threonine phosphatases: mechanism through structure. Cell *139*, 468-484.

Shipton, O.A., Leitz, J.R., Dworzak, J., Acton, C.E., Tunbridge, E.M., Denk, F., Dawson, H.N., Vitek, M.P., Wade-Martins, R., Paulsen, O.*, et al.* (2011). Tau protein is required for amyloid {beta}-induced impairment of hippocampal long-term potentiation. J Neurosci *31*, 1688-1692.

Sontag, E., Luangpirom, A., Hladik, C., Mudrak, I., Ogris, E., Speciale, S., and White, C.L., 3rd (2004). Altered expression levels of the protein phosphatase 2A ABalphaC enzyme are associated with Alzheimer disease pathology. Journal of neuropathology and experimental neurology *63*, 287-301.

Sontag, E., Nunbhakdi-Craig, V., Lee, G., Bloom, G.S., and Mumby, M.C. (1996). Regulation of the phosphorylation state and microtubule-binding activity of Tau by protein phosphatase 2A. Neuron *17*, 1201-1207.

Sontag, E., Nunbhakdi-Craig, V., Lee, G., Brandt, R., Kamibayashi, C., Kuret, J., White, C.L., 3rd, Mumby, M.C., and Bloom, G.S. (1999). Molecular interactions among protein phosphatase 2A, tau, and microtubules. Implications for the regulation of tau phosphorylation and the development of tauopathies. J Biol Chem *274*, 25490-25498.

Sontag, E., Nunbhakdi-Craig, V., Sontag, J.M., Diaz-Arrastia, R., Ogris, E., Dayal, S., Lentz, S.R., Arning, E., and Bottiglieri, T. (2007). Protein phosphatase 2A methyltransferase links homocysteine metabolism with tau and amyloid precursor protein regulation. J Neurosci *27*, 2751-2759.

Sontag, J.M., Nunbhakdi-Craig, V., Montgomery, L., Arning, E., Bottiglieri, T., and Sontag, E. (2008). Folate deficiency induces in vitro and mouse brain region-specific downregulation of leucine carboxyl methyltransferase-1 and protein phosphatase 2A B(alpha) subunit expression that correlate with enhanced tau phosphorylation. J Neurosci *28*, 11477-11487.

Sontag, J.M., Nunbhakdi-Craig, V., and Sontag, E. (2013). Leucine Carboxyl Methyltransferase 1 (LCMT1)-dependent Methylation Regulates the Association of Protein Phosphatase 2A and Tau Protein with Plasma Membrane Microdomains in Neuroblastoma Cells. J Biol Chem *288*, 27396-27405.

Stine, W.B., Jr., Dahlgren, K.N., Krafft, G.A., and LaDu, M.J. (2003). In vitro characterization of conditions for amyloid-beta peptide oligomerization and fibrillogenesis. J Biol Chem *278*, 11612-11622.

Sun, L., Liu, S.Y., Zhou, X.W., Wang, X.C., Liu, R., Wang, Q., and Wang, J.Z. (2003). Inhibition of protein phosphatase 2A- and protein phosphatase 1-induced tau hyperphosphorylation and impairment of spatial memory retention in rats. Neuroscience *118*, 1175-1182.

Tanzi, R.E. (2012). The Genetics of Alzheimer Disease. Cold Spring Harbor Perspectives in Medicine *2*.
Teich, A.F., Patel, M., and Arancio, O. (2013). A reliable way to detect endogenous murine beta-amyloid. PLoS One *8*, e55647.
Tolstykh, T., Lee, J., Vafai, S., and Stock, J.B. (2000). Carboxyl methylation regulates phosphoprotein phosphatase 2A by controlling the association of regulatory B subunits. The EMBO journal *19*, 5682-5691.
Troen, A.M., Shea-Budgell, M., Shukitt-Hale, B., Smith, D.E., Selhub, J., and Rosenberg, I.H. (2008). B-vitamin deficiency causes hyperhomocysteinemia and vascular cognitive impairment in mice. Proc Natl Acad Sci U S A *105*, 12474-12479.
Vogelsberg-Ragaglia, V., Schuck, T., Trojanowski, J.Q., and Lee, V.M. (2001). PP2A mRNA expression is quantitatively decreased in Alzheimer's disease hippocampus. Exp Neurol *168*, 402-412.
Voronkov, M., Braithwaite, S.P., and Stock, J.B. (2011). Phosphoprotein phosphatase 2A: a novel druggable target for Alzheimer's disease. Future Med Chem *3*, 821-833.
Wang, X., Blanchard, J., Kohlbrenner, E., Clement, N., Linden, R.M., Radu, A., Grundke-Iqbal, I., and Iqbal, K. (2010). The carboxy-terminal fragment of inhibitor-2 of protein phosphatase-2A induces Alzheimer disease pathology and cognitive impairment. FASEB J *24*, 4420-4432.
Watterson, D.M., Grum-Tokars, V.L., Roy, S.M., Schavocky, J.P., Bradaric, B.D., Bachstetter, A.D., Xing, B., Dimayuga, E., Saeed, F., Zhang, H.*, et al.* (2013). Development of Novel Chemical Probes to Address CNS Protein Kinase Involvement in Synaptic Dysfunction. PLoS One *8*, e66226.
Wei, W., Liu, Y.H., Zhang, C.E., Wang, Q., Wei, Z., Mousseau, D.D., Wang, J.Z., Tian, Q., and Liu, G.P. (2011). Folate/vitamin-B12 prevents chronic hyperhomocysteinemia-induced tau hyperphosphorylation and memory deficits in aged rats. J Alzheimers Dis *27*, 639-650.
Wisden, W., and Morris, B.J. (2002). In situ hybridization with oligonucleotide probes. International review of neurobiology *47*, 3-59.
Yin, Y.Y., Liu, H., Cong, X.B., Liu, Z., Wang, Q., Wang, J.Z., and Zhu, L.Q. (2010). Acetyl-L-carnitine attenuates okadaic acid induced tau hyperphosphorylation and spatial memory impairment in rats. J Alzheimers Dis *19*, 735-746.
Yoon, S.Y., Choi, H.I., Choi, J.E., Sul, C.A., Choi, J.M., and Kim, D.H. (2007). Methotrexate decreases PP2A methylation and increases tau phosphorylation in neuron. Biochem Biophys Res Commun *363*, 811-816.
Yu, X.X., Du, X., Moreno, C.S., Green, R.E., Ogris, E., Feng, Q., Chou, L., McQuoid, M.J., and Pallas, D.C. (2001). Methylation of the protein phosphatase 2A catalytic subunit is essential for association of Balpha regulatory subunit but not SG2NA, striatin, or polyomavirus middle tumor antigen. Molecular biology of the cell *12*, 185-199.
Zhang, C.E., Tian, Q., Wei, W., Peng, J.H., Liu, G.P., Zhou, X.W., Wang, Q., Wang, D.W., and Wang, J.Z. (2008). Homocysteine induces tau phosphorylation by inactivating protein phosphatase 2A in rat hippocampus. Neurobiology of aging *29*, 1654-1665.

Zhang, C.E., Wei, W., Liu, Y.H., Peng, J.H., Tian, Q., Liu, G.P., Zhang, Y., and Wang, J.Z. (2009). Hyperhomocysteinemia increases beta-amyloid by enhancing expression of gamma-secretase and phosphorylation of amyloid precursor protein in rat brain. Am J Pathol *174*, 1481-1491.

Zhuo, J.M., Portugal, G.S., Kruger, W.D., Wang, H., Gould, T.J., and Pratico, D. (2010). Diet-induced hyperhomocysteinemia increases amyloid-beta formation and deposition in a mouse model of Alzheimer's disease. Curr Alzheimer Res *7*, 140-149.

Zhuo, J.M., and Pratico, D. (2010a). Acceleration of brain amyloidosis in an Alzheimer's disease mouse model by a folate, vitamin B6 and B12-deficient diet. Experimental gerontology *45*, 195-201.

Zhuo, J.M., and Pratico, D. (2010b). Normalization of hyperhomocysteinemia improves cognitive deficits and ameliorates brain amyloidosis of a transgenic mouse model of Alzheimer's disease. FASEB J *24*, 3895-3902.

Zhuo, J.M., Wang, H., and Pratico, D. (2011). Is hyperhomocysteinemia an Alzheimer's disease (AD) risk factor, an AD marker, or neither? Trends Pharmacol Sci *32*, 562-571.

Supplemental Table 1:

Methyl metabolite levels in hippocampi of PME-1 over expressing animals and sibling controls:

	Hippocampus			ANOVA	
nmol/g	Double (N=11)	tTA (N = 7)	PME (N = 5)	F	P
SAM	11.9 ± 3.7	11.4 ± 4.0	11.1 ± 1.9		
SAH	0.21 ± 0.047	0.22 ± 0.06	0.19 ± 0.04		
SAM/SAH	57.7 ± 18.9	53.6 ± 18.5	60.3 ± 17.8		
CYSTA	19.6 ± 3.9	21.7 ± 3.1	18.4 ± 1.7		
BETAINE	27.6 ± 5.8	28.7 ± 4.0	27.1 ± 4.9		
CHOLINE	73.3 ± 14.3	79.5 ± 16.3	64.1 ± 16.7		
METHIONINE	39.6 ± 12.9	40.5 ± 11.5	44.3 ± 10.7		

Methyl metabolite levels in hippocampi of LCMT-1 over expressing animals and sibling controls:

	Hippocampus			ANOVA	
nmol/g	Double (N=7)	tTA (N = 9)	LCMT (N = 6)	F	P
SAM	10.9 ± 2.7	8.6 ± 3.0	10.7 ± 4.7		
SAH	0.28 ± 0.05	0.27 ± 0.04	0.24 ± 0.05		
SAM/SAH	42.6 ± 20.0	32.5 ± 12.0	45.0 ± 21.9		
CYSTA	20.8 ± 3.0	18.8 ± 1.7	19.6 ± 2.6		
BETAINE	24.2 ± 4.1	26.0 ± 3.5	26.0 ± 2.1		
CHOLINE	84.3 ± 12.8	80.9 ± 22.0	69.2 ± 16.6		
METHIONINE	41.7 ± 4.9	36.5 ± 3.6	34.7 ± 12.2		

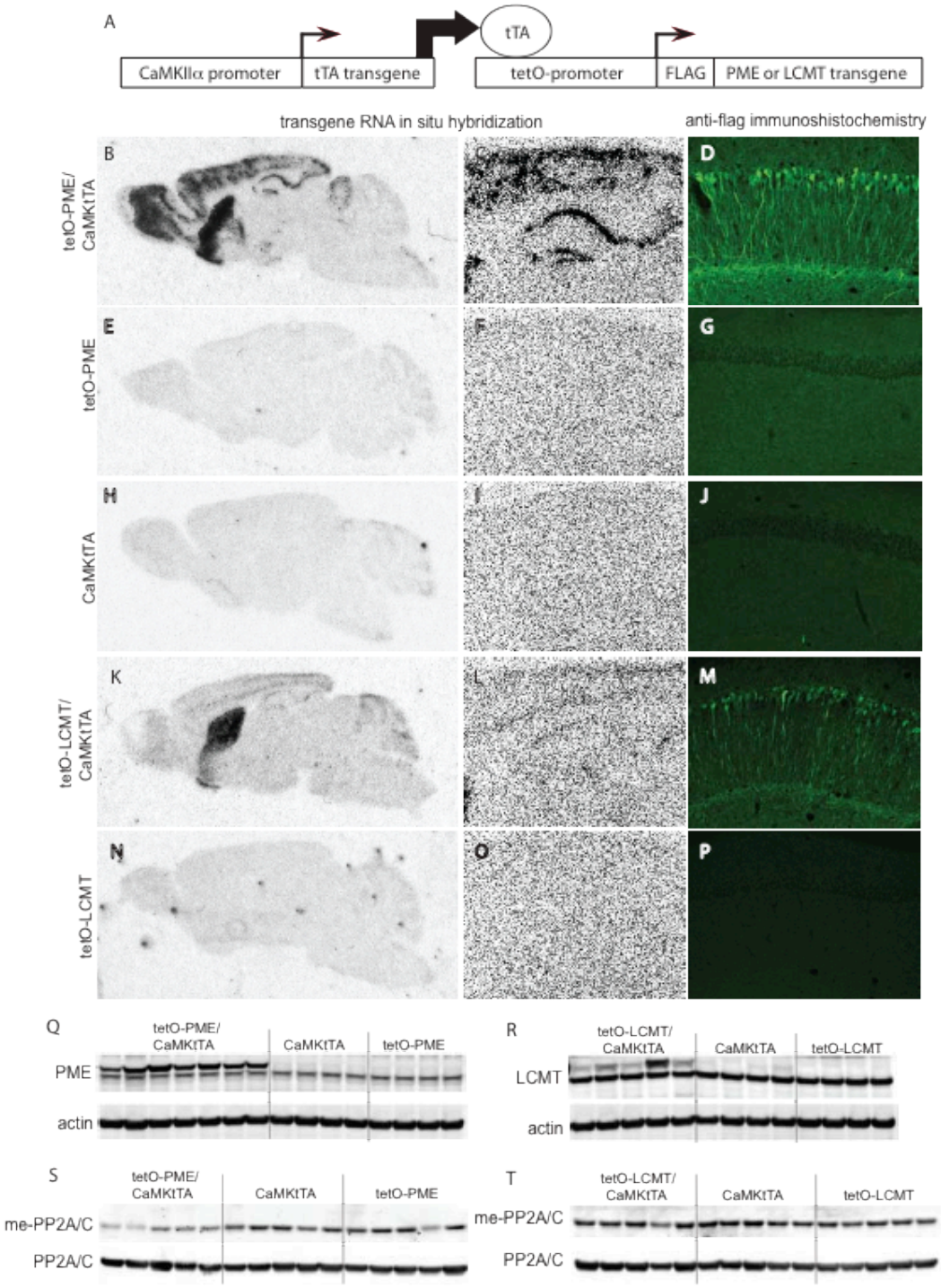
A
tTA
CaMKIIα promoter
tTA transgene
tetO-promoter
FLAG
PME or LCMT transgene
transgene RNA in situ hybridization
anti-flag immunoshistochemistry
tetO-PME/ CaMKtTA
tetO-PME
CaMKtTA
tetO-LCMT/ CaMKtTA
tetO-LCMT
B
C
D
E
F
G
H
I
J
K
L
M
N
O
P
Q
tetO-PME/ CaMKtTA
CaMKtTA
tetO-PME
PME
actin
R
tetO-LCMT/ CaMKtTA
CaMKtTA
tetO-LCMT
LCMT
actin
S
tetO-PME/ CaMKtTA
CaMKtTA
tetO-PME
me-PP2A/C
PP2A/C
T
tetO-LCMT/ CaMKtTA
CaMKtTA
tetO-LCMT
me-PP2A/C
PP2A/C

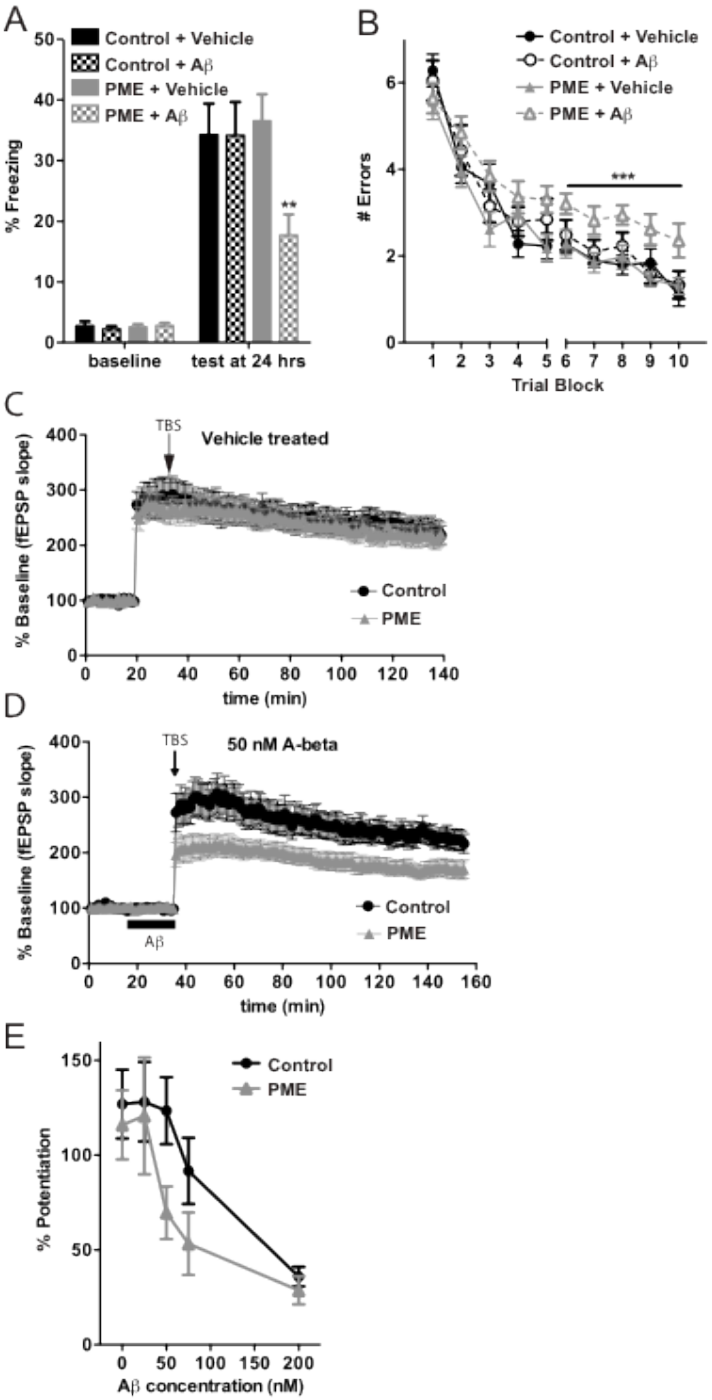
A
Control + Vehicle
Control + Aβ
PME + Vehicle
PME + Aβ
% Freezing
baseline
test at 24 hrs
**
B
Control + Vehicle
Control + Aβ
PME + Vehicle
PME + Aβ
Errors
***
Trial Block
C
TBS
Vehicle treated
% Baseline (fEPSP slope)
Control
PME
time (min)
D
TBS
50 nM A-beta
% Baseline (fEPSP slope)
Aβ
Control
PME
time (min)
E
Control
PME
% Potentiation
Aβ concentration (nM)

Figure 2

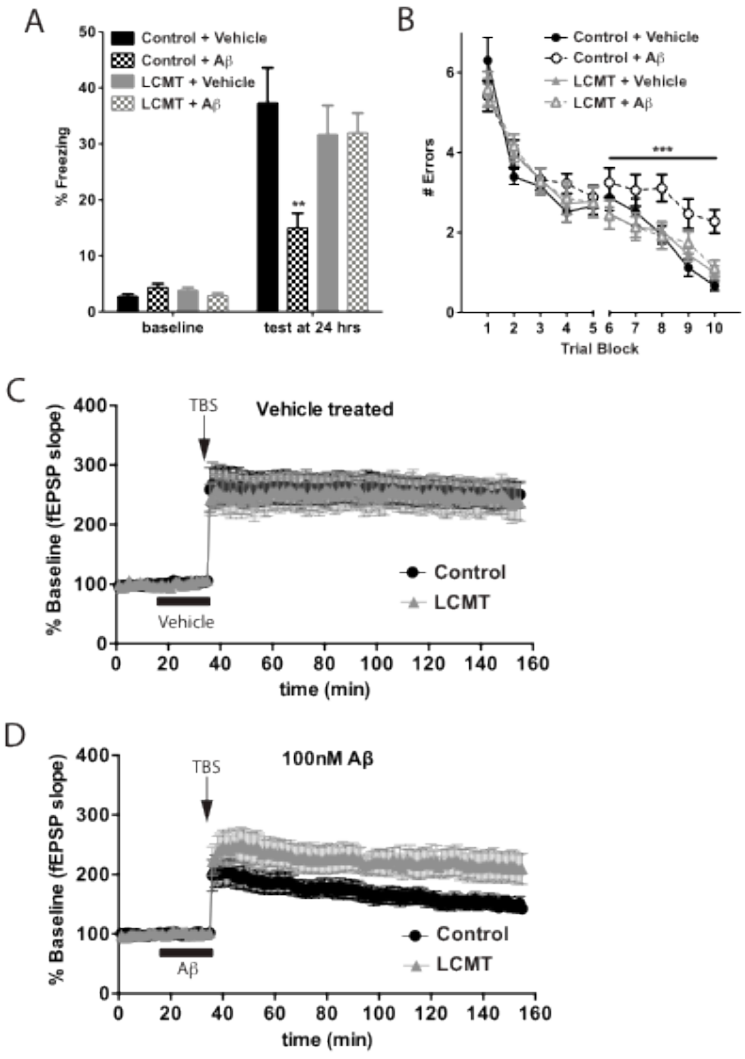
A
Control + Vehicle
Control + Aβ
LCMT + Vehicle
LCMT + Aβ
% Freezing
baseline
test at 24 hrs
**
B
Control + Vehicle
Control + Aβ
LCMT + Vehicle
LCMT + Aβ
Errors
***
Trial Block
C
Vehicle treated
TBS
% Baseline (fEPSP slope)
Vehicle
Control
LCMT
time (min)
D
100nM Aβ
TBS
% Baseline (fEPSP slope)
Aβ
Control
LCMT
time (min)

Figure 3

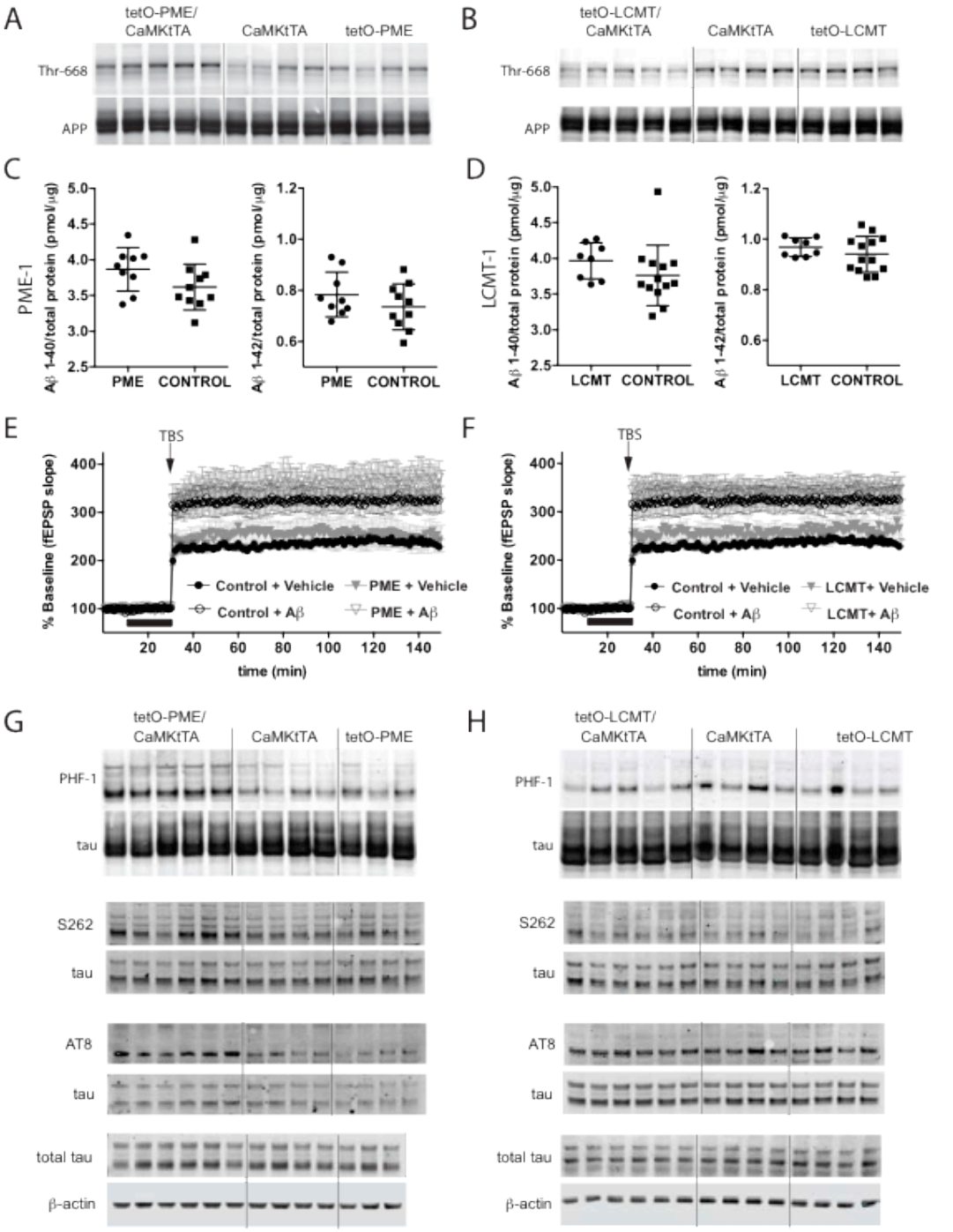
A
tetO-PME/ CaMKtTA
CaMKtTA
tetO-PME
Thr-668
APP
B
tetO-LCMT/ CaMKtTA
CaMKtTA
tetO-LCMT
Thr-668
APP
C
PME-1
Aβ 1-40/total protein (pmol/μg)
Aβ 1-42/total protein (pmol/μg)
PME
CONTROL
D
LCMT-1
Aβ 1-40/total protein (pmol/μg)
Aβ 1-42/total protein (pmol/μg)
LCMT
CONTROL
E
TBS
% Baseline (fEPSP slope)
time (min)
Control + Vehicle
PME + Vehicle
Control + Aβ
PME + Aβ
F
TBS
% Baseline (fEPSP slope)
time (min)
Control + Vehicle
LCMT+ Vehicle
Control + Aβ
LCMT+ Aβ
G
tetO-PME/ CaMKtTA
CaMKtTA
tetO-PME
PHF-1
tau
S262
tau
AT8
tau
total tau
β-actin
H
tetO-LCMT/ CaMKtTA
CaMKtTA
tetO-LCMT
PHF-1
tau
S262
tau
AT8
tau
total tau
β-actin

Figure 4

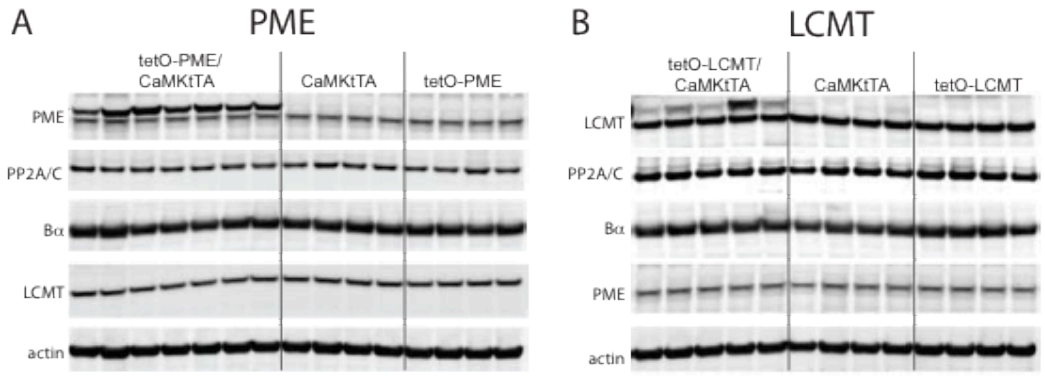
A
PME
tetO-PME/
CaMKtTA
CaMKtTA
tetO-PME
PME
PP2A/C
Bα
LCMT
actin
B
LCMT
tetO-LCMT/
CaMKtTA
CaMKtTA
tetO-LCMT
LCMT
PP2A/C
Bα
PME
actin

Figure S1

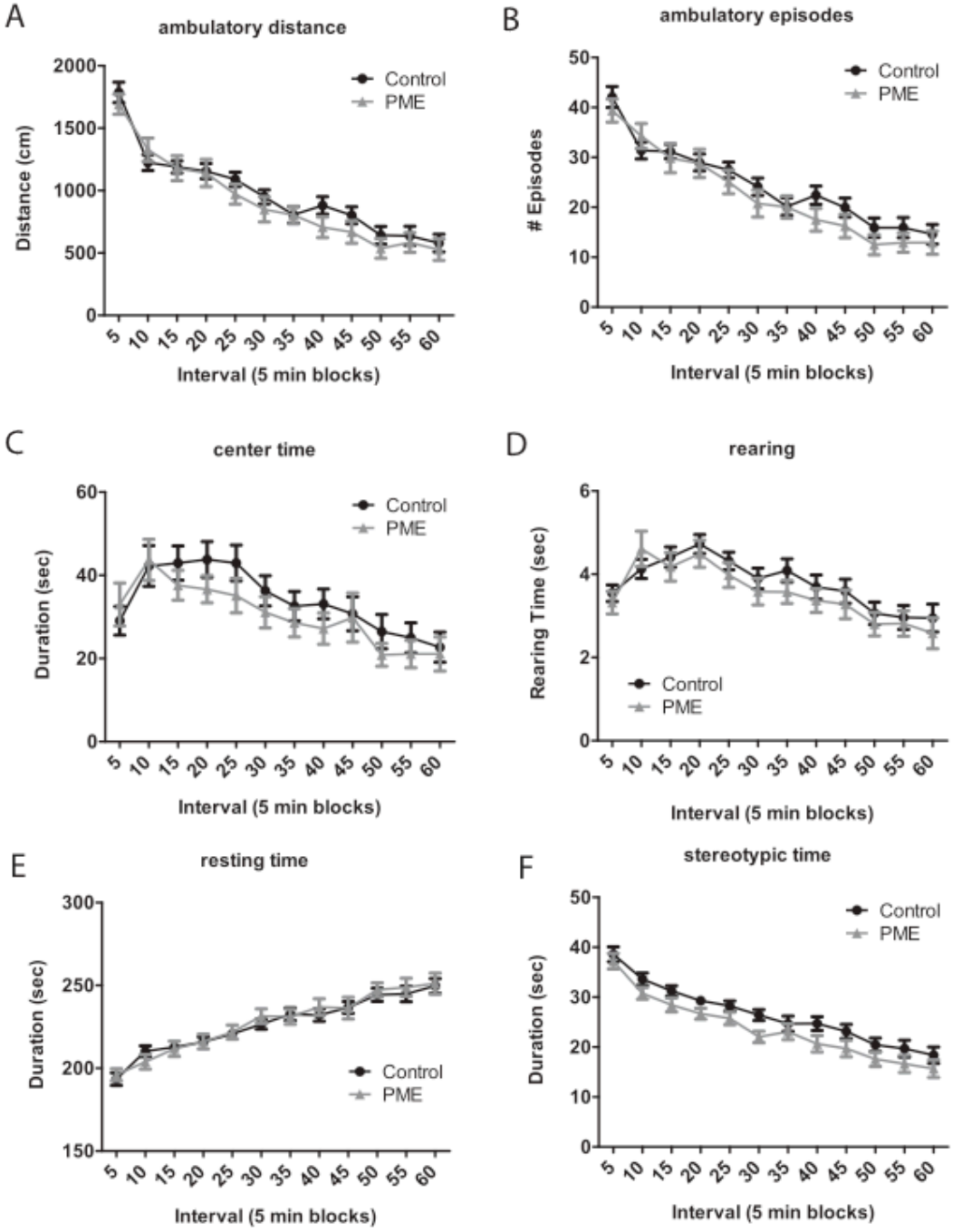

Supplemental Figure 2

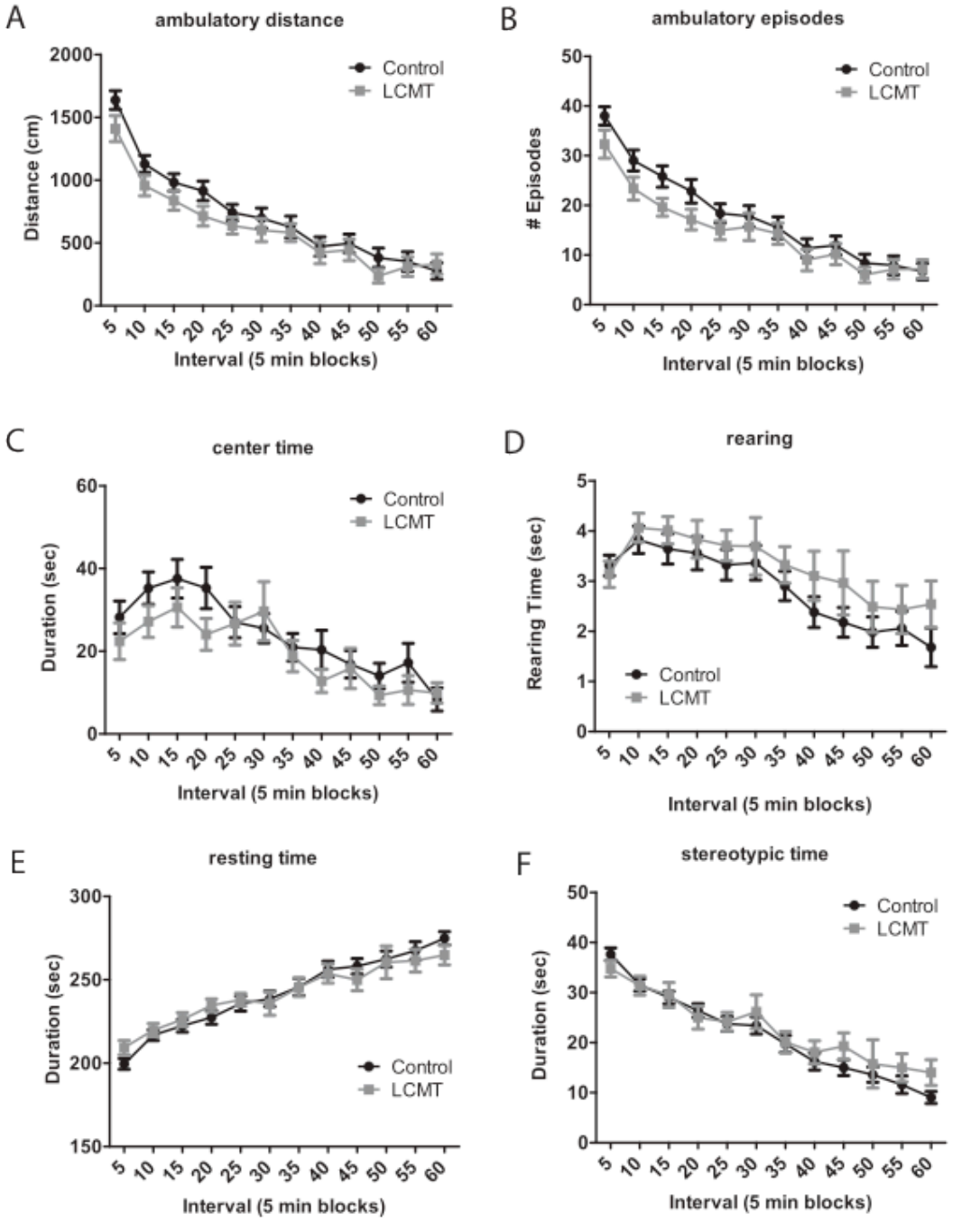

Supplemental Figure 3

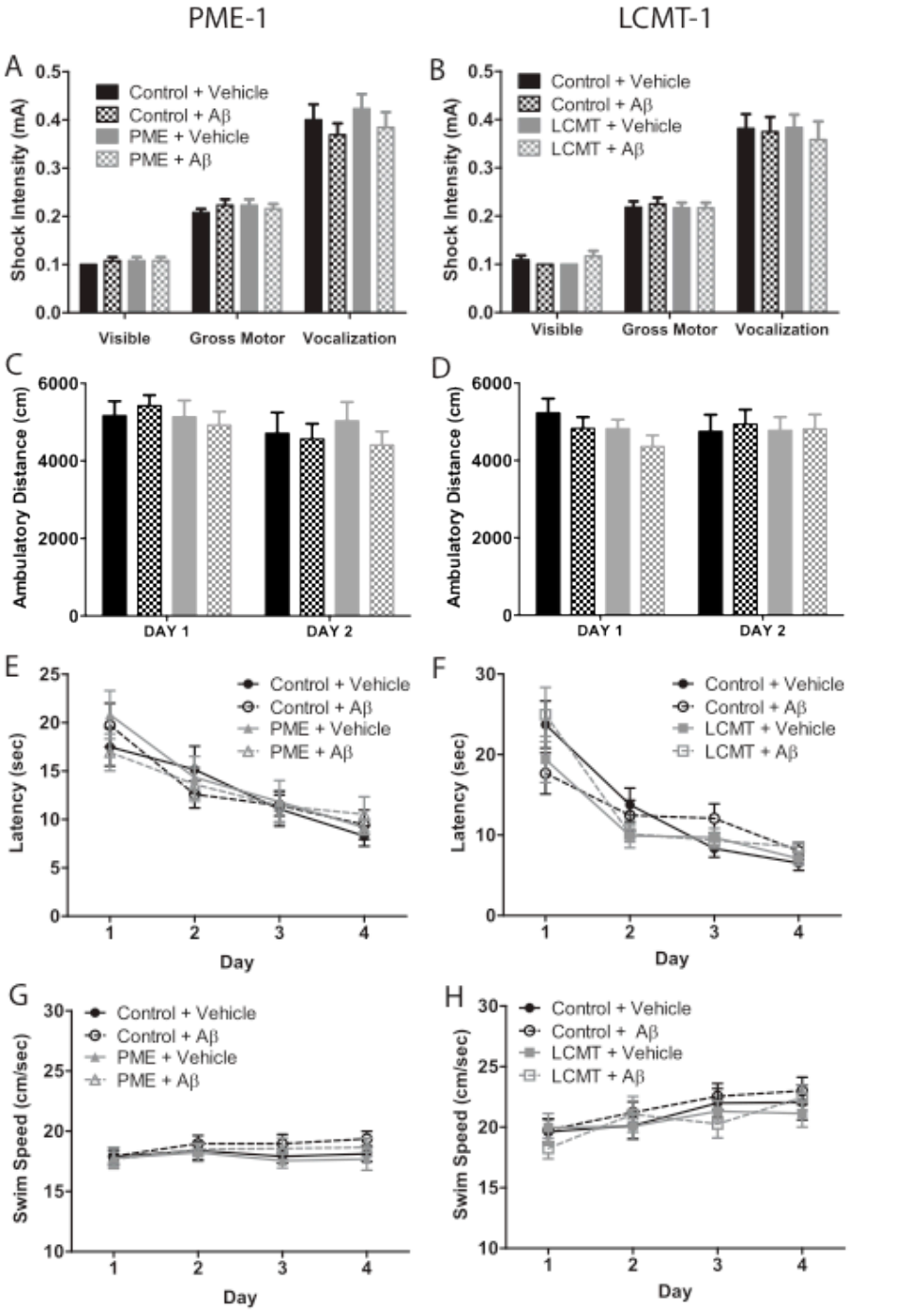

Supplemental Figure 4

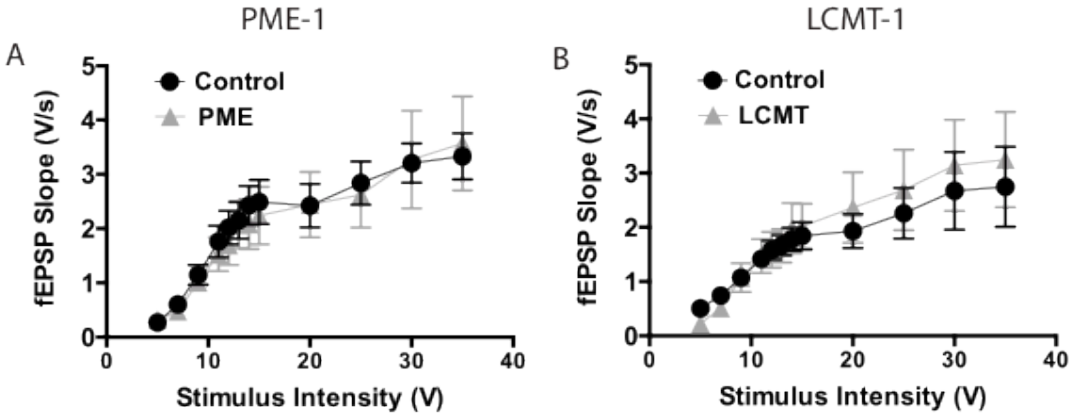

Supplemental Figure 5